DOI: 10.1070/RCR4712

Fullerene derivatives as nano-additives in polymer composites

Anastasia V. Penkova,[a] Steve F. A. Acquah,[b] Levon B. Piotrovskiy,[c] Denis A. Markelov,[a, d] Anna S. Semisalova,[e, f] Harold W. Kroto [b] (deceased)

[a] *Saint Petersburg State University*
Universitetskaya nab. 7 – 9, 199034 Saint Petersburg, Russian Federation
[b] *Florida State University*
W. College Avenue 600, Tallahassee, Florida 32306, USA
[c] *Institute of Experimental Medicine*
ul. Akademika Pavlova 12, 197376 Saint Petersburg, Russian Federation
[d] *St. Petersburg National Research University of Information Technologies, Mechanics and Optics (ITMO University)*
Kronverkskiy prosp. 49, 197101 Saint Petersburg, Russian Federation
[e] *Helmholtz-Zentrum Dresden – Rossendorf, Institute of Ion Beam Physics and Materials Research*
Bautzner Landstrasse 400, 01328 Dresden, Germany
[f] *Faculty of Physics, Lomonosov Moscow State University*
Leninskie Gory 1, str. 2, 119991 Moscow, Russian Federation

Since their discovery, fullerenes have become one of the most recognizable molecules in science. The 'beautiful molecule' described by Harold W.Kroto has been subtly referenced in movie, and has adorned the covers of many science-based textbooks. The physical and chemical properties of fullerenes have generated a lot of interest in the science community with many opportunities to develop new avenues for scientific research. Difficulties in the commercial use of fullerenes (*e.g.*, C_{60}) have likely been due to issues with solubility. Fortunately, the situation has improved over the last decade with research into fullerene derivatives. Once modified, fullerenes may have applications in a variety of areas including medicine, drug delivery, optoelectronics and electrochemistry. The addition of low concentrations of carbon nanoparticles to polymer matrices may result in significant changes in the function of polymer-based composite materials. This review will highlight the applications of fullerene derivatives as nano-additives for polymer composites. Various fullerene derivatives, *viz.*, water-soluble carbon nanoclusters modified with hydroxyl and carboxyl groups, as well as hydrophobic fullerenes (metallofullerenes and methanofullerenes) will be evaluated in regard to their potential impact on commercial applications, in particular, photovoltaic devices, fuel cells, membrane technology and biocompatible electroactive actuators. We, members of Harold W Kroto's research group in Florida and international collaborators, miss his exuberance and passion for engaging with young researchers, and we stand committed to preserving his legacy of science and outreach.
The bibliography includes 387 references.

Contents

I. Introduction 530
II. The structure of carbon nano-additives 532
III. The applications of fullerene derivatives 533
IV. Conclusion 558

I. Introduction

Polymer nanocomposites containing carbon nanoparticles as nanofillers are next-generation smart materials. As always, the researchers' goal is to transfer as much of the properties of the nanomaterials as possible from the nano- to the macroscale. The discovery of the buckminsterfullerene (C_{60}) was made in 1985 by R.Smalley, R.Curl and H.Kroto, who were awarded the 1996 Nobel Prize in chemistry. The subsequent years have seen a journey of discovery in the field of nanoscience and nanotechnology, a journey that continues with the recent discovery of C_{60}^{+} ions in space.

© 2017 Russian Academy of Sciences and Turpion Ltd.

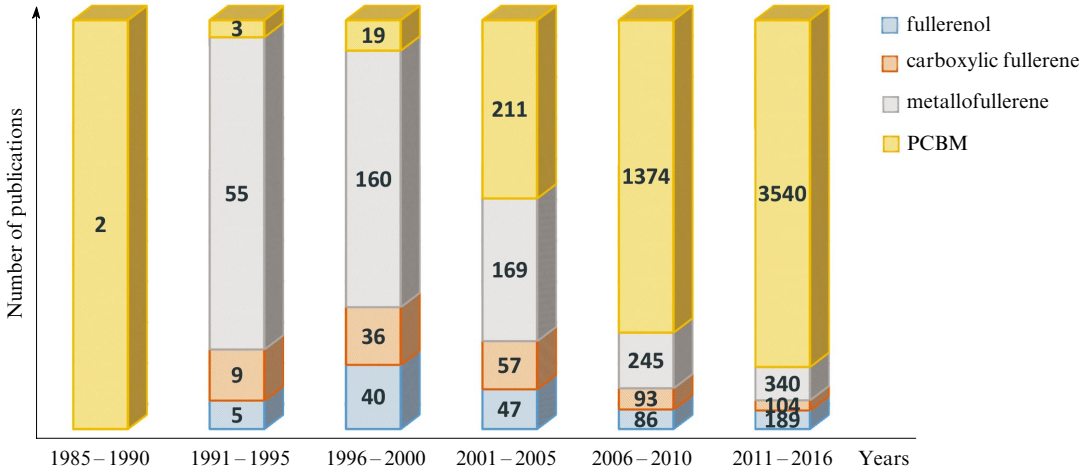


Figure 1. Comparison of the annual number of scientific publications devoted to fullerene derivatives in the past 30 years. Data analysis of publications was performed using the Scopus database with the terms 'PCBM', 'fullerenol', 'carboxylic fullerene', and 'metallofullerenes' as of the 28th August 2016.

The inherent properties of fullerenes have been investigated for potential use in some applications including light-activated antimicrobial agents, heat-resistant materials, superconductivity and biocompatibility in the field of medicine. Fullerenes have been used in photovoltaic devices,[1] biomedical devices,[2] fuel cells[3] and membrane processes.[4–11] Incorporating fullerenes into polymer matrices has been shown to improve the physical and transport properties of the host polymers.[12, 13]

Fullerenes are typically produced by arc or combustion methods and subsequent purification of reaction products. The resulting fullerenes can then be mixed with polymers. However, the poor adhesion and low miscibility of fullerenes with conventional organic solvents typically prevent them from being well-dispersed in polymer matrices. To overcome these difficulties, fullerenes can be functionalized with hydrophilic and hydrophobic groups, which enhance their physicochemical properties and promote their dispersion and strong adherence in polymer matrices. Fullerene derivatives have improved miscibility with host polymers without significant agglomeration, an essential characteristic for a wide range of applications.

In this review, a number of fullerene derivatives will be highlighted, including water-soluble fullerene derivatives (polyhydroxylated fullerenes, carboxyfullerenes and malonic acid derivatives) and hydrophobic fullerenes (metallofullerenes and methanofullerenes).

A survey of publications related to fullerene derivatives in the past 30 years is shown in Fig. 1.

First of all, Fig. 1 highlights a trend of increasing focus on fullerene derivatives over the last 30 years. This led to the creation of hybrid materials composed of polymer matrices and carbon additives. Pioneering publications on polymer nanocomposites appeared in the early 1990s. Over 4000 publications on polymer-carbon nanoparticles have been reported to date.

Water-soluble fullerene derivatives have been considered for applications in biology and medicine. In particular, hydrophilic fullerene derivatives can be used as antioxidants and help to prevent biological structures from the action of reactive oxygen species (ROS). A recent review on the physicochemical properties and

A.V.Penkova. Candidate of Chemical Sciences, Associate Professor at the Institute of Chemistry, SPbSU.
Telephone: +7 (812) 428 – 4805, e-mail: a.penkova@spbu.ru
Current research interests: membranes, polymers, polymer nanocomposites.
S.F.A.Acquah. Associate Research Professor of Chemistry, Department of Chemistry and Biochemistry, Florida State University (USA), Director of the H.W.Kroto Legacy Research Group and Director of Global Educational Outreach for Science, Engineering and Technology (GEOSET) Programme at the same University.
Telephone: +1 (850) 320 – 4686, e-mail: sacquah@chem.fsu.edu
Current research interests: carbon nanoparticles (carbon nanotubes, fullerenes, *etc.*), nanotechnology, polymer nanocomposites, solar cells.
L.B.Piotrovskiy. Doctor of Biological Sciences, Professor, Head of the Laboratory of Drug Synthesis and Nanotechnology, IEM.
Telephone: +7 (812) 234 – 6868, e-mail: levon-piotrovsky@yandex.ru
Current research interests: drug design, carbon nanostructures.
D.A.Markelov. Doctor of Physical and Mathematical Sciences, Associate Professor of Faculty of Physics, SPbSU, Researcher at the ITMO University.
Telephone: +7 (812) 428 – 9948, e-mail: markeloved@gmail.com
Current research interests: polymers, nanoparticles, membranes, modelling, molecular dynamics simulation, NMR.
A.S.Semisalova. Candidate of Physical and Mathematical Sciences, Assistant Professor of Department of Physics at the MSU, Postdoctoral Researcher of the Institute of Ion Beam Physics and Materials Research, Helmholtz-Zentrum Dresden – Rossendorf (Germany).
Telephone: +7 (495) 939 – 1847, e-mail: semisalova@magn.ru
Current research interests: magnetic materials, smart magnetorheological elastomers, nanoparticles.
H.W.Kroto. Eppes Professor of Chemistry, Florida State University (USA), 1996 Nobel Prize laureate in chemistry (deceased in 2016).

Received 24 November 2016

applications of fullerenols, promising pharmaceutical additives for the treatment of oxidative stress-related diseases, is available.[14] Fullerenols can also be used in biocompatible actuators as part of electroactive artificial muscles. Fullerenols and carboxyfullerenes can be incorporated into chemosensors and biosensors. The application of fullerenols in membrane technology leads to improvement in the properties of diffusive pervaporation membranes and the conductivity in fuel cells, especially at low relative humidity (RH). Fullerenols have demonstrated the potential for application in photocatalysis and photovoltaic devices. They show excellent optical transmission and electron transporting properties. For example, the surface morphology and wettability of fullerenol thin films on indium tin oxide-coated glass could be tuned by simply changing the annealing temperature; this causes changes in the photovoltaic performance of the inverted devices with fullerenol as a cathode buffer layer.[15]

Hydrophobic fullerene derivatives, metallofullerenes and methanofullerenes are being investigated in regard to application in sensors and photovoltaic devices. A poly(3-hexylthiophene): [6,6]-phenyl-C_{61}-butyric acid methyl ester (P3HT: PCBM) composite is a promising active layer material for photovoltaic solar cells (PSCs) with power conversion efficiencies (PCE) approaching 5% – 6%. Metallofullerenes demonstrate good potential for applications in catalysis.

Despite the broad use of polymer composites with carbon additives, the annual number of papers did not significantly change from 2005 to 2016 (except publications on polymer – PCBM composites whose number has been increasing dramatically over the last years). The groundbreaking experiments on graphene by A.Geim and K.Novoselov, which resulted in the 2010 Nobel Prize in physics, provide a renewed perspective on the application of carbon nanoparticles and nanoscience in general.

In the forthcoming Sections, the progress towards the development of fullerene derivatives as nano-additives in polymer composites will be reviewed, with applications of polymer nanocomposites in biology, medicine, physics, chemistry, engineering and material science.

Notations used in the review are as follows:

AFM — atomic force microscopy
ATP — adenosine 5′-triphosphate
BHJ — bulk heterojunction
BSA — bovine serum albumin
DDAB — didodecyldimethylammonium bromide
DIO — 1,8-diiodooctane
DOP — dioctyl phthalate
DOTA — 1,4,7,10-tetraazacyclododecane-1,4,7,10-tetraacetic acid
dPCBA — 3,4-dihexyloxyphenyl-C_{61}-butyric-acid
DTPA — diethylenetriaminepentaacetic acid
EMF — endohedral metallofullerene
EQE — external quantum efficiency
FF — fill factor
HSA — human serum albumin
HOMO — highest occupied molecular orbital
IPMC — ionic polymer metal composite
J_{SC} — short circuit current
LUMO — lowest unoccupied molecular orbital
MEH-PPV — poly{2-methoxy-5-(2′-ethylhexyloxy)-1,4-phenylenevinylene}
MIP — molecularly imprinted polymer
MRI — magnetic resonance imaging
P3HT — poly(3-hexylthiophene)
P3OT — poly(3-octylthiophene)
PCBM — [6,6]-phenyl-C_{61}-butyric acid methyl ester
$PC_{70}BM$ — [6,6]-phenyl-C_{71}-butyric acid methyl ester
$PC_{84}BM$ — [6,6]-phenyl-C_{85}-butyric acid methyl ester
PCDTBT — poly[*N*-9″-heptadecanyl-2,7-carbazole-*alt*-5,5-(4′,7′-di-2-thienyl-2′,1′,3′-benzothiadiazole)
PCE — power conversion efficiency
PEG — polyethylene glycol;
PEM — polymer electrolyte membrane
PSC — photovoltaic solar cell
PSVPy — poly(styrene-*co*-4-vinylpyridine)
PTB4 — poly({4,8-bis(n-octyloxy)-benzo[1,2-*b*:4,5-*b*′]dithiophene-2,6-diyl}{3-fluoro-2-[(2-ethylhexyl)-carbonyl]thieno[3,4-*b*]thiophenediyl});
PTB7 — poly({4,8-bis[(2-ethylhexyl)oxy]benzo[1,2-*b*:4,5-*b*′]dithiophene-2,6-diyl}{3-fluoro-2-[(2-ethylhexyl)-carbonyl]thieno[3,4-*b*]thiophenediyl});
PUE — polyurethane elastomer
PVA — polyvinyl alcohol
PVP — polyvinylpyrrolidone
ROS — reactive oxygen species
SPEI — sulfonated poly(ether imide)
TEM — transmission electron microscopy
ThCBM — [6,6]-thienyl-C_{61}-butyric acid methyl ester
TNT-EMF — trimetallic nitride template endohedral metallofullerene
UV — ultraviolet
V_{OC} — open circuit voltage

II. The structure of carbon nano-additives

Among covalent fullerene derivatives, mention should be made of the widely used polyhydroxylated fullerenes (so-called fullerenols) .

Polyhydroxylated fullerenes are fullerene derivatives containing different numbers of hydroxyl groups. After the synthesis, a fullerenol is a complex radical anion of the general formula $Na_n^+[C_{60}O_x(OH)_y]^{n-}$ rather than simply polyhydroxylated C_{60} molecule.[16] Figure 2

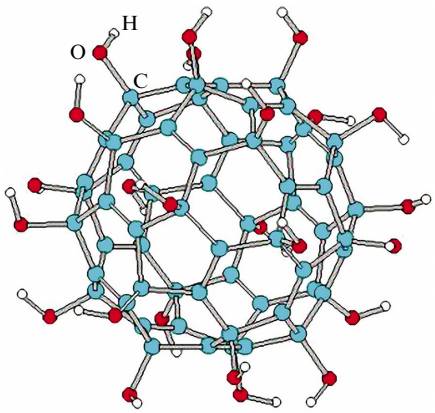


Figure 2. Molecular structure of fullerenol.

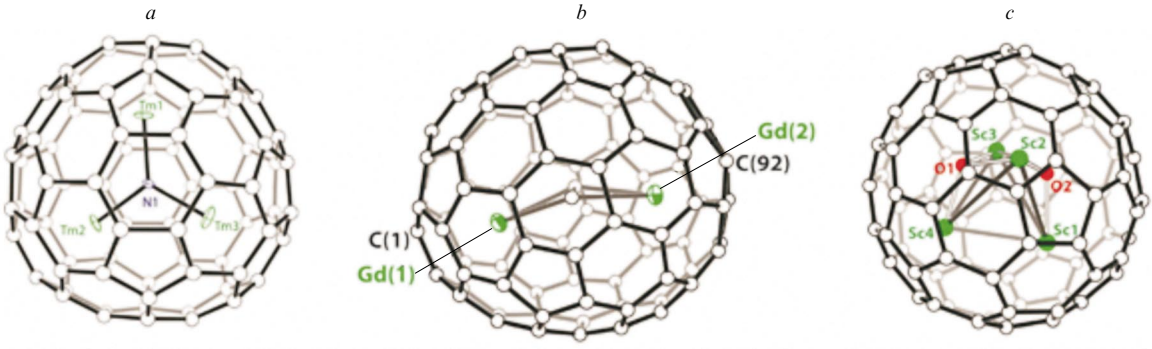


Figure 3. Molecular structures of EMFs containing encapsulated trimetallic nitride $Tm_3N@I_h$-C_{80} (*a*), metal carbide $Gd_2C_2@D_3(85)$-C_{92} (*b*) and a metal oxide cluster $Sc_4(\mu_3\text{-}O)_2@I_h$-$C_{80}$ (*c*).[19]

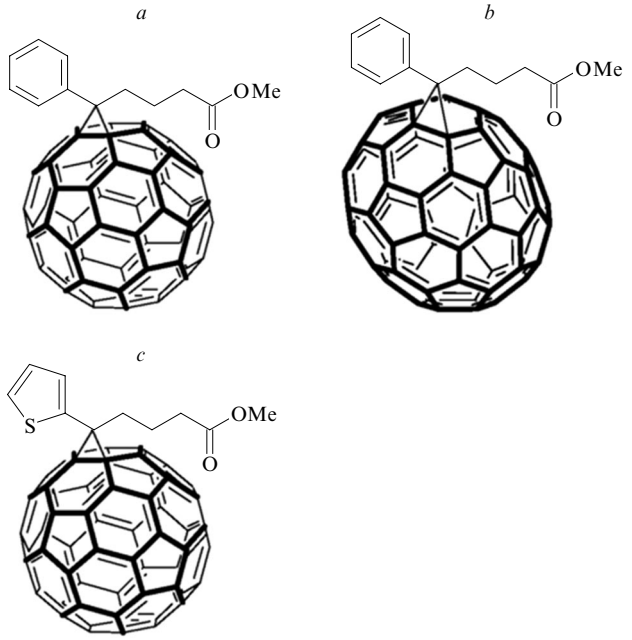


Figure 4. Molecular structures of methanofullerenes PCBM (*a*), $PC_{70}BM$ (*b*) and ThCBM (*c*).

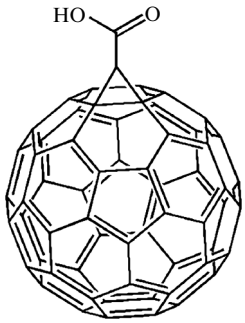


Figure 5. Molecular structure of (1,2-methanofullerene-C_{60})-61-carboxylic acid.

presents the molecular structure of fullerenol.[17] The formula $C_{60}(OH)_n$ corresponds to the structure averaged over a mixture of fullerenols bearing different number of hydroxyl groups, each with its own regioisomers. The solubility of fullerenols depends on the number of hydroxyl groups.

Endohedral metallofullerenes (EMFs) are produced by encapsulating a metal atom (Li, Ca, Sr, Ba, Ti, U, Zr, Hf, Sc, La and other lanthanide atoms, *etc.*) or metal clusters within the fullerene cage. These systems are classified by their inner composition and the size of the carbon cage. Mono- and dimetallofullerenes (*e.g.*, $La@C_{82}$ and $LaR_2R@C_{80}$) have been successfully synthesized, as well as complexes of fullerenes with metal nitrides (*e.g.*, $Sc_3N@C_{2n}$) and more complex species, namely, encapsulated metal carbides (M_nC_2, $n = 2-4$), hydrogenated metal carbides (Sc_3CH), metal nitrogen carbides (M_xNC, $x = 1, 3$), metal oxides (Sc_yO_z, $y = 2, 4$; $z = 1-3$) and metal sulfides (M_2S).[18]

Endohedral metallofullerenes are a new class of compounds combining nanotechnology with organic and inorganic chemistry. Due to unique electronic structure, they have found wide application in various fields. The properties of metallofullerenes are completely different from those of pure fullerene, partially because the interaction between the encapsulated metal atom or cation and fullerene leads to emergence of unique electronic properties. The intrinsic charge transfer from the encapsulated metal atom(s) to the carbon cage, which was predicted theoretically and observed experimentally, can stabilize the fullerenes whose structure does not obey the isolated pentagon rule. The structures of some EMFs are presented in Fig. 3.[19]

Methanofullerenes are fullerenes with a methano bridge (a bond between two six-membered rings; it is present in all the reported methanofullerenes). Figure 4 presents the structures of methanofullerenes that are most widely used as electron acceptors, *viz.*, [6,6]-phenyl-C_{61}-butyric acid methyl ester (PCBM), [6,6]-phenyl-C_{71}-butyric acid methyl ester ($PC_{70}BM$) and [6,6]-thienyl-C_{61}-butyric acid methyl ester (ThCBM).

Carboxyfullerenes are fullerenes functionalized with carboxyl groups and having a methano bridge. A typical example of a carboxyfullerene is (1,2-methanofullerene-C_{60})-61-carboxylic acid (Fig. 5).

III. The applications of fullerene derivatives

III.1. Photovoltaic devices and photocatalysts

The unique combination of physical and chemical properties of carbon nanomaterials including fullerenes has stimulated advanced research in many areas of applied

science.[20–26] One of the most promising areas of research into fullerene derivative is photovoltaics.[27,28] The sun delivers 1368 $W\,m^{-2}$ (so-called solar constant) to our planet. After reflection and absorption by the atmosphere, this value decreases to 198 $W\,m^{-2}$.[29] About 40% of solar radiation is visible light, 10% is UV, and 50% is IR radiation. In total, the yearly solar energy that reaches the planet is approximately 6200 times more than the world's energy consumption in 2008 and 4200 times more than the energy that is expected to be demanded by humankind in 2035 (following the IEA's Current Policies Scenario[30]).

Thus, it takes about 1.5 h for the Sun to cover the year's primary consumption of energy.[31] This fact makes the Sun the largest energy resource on the planet and explains the colossal scientific and technological interest in solar energy. Photovoltaic devices offer an opportunity to convert the solar energy into electricity and electric power.

Organic photovoltaics is considered a very promising technology due to several key advantages, in particular, light weight and flexibility. The low cost of material components and peculiarities of the production process allow easy fabrication of large-area solar cells.[32–34] Fullerenes are characterized by high electron affinities and thus belong to the most important components of organic solar cells. A comparison of third-generation solar cells including organic photovoltaic devices can be found in a detailed review.[27]

III.1.a. Basics of solar cells

Photoinduced charge transfer to fullerenes was for the first time demonstrated in 1992.[35] This was followed by a report about the first photovoltaic cell based on a heterojunction between the semiconducting polymer MEH-PPV (donor) and C_{60} acting as an acceptor.[36] Following the method introduced in Ref. 35, charge transfer from the conjugated polymer MEH-PPV to fullerene can be described within five steps:

excitation of donor

$$D + A \longrightarrow D^* + A$$

delocalization of excitation on the D–A complex

$$D^* + A \longrightarrow (D-A)^*$$

initiation of charge transfer

$$(D-A)^* \longrightarrow (D^{\delta+}-A^{\delta-})^*$$

formation of radical ion pair

$$(D^{\delta+}-A^{\delta-})^* \longrightarrow (D^{+\bullet}-A^{-\bullet})$$

charge separation

$$(D^{+\bullet}-A^{-\bullet}) \longrightarrow D^{+\bullet} + A^{-\bullet}$$

the process of electrical current generation in organic solar cells is schematically shown in Fig. 6.[27,37]

Light absorption in organic solar cells is followed by generation of excitons (bound electron–hole pairs). Their dissociation into two charged counterparts at interfaces between materials with different electron affinities leads to energy conversion. Such dissociation can also be guided by an electric field.

The efficiency of the original bilayer fullerene-based solar cells was limited by the low surface area of heterojunctions. This problem was resolved using fullerene derivatives.[38] The chemically improved solubility of C_{60} in organic solvents was achieved in its modified form, PCBM. This allowed for the creation of a bulk heterojunction (BHJ)-based solar cells where the semiconducting polymer (donor) and fullerene derivative (acceptor) were intermixed, thus providing a larger interfacial area than in the initial bilayer structure. A typical architecture of a BHJ solar cell includes a solvent-cast π-conjugated polymer/fullerene derivative blend film sandwiched between electrodes.[39]

There are many donor polymers currently used for BHJ solar cells.[40,41] Early reports demonstrated high efficiency of bulk heterojunctions. In particular, it was reported that the PCE of solar cells based on a MEH-PPV–PCBM blend is equal to 2.9% and can be further increased to 5.5%.[42] The enhanced efficiency of up to 4.5%–5% for P3HT:PCBM solar cells was achieved through careful control of the growth and morphology of the active layer, reduction of the free volume and the number of trapping sites, as well as improvement of the interfaces and the quality of the contact with electrodes.[43,44]

Solar cells based on poly({4,8-bis(n-octyloxy)-benzo[1,2-*b*:4,5-*b*′]dithiophene-2,6-diyl}{3-fluoro-2-[(2-ethylhexyl)carbonyl]thieno[3,4-*b*]thiophenediyl}) (PTB4)/

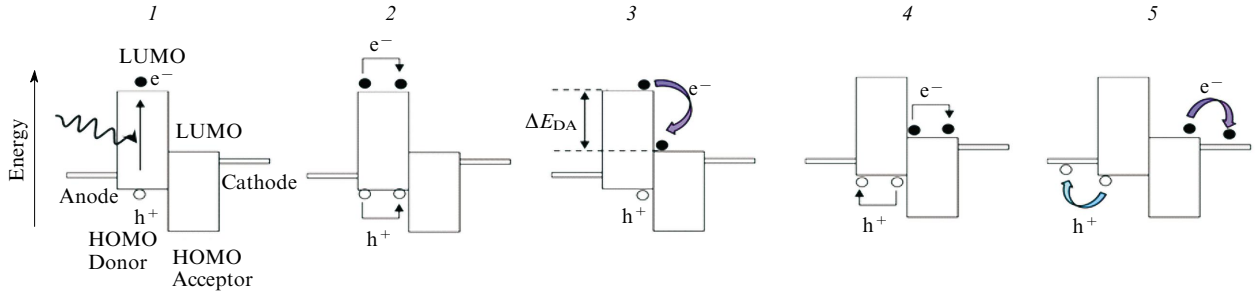


Figure 6. Diagram of the fundamental process of energy conversion.[27]
Light absorption and exciton generation (*1*); diffusion of excitons (*2*); electron transfer from excited donor to acceptor at the donor-acceptor interface (ΔE_{DA} is the LUMO energy difference between the donor and acceptor, or the donor/acceptor LUMO offset) (*3*); negative charge carriers in the acceptor and positive charge carriers in the donor diffuse and/or drift by hopping to neighbouring molecules (*4*); and collection of charges at the electrodes and subsequent transfer to the external circuit (*5*).
Electrons and holes are denoted as e^- and h^+, respectively.

PCBM have a PCE of up to 6.1%; here, the newly developed polymer with higher hole mobility and miscibility was used to achieve better interpenetration with the fullerene derivative.[45] The electrical properties of fullerene derivatives and their influence on the photovoltaic performance have been studied.[46–48] Compounds $PC_{70}BM$ and ThCBM are also often used as acceptors in photovoltaic devices.[28,49]

Limitations on the efficiency of PCBM-based solar cell were studied[50] using poly({4,8-bis[(2-ethylhexyl)-oxy]benzo[1,2-*b*:4,5-*b*′]dithiophene-2,6-diyl}{3-fluoro-2-[(2-ethylhexyl)carbonyl]thieno[3,4-*b*]thiophenediyl}) (PTB7) as donor polymer. It was shown that the main factor influencing the device performance is the relatively poor electron mobility due to inefficient formation of the PCBM network within the blend. The microstructure of polymer–fullerene derivative blends was studied using energy-filtered transmission electron microscopy (TEM) and photoluminescence quenching. It was proposed to tune the PCBM phase connectivity for a significant increase in the solar cell efficiency without improving the hole mobility in the polymer. Also, the role of the solvent additive (1,8-diiodooctane, DIO) was investigated and it was shown that DIO reduces the geminate recombination probability.

Currently, PCBM-based solar cells are still considered among the most efficient ones. The well-known advantage of PCBM is good solubility in many organic solvents. However, weak absorption of PCBM in the visible region[21] due to high symmetry of the molecule, which makes the lowest-energy transitions formally dipole forbidden, motivates further development of fullerene derivatives, which could absorb solar energy more effectively.

A higher fullerene analogue of PCBM based on C_{70}, $PC_{70}BM$ (see Fig. 4 *b*), exhibits enhanced light absorption in the visible region.[51] Solar cells based on $PC_{70}BM$ provide more effective light absorption in the UV and visible regions compared to the PCBM-based cells and a PCE improvement up to 10%. Liang *et al.*[52] compared the efficiency of solar cells using a donor polymer based on alternating thieno[3,4-*b*]thiophene and benzodithiophene units (PTB1) and PCBM and $PC_{70}BM$ as acceptors. The device based on the higher fullerene derivative demonstrated enhanced external quantum efficiency (EQE) in the wavelength range from 400 to 750 nm, with a maximum of 67% at 650 nm. For the PCBM-based solar cell, the maximum EQE was ~60% at the same wavelength. The corresponding PCE values were 5.6% and 4.76%, which confirms the significant role of $PC_{70}BM$ in the improvement of the solar cell performance without additional engineering treatment.

A PCE of 6.1% was reported for PCDTBT : $PC_{70}BM$ solar cells.[53] An extremely high internal quantum efficiency almost corresponding to 'one absorbed electron–one pair of charge carriers' was achieved through the optimized ratio of the polymer and $PC_{70}BM$.[53]

The difference in the shape of PCBM and $PC_{70}BM$ molecules (sphere *vs.* ellipsoid with an aspect ratio of the fullerene moiety of 1.14)[54] leads to a discrepancy in the molecular packing of these fullerene derivatives and consequently to different, orientation-dependent intermolecular electronic coupling. Molecular dynamics simulations revealed an apparent difference in the formation of a layer of the nearest neighbours including their distribution, the number of molecules in the shell and the distance to the neighbouring molecules. All these parameters specify the electronic coupling and properties of fullerene aggregates.

The stability of photovoltaic devices based on PTB7:$PC_{70}BM$ and possible ways to protect the solar cell against degradation and to increase its lifetime using additional optically active layers were explored.[55] The influence of the molecular mass (M_n) of polymer and the solvent additive (1-chloronaphthalene, CN) on the performance efficiency of a $PC_{70}BM$-based solar cell was studied[56] using poly[di(2-ethylhexyloxy)benzo[1,2-*b*:4,5-*b*′]-dithiophene-*co*-octylthieno[3,4-*c*]pyrrole-4,6-dione] (PBDTTPD) as donor polymer. It was found that low molecular mass of PBDTTPD resulted in poor efficiency mostly because of the phase separation of the polymer and fullerene derivative and the formation of $PC_{70}BM$-enriched domains, which was avoided in the case of the high-M_n polymer. That study[56] and several similar publications[57,58] have demonstrated that the correlation between the BHJ solar cell performance and the molecular mass of the donor polymer may appear to be a promising method for optimization of the solar cell morphology and design of highly efficient structures.

Enhanced performance of a photovoltaic device can be achieved using solvent additives.[59,60] A study of a solar cell based on PTB7:$PC_{70}BM$ with the DIO and 1,8-dibromooctane additives revealed an increase of almost 150% in PCE (from 2.74% to 6.76%) in comparison with the initial devices fabricated without additives.[61] Improved charge transport and charge collection efficiency, as well as more effective light absorption in the blended solar cell with additives are the main factors responsible for the PCE enhancement.[62] Formic acid (FA) was also suggested[63] as a novel additive to improve the performance of a PTB7:$PC_{70}BM$ solar cell and to increase the short circuit current J_{SC}. A significant increase in J_{SC} from 14.57 to 24.11 mA cm^{-2} upon the addition of FA was attributed to enhanced charge carrier mobility, enhanced light absorption and more effective exciton generation.

High PCE values have recently been reported for photovoltaic devices based on $PC_{70}BM$ and new molecular donors. Sun *et al.*[64] presented a benzodithiophene terthiophene rhodanine (BTR) with benzo[1,2-*b*:4,5-*b*′]dithiophene core and rhodanine peripheral moieties as a new thermally stable material for roll-to-roll techniques in large-scale production of organic solar cells. Photovoltaic devices based on BTR:$PC_{70}BM$ demonstrated an efficiency of up to 9.3% with a fill factor (FF) of 77%. Strong intramolecular interactions in BTR, which determine the liquid-crystalline properties of the material, also provide very high hole mobility, resulting in the record high value of PCE.

Another example of outstanding efficiency of $PC_{70}BM$-based solar cells was shown by He *et al.*[65] They used a newly synthesized, narrow-band-gap semiconducting polymer poly{[2,6′-4,8-di(5-ethylhexylthienyl)benzo[1,2-*b*;3,3-*b*]dithiophene][3-fluoro-2[(2-ethylhexyl)carbonyl]thieno[3,4-*b*]thiophenediyl]} (PTB7-Th). Compared to PTB7, PTB7-Th has a narrow band gap of 1.59 eV and its highest occupied molecular orbital (HOMO) level lies 0.07 eV deeper (at −5.22 eV); also,

the new polymer strongly absorbs between 500 and 800 nm. These results looked very promising, and the expectation of better performance of the new donor in combination with $PC_{70}BM$ was confirmed experimentally. The parameters of the fabricated device were $V_{OC} = 0.815$ V, $J_{SC} = 17.52$ mA cm^{-2}, FF = 72% and PCE = 10.28%.

Since the same research group earlier reported an efficiency of 9.15% for a PTB7-$PC_{70}BM$ solar cell,[66] the success of tuning V_{OC} and photocurrent in the $PC_{70}BM$-based device by deepening the lowest unoccupied molecular orbital (LUMO) level and narrowing the polymer band gap was justified. A recent study[67] showed that long-term photostability of organic solar cells based on PTB7-Th can be improved by removing the residual solvent (DIO) required to cast the polymer – fullerene blend film.

Highly efficient BHJ solar cells based on a mixture of PTB7 and $PC_{70}BM$ dissolved in *o*-xylene were reported.[68] The possibility of designing solar cells using non-chlorinated and, therefore, less toxic solvents (*e.g.*, xylene) is of high priority in the development of photovoltaic devices for common consumption.[69]

There are reports on interesting ways to use fullerene as a dopant in the active layers of photovoltaic devices. For instance, an impressive improvement of the PCE of an inverted PTB7-Th:$PC_{70}BM$ polymer solar cell from 7.64% up to 9.35% was achieved when the ZnO cathode was modified with [6,6]-phenyl-C_{61}-butyric acid hydroxyethyl ester (PCBE-OH).[70] The modified ZnO – C_{60} cathode enhances the electron collection and electronic conductivity at the interface and in the bulk of the cathode.

The further increase in the size of fullerene derivatives entailed the synthesis of $PC_{84}BM$.[71] In spite of more efficient light absorption (extended to near-IR region) and electron mobility observed in C_{84},[27,72] this fullerene derivative has not found practical application in the BHJ solar cells due to low solubility, weak photocurrent and increased recombination of charge carriers.[71] A comparison of the absorption spectra of three methanofullerenes is presented in Fig. 7. Recently, the role of $PC_{84}BM$ impurities in the polymer BHJ solar cells was explored in charge trapping and trap-assisted recombination.[73,74] The Shockley – Read – Hall recombination from inorganic material (through a single defect state in the energy gap) was shown to be significantly affected by $PC_{84}BM$ traps in the active layer of the solar cell. Experiments with BHJ solar cells composed of a copolymer of PCDTBT with PCBM showed that all characteristics of the photovoltaic devices decreased upon the addition of $PC_{84}BM$. Femtosecond transient absorption spectroscopy measurements were performed to study the decay dynamics of polarons. Measurements revealed increased polaron trapping and trap-induced recombination. This conclusion was confirmed in a more recent study[75] where the photophysical processes associated with impurities were analyzed and compared with the results obtained upon doping with $PC_{84}BM$ and 7,7,8,8-teracyanoquinodimethane (TCNQ).

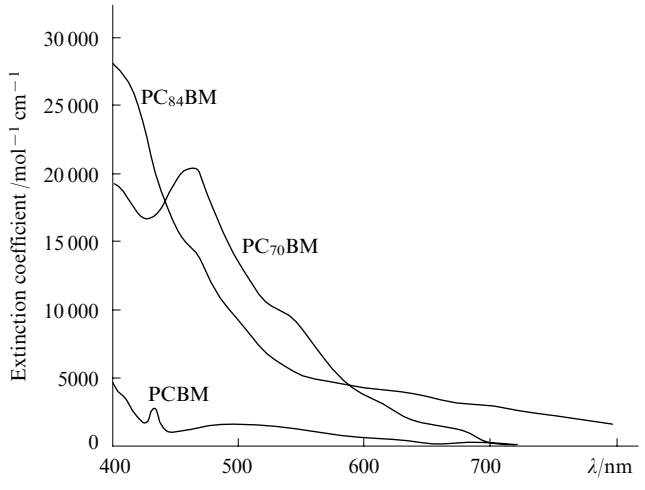


Figure 7. Absorption spectra of various methanofullerenes.[27]

The PCBM-like thienyl-containing fullerene derivative ThCBM (see Fig. 4*c*) was developed for better polymer-to-fullerene conformity in photovoltaic devices.[76]

A higher efficiency of organic photovoltaic cells can be obtained by increasing J_{SC} and V_{OC}. The modification of active layers in photovoltaic devices was successfully used for developing short circuit current.[77,78] In particular, the increase in J_{SC} can be reached by enhancing the optical absorption upon symmetry reduction of the fullerene core.[79]

The V_{OC} value of a solar cell depends on the energy difference between the donor HOMO and the acceptor LUMO.[80–82] For efficient exciton dissociation and electron transfer from donor to acceptor, the LUMO of the donor should lie 0.3 – 0.5 eV higher than that of the acceptor.[83,84] In a typical organic photovoltaic cell based on regioregular P3HT and PCBM, this energy difference is 1.17 eV, which is much higher than the desirable value and, consequently, leads to a suppression of V_{OC}. The difference between the LUMO energies can be decreased by lowering the donor LUMO[85] or by raising the acceptor LUMO,[86] both ways being theoretically promising.[87] In the former case, the photocurrent increases due to enhanced overlapping between the donor absorption spectrum and the solar spectrum.[88] In the latter case, V_{OC} increases directly since it is proportional to the energy difference between the fullerene LUMO and the polymer HOMO.

The further optimization of fullerene derivatives was proposed in a series of reports[89–94] where the bisadduct analogues of PCBM, ThCBM and other fullerene derivatives were introduced as new fullerene-based high-LUMO semiconductors for organic photovoltaics (Fig. 8). Since the synthesis of PCBM-like fullerene derivatives affords a mixture of mono- and multiadducts, the desired fractions can be separated by column chromatography.

In an early study, an increase of up to 100 meV (corresponds to −3.7 eV) in the LUMO level of bis-PCBM was reported. Compared to the P3HT:PCBM solar cell, the PCE increased by almost 20% up to 4.5% due to V_{OC} enhancement. Higher fullerene adducts were experimentally studied using photovoltaic cells based on P3HT as donor.[90] Despite relatively high V_{OC} values obtained by shifting the LUMO level, the PCE was found to be the same as that of the PCBM-based

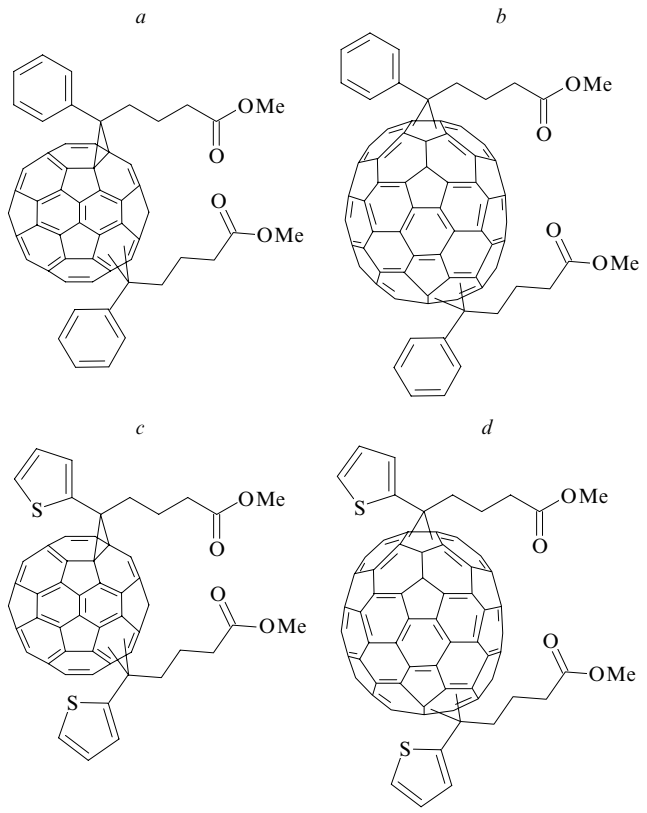


Figure 8. Fullerene bisadducts: bis-PCBM (*a*), bis-$PC_{70}BM$ (*b*), bis-ThCBM (*c*) and bis-$ThC_{70}BM$ (*d*).[90]

solar cell or even lower. This was explained by the reduced electron mobility and lower J_{SC} in the devices based on the bisadducts.

Later, Liu *et al.*[95] tested the influence of bis-PCBM substitution on the stability and performance of P3HT:PCBM solar cells and found that this bisadduct can be successfully used as an inhibitor of phase separation, providing high miscibility of the fullerene derivative and the polymer. The PCE of the device based on bis-PCBM was surprisingly stable against thermal ageing (150 °C at 15 h).

Polymer solar cells based on PBDTBDD:bis-PCBM with an efficiency of 6.07% were studied.[96] The optimized mass ratio of the polymer and fullerene derivative, as well as treatment with DIO were the key factors in reaching high values of PCE, V_{OC} (1.00 V), J_{SC} (10.02 mA cm^{-2}) and a fill factor of 60.54% through the efficient exciton dissociation and charge separation.

A detailed comparison of solar cells based on different fullerene derivatives including bis-PCBM and $PC_{70}BM$ using neutron reflectivity experiments was performed by Chen *et al.*[97] The main parameter addressed in this study was the miscibility of different acceptors and its influence on the morphology of photovoltaic devices. It was shown that, depending on the miscibility of fullerene, the size of domains and interfacial area in the blended films based on bis-PCBM affect the resulting exciton dissociation and charge transport, being the limiting factors for the photovoltaic device performance. Chen *et al.*[97] also determined the surface-to-surface distance between adjacent fullerene derivatives that was considered sufficient for the recombination process. Earlier, a comparison of parameters of solar cells based on $PC_{70}BM$- and bis-$PC_{70}BM$ and the influence of intercalation in the case of poly{2,5-bis(3-hexadecylthiophen-2-yl)thieno[3,2-*b*]thiophene} (pBTTT) was reported.[98]

Methanofullerenes ThCBM and bis-ThCBM were introduced as acceptors for solar cells based on P3HT.[99] The efficiency of the ThCBM-based devices was comparable with that of PCBM-based ones (3.97% *vs.* 4.18%, respectively), whereas the maximal efficiency of the device based on bis-ThCBM was only 1.72% in spite of higher V_{OC} provided with the raised LUMO energy level.

A review of the state of the art in application of fullerene bisadducts is available.[100]

Vandewal *et al.*[101] suggested to increase the V_{OC} of polymer-fullerene solar cells by controlling the spectral position of the charge-transfer band[102] and changing the electronic coupling between donor and acceptor materials; the latter was demonstrated by Thompson and co-workers.[103] Using PCBM and $PC_{70}BM$-based solar cells, Vandewal *et al.*[101] revealed a correlation between electroluminescence and the photovoltaic EQE spectra in the charge-transfer region, which opens an additional pathway to tune the generated V_{OC}.

To find an alternative way to reach a higher PCE is a challenging task, which can be solved by increasing the fill factor. Inverted BHJ solar cells based on $PC_{70}BM$ and new in-chain donor – acceptor polymers with close π – π-stacking demonstrated a fill factor up to 80%.[104]

A relatively new approach to achieve higher electron mobility and PCE is to prepare hybrid inorganic-organic nanocomposites containing metal nanoparticles and nanowires. Enhanced functionality achieved through an increase in electron mobility was reported for the hybrid materials composed of gold nanowires and ThCBM (Fig. 9).[105]

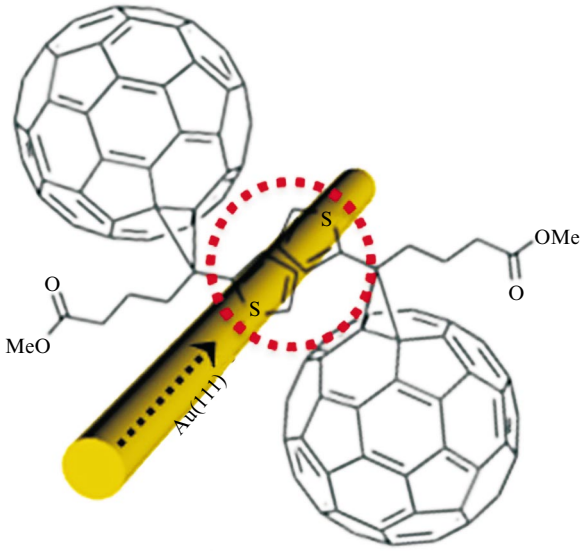


Figure 9. Hybrid nanocomposite composed of Au nanowire and ThCBM (n-type semiconductor).[105]

Semiconducting molecular nanowires (in particular, MoSI) were used to improve the P3HT:PCBM solar cell efficiency.[106] Increased hole mobility and good transport properties of nanowires resulted in 52% enhancement of PCE. Moreover, it was found that adding MoSI nanowires on top of the active layer extends the absorption spectrum of the active layer, thus providing an additional way to tune the conversion of photons to electric current.

Semiconducting single-walled nanotubes (SWNT) were shown to be promising additives for use in organic solar cells.[107] Doping of a solar cell based on regioregular P3HT and PCBM with semiconducting SWNT resulted in not only enhanced hole mobility in the fullerene-polymer blend, but also improved thermal stability of the device.

Recently, Zhang *et al.*[108] demonstrated the spin enhancement of organic BHJ PSC doped with spin 1/2 radicals. Recombination of polaron pairs appearing as a result of the separation of excitons at donor/acceptor interfaces can be effectively suppressed using a π-conjugated radical galvinoxyl (2,6-di-*tert*-butyl-4-[(3,5-di-*tert*-butyl-4-oxocyclohexa-2,5-dien-1-ylidene)methyl]-phenoxyl). Spin 1/2 radicals resonantly induced the spin-flip process of electron acceptor *via* an exchange mechanism, converting the polaron pair from spin singlet to triplet and enhancing its separation into free charges. The PCE of PCBM-based solar cells increased by almost 340%, which clearly shows the benefits of this approach. Remarkably, the enhancement of the photovoltaic performance was observed only for PCBM, whereas neither bis-PCBM nor indene-C_{60} bisadduct (ICBA) demonstrated a similar response to doping with spin 1/2 radicals.

Efforts are now aimed at better understanding of the process of charge separation and hopping type transport in organic photovoltaic solar cells with a focus on the electron spin dynamics.[109 – 111] A BHJ is highly disordered system where materials with different properties are intermixed, and this affects the generation and dynamics of charge-transfer states.[112]

Predominant formation of singlet charge-transfer states was studied recently using electron paramagnetic resonance (EPR).[113, 114] The evolution of the EPR spectra of polymer-fullerene blends based on P3HT, PCDTBT, PTB7 and PCBM was followed using the time-resolved technique. A correlation between the lifetime of the intermediate radical pairs and the delocalization length of the hole along the polymer chains was revealed. The effect might be due to a stronger Coulomb interaction between separated charges, leading to the stable state of the radical pair. Stabilization of such pairs is an intermediate step in electron transfer mediated by hopping between electron acceptors and formation of charge-separated states.[115]

The possibility of fullerene dimerization opens the way of designing new types of acceptors for PSCs.[116] Despite the fact that PCBM-based dimer containing hydroxyl groups demonstrated lower photovoltaic response,[117] covalent aggregation of fullerenes can significantly improve the final device efficiency.[118] It was shown[119] that a PSC based on P3HT and a PCBM derivative with the dumbbell-shaped structure[120] has a higher PCE (3.7%) compared to the PCBM-based device (3.22%). Interestingly, the LUMO energy level of the dimeric fullerene derivative remained nearly the same as that of PCBM. The increase in efficiency was due to the significant enhancement of J_{SC} to 10.34 mA cm^{-2} for the solar cell based on the dumbbell-shaped dimer from 8.45 mA cm^{-2} for a standard solar cell based on PCBM.

Morinaka *et al.*[121] performed a detailed study on the influence of (i) fullerene dimerization and (ii) structure of the dumbbell-shaped fullerene C_{60} derivatives on the solar cell efficiency. Two fullerenes linked at *para*- and *meta*-position of the phenyl ring were synthesized and the photovoltaic properties of the P3HT- and PTB7-based solar cells were investigated. The authors demonstrated an important role of the molecular structure of the dimers in achieving high J_{SC} and FF values and in tuning the morphology of the active layer. A PCE of 6.14% was reported for the solar cell based on PTB7 (donor) and the *para*-linked dumbbell-shaped dimer (acceptor), which is comparable with a PCE of 6.24% obtained for PCBM.

Ongoing research activity and a better understanding of the physics behind the performance control of polymer solar cells has led to progress in the development and design of highly efficient devices. Among them, molecular solar cells[122, 123] and tandem (multiple junction) solar cells[124, 125] with efficiencies over 10% can be specified. Great efforts are being undertaken to create novel types of acceptors, *viz.*, methanofullerene derivatives[126, 127] and others.[128] An extensive review of recent progress in the field is available.[129]

III.1.b. Metallofullerenes

Trimetallic nitride template endohedral metallofullerenes (TNT-EMFs). Endohedral metallofullerenes[130, 131] are fullerene C_{60} derivatives with encapsulated metal atoms. They look promising for photovoltaic applications since they are materials with the LUMO level shifted closer to the HOMO level of the polymer acting as donor.[132] Good examples of metallofullerenes are provided by the nitrides TNT-EMFs $M_3N@C_{80}$ (M = Sc, Y, Gd, Tb, Dy, Ho, Er, Tm, Lu) in which the metal is bound.[133, 134]

There are several reports on TNT-EMFs used as electron acceptors in polymer conjugates. The thermal stability and photophysical properties of the $Sc_3N@I_h$-C_{80} and $Y_3N@I_h$-C_{80} dyads blended with triphenylamine (TPA), ferrocene (Fc), extended tetrathiafulvalene (exTTF) and phthalocyanine (Pc) have been studied and compared with C_{60}-based analogues by Pinzon *et al.*[135, 136] It was found that photoinduced charge separated states have a longer lifetime in the case of the $Sc_3N@I_h$-C_{80} derivative.

A photoinduced electron-transfer reaction in the $Sc_3N@C_{80}$-Fc donor-acceptor dyad[138] was reported.[137] *N*-methyl-2-ferrocenyl[5,6]-$Sc_3N@I_h$-C_{80}-fulleropyrrolidine was prepared by thermal reaction of $Sc_3N@I_h$-C_{80} with sarcosine and ferrocenecarboxaldehyde in a toluene/*o*-dichlorobenzene (*o*-DCB) mixture. Cyclic voltammograms revealed three one-electron reversible reduction peaks at −1.14, −1.53 and −2.25 V. The radical ion pair state was found to be more stable than that for an analogous C_{60} – Fc derivative. Additionally, the charge-separation and charge-recombination dynamics were followed by time-resolved transient absorption spectro-

scopy in order to demonstrate the potential of TNT-EMFs in organic photovoltaics.

New metallofullerene derivatives $M_3N@PC_{80}BM$ (M = Y, Sc), analogues of PCBM, were synthesized and studied[139] and their importance for BHJ solar cells was demonstrated. The synthesis and electrochemical properties of a large family of TNT-EMFs $M_3N@C_{2n}$ (M = Gd, Ce, Pr, Nd; $2n$ = 80, 82, 84, 86, 88) were reported.[140] The influence of the carbon cage symmetry and size on the electrochemical properties of fullerenes were investigated and it was concluded that the LUMO is localized on the metallic cluster while the HOMO is localized on the carbon cage. Due to the intrinsic stability and unique properties of TNT-EMFs, they can be considered as candidates for many applications besides photovoltaics, *e.g.*, as contrast agents for magnetic resonance imaging (MRI).

First synthesized by Ross *et al.*,[86] $Lu_3N@C_{80}$ derivatives revealed better performance in P3HT-based organic solar cells as compared with an analogous P3HT:PCBM-based device, namely, the higher LUMO provided a higher V_{OC}. An important role of the donor/acceptor LUMO offset tuning approach in organic photovoltaic devices based on metallofullerenes and narrow-band-gap donor polymers was demonstrated. The PCE and V_{OC} values for the 1-[3-(hexyloxycarbonyl)propyl]-1-phenyl-[6,6]-$Lu_3N@C_{81}$ system ($Lu_3N@PC_{80}BH$) reached up to 4.2% and 890 mV, respectively. Remarkably, due to the increased size of this EMF, the optimum blend ratio of P3HT and $Lu_3N@PC_{80}BH$ was 50 mass% of fullerene loading, which is not the same for the C_{60}-based analogue.[132]

Later, an organic solar cell based on $Lu_3N@C_{80}$ was investigated in terms of the influence of the metallofullerene on the simultaneous reduction of photocurrent J_{SC}.[141] The reasons responsible for the decrease in J_{SC} were analyzed using photoluminescence and photoinduced absorption techniques and it was found that the formation of triplet molecular excitons and corresponding intramolecular electron transfer may decrease the efficiency of the solar cells. The existence of triplet excitons was also proved using photoluminescence-detected magnetic resonance where the triplet in the resonance spectra quenched by charge transfer in the blends with PCBM appears in the case of a blend based on $Lu_3N@C_{80}$.

The dual role of EMFs in bulk heterojunctions was shown by Feng *et al.*[142] in a study on fullerene bonding to electron acceptors in solar cells taking a conjugate of a [6,6]-phenyl-C_{81}-butyric acid derivative $Lu_3N@PC_{80}BM$ (electron donor) with 1,6,7,12-tetrachloro-3,4,9,10-perylenediimide (PDI) as an example. PDI is known for its light-harvesting electron-accepting properties. Using femtosecond transient absorption spectroscopy, photoinduced electron transfer from the ground state of $Lu_3N@C_{80}$ to the excited state of PDI was observed, which is opposite to what occurs when C_{60}–PDI is used. This example demonstrates that there are many new interesting aspects in the application of metallofullerenes in organic photovoltaics to be explored.

Metallofullerenes of the general formula $Me@C_{2n}$. The interest in metallofullerenes in organic photovoltaics is not limited to TNT-EMFs. Fujii *et al.*[143] studied the optical and photovoltaic properties of $La@C_{82}$ and reported about photoinduced charge transfer in P3HT–$La@C_{82}$ composite films. They demonstrated the enhancement of photocurrent upon introducing a small amount of $La@C_{82}$ into the polymer, which points to a significant role of metallofullerenes in highly efficient photoinduced charge separation. A positive effect of doping with $Dy@C_{82}$ on the photocurrent in a photovoltaic solar cell based on P3HT caused by photoinduced electron transfer between donor and acceptor was reported by Yang *et al.*[144,145] Using atomic force microscopy (AFM) and absorption measurements, they investigated the optimal composition of the polymer : $Dy@C_{82}$ film and revealed the formation of a $Dy@C_{82}$ segregated phase in the case of metallofullerene excess in the film. More recently, successful incorporation of $Dy@C_{82}$ into polythiophene (PT) was demonstrated.[146]

Stable conjugates based on $La_2@I_h$-C_{80} and exTTF were reported by Takano *et al.*[147] The electronic interaction between the polymer and fullerene molecules in the ground state was found to be relatively weak. However, rapid formation of a radical ion pair state of $La_2@C_{80}^{-\bullet}$-$exTTF^{+\bullet}$ with a lifetime of 3260 ps was observed using transient absorption spectroscopy in the visible and near-IR regions.

An interesting case of charge transfer in a donor-acceptor conjugate $Ce_2@I_h$-C_{80}-ZnP (ZnP is zinc tetraphenylporphyrin) was studied by Guldi *et al.*[148] They revealed different strength of electronic coupling affecting the charge transfer kinetics of radical ion pairs in the conjugates. Reductive charge transfer [formation of $(Ce_2@I_h\text{-}C_{80})^{-\bullet}$-$(ZnP)^{+\bullet}$] was found to dominate in nonpolar media (toluene, THF), whereas oxidative charge transfer [formation of $(Ce_2@I_h\text{-}C_{80})^{+\bullet}$-$(ZnP)^{-\bullet}$] dominated in polar media (benzonitrile, DMF). This work demonstrated the possibility to use EMFs as electron donors and opened a new and intriguing direction of employing fullerene derivatives in photovoltaics.

Currently, the application of metallofullerenes in photovoltaics is not yet clear. However, numerous reports have already demonstrated that these fullerene derivatives seem to be more promising than conventional fullerenes commonly used in organic solar cells. One of the stumbling blocks towards applying these unique materials in photovoltaics and realization of operating devices are the difficulties associated with their synthesis.

Novel strategies for the chemical synthesis of metallofullerenes are an important area of research. A recently proposed methodology is the bottom-up formation of the $M@C_{2n}$ (M is metal; $2n$ = 44, 50, 60, 70, 80, 90) EMFs from metal-doped graphite.[149] Metallofullerenes were produced from graphite–metal oxide mixtures containing up to 2% of incorporated metal by pulsed evaporation using a Nd:YAG laser.

III.1.c. Photocatalysis

Fullerene derivatives are being actively investigated in the context of photocatalytic applications. The oxides TiO_2 and ZnO commonly used in photocatalysis are inefficient in the visible region due to their wide band gaps. Sensitization by visible light absorbing fullerene

derivatives through the charge transfer mechanism[150] is a way to solve the problem.[151–153]

Photocatalytic activity of PCBM-modified TiO_2 was studied by Liu *et al.*,[154] who showed that photodegradation of dyes under visible light irradiation significantly enhanced upon adsorption of PCBM on the surface of TiO_2 photocatalyst. A TiO_2 powder was mixed with PCBM sonicated in toluene and stirred. Then, the solvent was evaporated. The fullerene derivative acted as a shuttle transferring photoexcited electrons from the conduction band of TiO_2 to the surface to take part in the surface reactions. Consequently, efficient separation of electron–hole pairs was achieved.

Oh *et al.*[155] reported two composite photocatalysts, C_{60}/TiO_2 and $V-C_{60}/TiO_2$, with enhanced photogenerated electron transfer. The photocatalytic efficiency of the composites was evaluated taking degradation of methylene blue in water under UV irradiation as an example. Homogeneous aggregation of fullerene in TiO_2 aggregates was confirmed by scanning electron microscopy. Such homogeneity was supposed to lead to the positive combination effect with increasing degradation rate. Fullerene C_{60}-modified TiO_2 was tested as photocatalyst taking the degradation of salicylic acid in aqueous solution and gaseous formaldehyde under UV light as examples.[156] The efficiency of electron–hole pair separation and consequently the photocatalytic activity was enhanced due to a decrease in the charge recombination rate in the presence of C_{60}.

Polyhydroxyfullerene (fullerenol) $C_{60}(OH)_x$ is attractive for photocatalytic applications since this fullerene derivative is water soluble, biocompatible, biodegradable and spontaneously forms nanocomposites with TiO_2 without the requirement of expensive technological treatment (*e.g.*, sol–gel process). In particular, fullerenol $C_{60}(OH)_x$ was used to activate TiO_2 in the visible region through the surface–charge-transfer complex mechanism, where the electrons are photoexcited from the adsorbate ground state (HOMO) to the semiconductor conduction band.[151]

A model for the formation of surface complexes and charge transfer proposed by Park *et al.*[151] assumes that absorption of visible light is mediated by the formation of covalent bonds between the titanol group $\equiv Ti-OH$ and fullerenol similarly to the case of phenolic compounds $OH-C_6H_4X$:

$$\equiv Ti-OH + HO-C_{60}(OH)_{x-1} \longrightarrow$$

$$\longrightarrow \equiv Ti-O-C_{60}(OH)_{x-1} + H_2O$$

Importantly, fullerenol molecules bearing multiple hydroxyl groups can be gripped to the titania surface through oxygen linkages. Absorption of visible light leads to direct excitation of electrons from the fullerenol HOMO to the oxide conduction band without involving the excited state of fullerenol. The resulting radical cation undergoes recombination, thus causing one of the limitations on the efficiency of the photocatalytic process. The application of fullerenol to photocatalysis in the visible region for the reduction of Cr^{VI}, degradation of 4-chlorophenol (4-CP) and H_2 generation was successfully proved in another study.[151]

An interesting example of combined bulk and surface modification of TiO_2 with fullerenol was reported.[157] The surface adsorption of $C_{60}(OH)_x$ was used for photosensitization of titania. Also, the 'bulk' Nb-doping was initially applied to increase the electron concentration and transport efficiency due to the charge compensation as a result of Nb-substitution of Ti ions.[158] The photocatalytic properties were tested using the photoinduced oxidation of 4-CP and iodide to triiodide as well as photoreduction of Cr^{VI}. The visible light photocatalytic performance of fullerenol/Nb-TiO_2 nanoparticles was found to be higher than in the case of non- or single-modified (through either Nb-doping or fullerenol sensitization) samples. The improvement of efficiency was described as being due to the synergistic effect of the modification with fullerenol and Nb-doping causing the formation of defects. The latter reduced the electron transfer from fullerenol and charge recombination.

Fullerenes and their derivatives can be used for application in oxidative damage in biological objects and cellular systems as ROS through photosensitization involving UV or visible light.[159,160] Fullerene C_{60} and $C_{60}(OH)_{18}$ have the potential to damage biological membranes in both hepatic and tumour microsomes *via* the action of $^1O_2$ and other radical species, respectively.[161]

Enhancement of UVA-photocatalytic performance of a fullerenol/TiO_2 nanocomposite in transparent antimicrobial coatings was demonstrated.[162] A comparison of the organic dye degradation and fungal spore inactivation kinetics on the photocatalytic and non-photocatalytic surfaces revealed a significant increase in the rate of both processes. Optimization tests made it possible to determine the most efficient fullerenol/TiO_2 ratio in the nanocomposites studied when the titania surface becomes saturated with the functionalized fullerene.

The enhanced photocatalytic activity of titanium dioxide modified with fullerenol was studied by Krishna *et al.*[163,164] It was shown that the fullerenol additives enhance the hydroxyl radical generation and degradation of Procion red dye which is accelerated by a factor of up to 2.6. The rate of inactivation of *Escherichia coli* was found to be almost two times higher for the modified TiO_2. The authors also discussed the potential of fullerenol as a scavenger of hydroxyl radicals, which were expected to decrease the efficiency of photocatalysis, and concluded there would be a limited role of $C_{60}(OH)_x$ as a scavenger due to the short lifetime of the hydroxyl radical. However, fullerenol can successfully scavenge the photogenerated electrons from titanium dioxide, which leads to faster generation of the $^{\bullet}OH$ radicals.

It was proposed to use fullerene derivatives for photosensitive ROS generation and subsequent inactivation of MS2 bacteriophage under UV irradiation.[165] The production of singlet oxygen $^1O_2$ and superoxide radical anion $O_2^{-\bullet}$ (key factors of MS2 inactivation) by fullerenol in these conditions was confirmed by EPR and reduction of nitrotetrazolium blue.

Brunet *et al.*[166] tested the ROS production in aqueous suspensions of fullerenol and a complex of PVP with fullerene C_{60} and compared it with nano-TiO_2. They found more efficient $^1O_2$ generation by the hydroxylated and polymer-coated fullerenes. However,

no hydroxyl radical production was detected in both cases.

The efficiency of novel fullerene C_{60} derivatives for photocatalytic applications including antimicrobial was shown to be higher than that of fullerenol.[167] Four NH_3^+-, CO_2H- and OH-terminated multi-functionalized fullerene C_{60} derivatives were synthesized using high-purity C_{60} and malonate analogues. These materials exhibit unique photochemical properties, especially in photoinduced bacterial and virus inactivation. These agents had a much higher efficiency as compared with fullerenol and TiO_2. Interestingly, the lifetime of the triplet states of the functionalized C_{60} derivatives was comparable with that of pristine C_{60} samples and much longer than that of fullerenol. Such intrinsic energy transfer is responsible for efficient $^1O_2$ production by these derivatives in water despite the formation of large particles due to aggregation.

The photocatalytic properties of fullerenes are of interest for hydrogen energetics. The photoelectrochemical activity of n-type organic semiconductors based on PCBM and 3,4,9,10-perylenetetracarboxylic dianhydride (PTCDA) was studied.[168] Three-layer PTCDA/PTCDA:PCBM/PCBM photoactive anodes of water splitting cells for H_2 generation have been constructed and tested for stability. The efficiency of this structure was shown to be higher than that of the one- or two-layered anode structures. The possibility of generating hydrogen and oxygen in almost a stoichiometric ratio (2 : 1) was demonstrated in a three-electrode cell with the mixed layer. This result can be associated with two possible paths of charge separation under illumination with visible light depending on what component (PCBM or PTCDA) is first excited.

III.2. Membrane technology

Membrane processes are widely used for purification of natural water and wastewater and for concentration and fractionation of industrial liquid and gas mixtures. Owing to environmental and material advantages, membrane methods have been extensively developed and applied in various fields.[169–171] Rapid progress of membrane techniques requires the design of new membrane materials with improved transport and physicochemical properties. In this connection, modification of well-known polymer materials with fullerene and fullerene derivatives seems to be promising. This approach and the applications of the thus-modified materials in diffusive processes,[4,5] pressure-driven processes[6–11] and fuel cells[3] have been documented.

III.2.a. Diffusive membrane processes

Mixed-matrix membranes are most widely used in diffusive membrane processes, *viz.*, pervaporation and gas separation, since carbon nanomodifiers change the crystallinity of polymer matrices, the mechanical properties and the free volume of polymer membranes. Studies on the properties of hybrid membranes in diffusive membrane processes allow one to evaluate the contribution of modification to the transport properties of polymeric membranes.

In pervaporation, separation of low-molecular-mass liquids occurs due to diffusion through a membrane.[172] This method is used for the separation of azeotropic mixtures, mixtures of isomers and thermally unstable substances. Since pervaporation is a low-power and eco-friendly technology, it is used in various fields, especially in chemical[173] and petrochemical[173,174] industries and in biochemistry.[175] The main characteristics influencing the selectivity of the pervaporation process include the structure and chemical nature of the membrane.

Membranes based on the PVA–fullerenol $C_{60}(OH)_n$ composites (n = 12, 22–24) were prepared.[13,176,177] It was shown that PVA forms hydrogen or covalent bonds with fullerenol depending on the cross-linking method. The structure of the PVA–fullerenol membranes with hydrogen bonds is shown in Fig. 10.

The transport properties of membranes in the dehydration of different types of binary and multicomponent systems were studied by pervaporation. It was shown that the fullerenol-modified PVA membranes had different transport properties depending on the cross-linking procedure,[176] namely, heat-treated membranes had high selectivity but low permeability, while the membranes chemically treated by maleic acid had high selectivity and permeability. During the separation of water–alcohol mixtures[176] using chemically cross-linked PVA-fullerenol membranes the flux increased by 260%. The same result was obtained in the study of the synthesis of n-propyl acetate using a hybrid process 'esterification with pervaporation'.[177] During the separation of the n-propanol–n-propyl acetate–water ternary azeotropic mixture the flux increased by 170% compared to the unmodified PVA membrane.[177] All membranes were highly selective to water. These results show a promise in the application of these chemically cross-linked membranes in the separation of water-containing mixtures.

The mechanism of the gas separation process is similar to that of pervaporation. Like in pervaporation, the separation of gaseous mixtures proceeds by the 'solution–diffusion' mechanism by diffusion of gas molecules through a nonporous membrane.

To improve the gas barrier properties of thermoplastic polyurethane elastomers (PUE), fullerenol $C_{60}(OH)_{6-12}$ and a polyurethane fullerene derivative

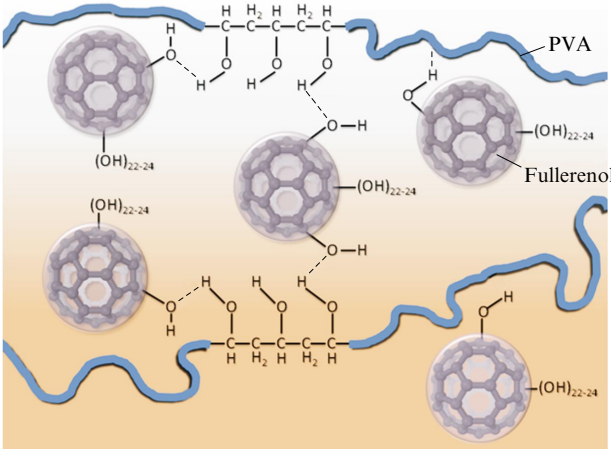


Figure 10. The structure of non-heat-treated PVA–$C_{60}(OH)_{22-24}$ membranes.[176]
Dashed lines denote hydrogen bonds.

prepared by the chemical modification of fullerenol were added as fillers.[178] To study the transport properties, the O_2 and CO_2 permeabilities were investigated. It was shown that the decrease in the gas permeability of the modified membranes is due to inhibited diffusion of gas molecules by fullerene particles (this fact was confirmed by changes in the diffusion coefficient with temperature) rather than changes in the hole volume which varied only slightly for the neat and modified membranes. It was found that the gas barrier properties of the polyurethane fullerene derivative improved almost fourfold for O_2 and fivefold for CO_2 as compared to fullerenol. The addition of fullerenol (5 mass %) reduced the gas permeability by about 10% – 20%, which was explained by higher dispersibility of the polyurethane fullerene derivative in thermoplastic PUE compared to that of fullerenol.

III.2.b. Fuel cells

A fuel cell converts the chemical energy of fuel and an oxidant into electricity. Fuel cells consist of an anode, a cathode and an electrolyte. The anode and cathode contain catalysts that cause the fuel to undergo oxidation reactions that generate positively charged hydrogen ions and electrons.

The main challenges affecting the commercialization potential of fuel cells are their performance, reliability, durability, and cost. Polymer electrolyte membrane (PEM) fuel cells or proton-exchange membrane fuel cells consist of a polymer electrolyte sandwiched between two electrodes to form a membrane-electrode assembly.

PEM fuel cells have been considered as candidates for use in different fields since they can vary their output quickly to meet shifts in power demand and thus are suited for applications requiring quick startup.[179] Water management is one of the most difficult issues in operating polymer electrolyte fuel cells. A breakdown in water balance at the cathode side often results in water flood, while the anode interface with the membrane may suffer from water depletion due to water transportation by electro-osmotic drag.

Tasaki *et al.*[180] modified the Nafion® 117 membranes with fullerene C_{60} and fullerenol $C_{60}(OH)_{12}$. The modified membranes had higher proton conductivities and held more water than the parent Nafion membranes, especially at low RH < 50%. The composite Nafion – C_{60} (1 mass %) was characterized by increased dry water uptake and a higher conductivity compared to the Nafion – fullerenol composite despite its hydrophilicity. The results obtained were explained by the presence of interfacial water (extra water) between the C_{60} particles and the Nafion domain and a likely morphological change in the Nafion membranes.

Postnov *et al.*[181] prepared Nafion – fullerenol ($C_{60}(OH)_n$ ($n = 22 – 24$), $C_{70}(OH)_{12}$) and Nafion – tris-malonate $C_{60}[C(COOH_2)_3]$ composite films and studied their proton conductivity at different RH levels. The composite containing 1.7 mass % of tris-malonate demonstrated the maximum proton conductivity at low RH, *viz.*, nearly 6.3×10^{-5} S cm^{-1} at RH = 32%, which was about 30 times higher than that of pure Nafion. The Nafion – fullerenol composite films containing from 1 mass % to 6 mass % of dopant showed no significant dependence of conductivity on the concentration and type of dopant.

PEM fuel cells transform hydrogen and oxygen gases into water and electricity. However, the complicated reaction pathway to do this transformation needs a catalyst to be efficient. Platinum is an effective catalyst for the hydrogen oxidation reaction and the oxygen reduction reaction in PEM fuel cells, but it is also an expensive one. The expense and the stability problems for platinum/carbon black catalysts have led scientists to search for alternative catalyst materials. Metallofullerenes have also been suggested as alternative catalysts with ultralow Pt loading. Since fullerene C_{60} is rather stable, a metallofullerene also may appear to be stable enough to decrease carbon corrosion and at the same time to maintain the catalytic activity on the metal atom(s).†

III.3. Biomedical applications

The study of the biological properties of fullerenes is important from both theoretical and practical perspective because it is important to identify and assess the potential of these fundamentally new structures.

Studies on the possibility of using fullerenes in drug design started fairly quickly after their discovery.[182, 183] This was 4,4′-bis{[2-(2-carboxyethyl)carbonylaminoethyl]phenyl}-(3′H-cyclopropa[1,9](I_h-C_{60})[5,6]fullerene, which can block the hydrophobic cavity of HIV protease.

Since then the number of studies on the biological activity of fullerene has increased and currently reaches thousands of articles annually. In this review only some of the recent publications on the general problem and some unusual aspects[184 – 190] will be mentioned. This Section focuses mainly on those examples of the application of fullerenes and their derivatives where the role and use of polymers are significant.

The biological activity of fullerenes, as any other class of compounds, is determined by the physical, chemical and topological properties of their molecules. The most important physical property of fullerene molecules is their ability to convert triplet oxygen into a variety of ROS. The most important chemical property is the unsaturated nature of the molecules, which makes them active radical scavengers.

Furthermore, fullerene molecules can form covalent bonds and supramolecular conjugates with various types of molecules including macromolecules. Another crucial feature of the fullerene molecules, distinguishing them from the majority of other organic compounds, is the presence of an internal cavity, which can include a variety of atoms or groups of atoms. Endohedral fullerenes can be very useful in the development of contrast agents for different types of tomography (see below).

Using EMFs, it is also possible to engineer theranostic agents, *i.e.*, single agents that are both therapeutic and diagnostic by design.[191, 192] The rigid shape (sphere for C_{60}) allows them to react with various

† See M A Gabriel, T Deutsch, A A Franco *ECS Trans.* **25** (22) 1 (2010); M A Gabriel, L Genovese, G Kronsicki, O Lemaire, T Deutsch, A A Franco *Phys. Chem. Chem. Phys.* **12** 9406 (2010).

biological molecules and structures. The driving force of this interaction is lipophilicity.

Therefore, fullerenes C_{60}, C_{70} and higher analogues, as well as their derivatives can be used in medicinal chemistry as:

— photosensitizers for photodynamic therapy (PDT);

— antioxidants; and

— membranotropic compounds.

On the basis of fullerenes and their derivatives it is possible to design:

— antitumour and antiviral chemotherapeutic agents;

— contrast agents;

— vehicles for drug or gene delivery systems; and

— diagnostic and theranostic agents.

However, there are two challenges that complicate the study of the biological activity of fullerenes. At first, fullerenes are almost entirely insoluble in water, which reduces the availability of biologically active molecules.[193] Secondly, hydrophobic fullerene molecules tend to form aggregates. At the same time, it is well known that the physicochemical and biological properties of fullerenes can significantly influence the development and degree of biological response.[194]

Aggregation leads to fundamental differences in the interaction of single fullerene molecules and fullerene nanoparticles with biological structures due to not only different properties, but also different size. The size of fullerene molecules is quite biological. For instance, the C_{60} molecule is $\sim$1 nm in size, which is biologically attractive. But this is valid only for isolated molecules, because aggregate forms of C_{60} represent nanoparticles. For example, a small C_{60} fullerene molecule can embed into a human serum albumin (HSA) molecule having a size of 8.0×3.8 nm.[195, 196] However, nanoparticles behave in a completely different manner, namely, HSA molecules adsorb onto the surface of C_{60} nanoparticles in an aqueous dispersion, the process being accompanied by changes in the conformation of the protein molecules.[197]

As a result, depending on the degree of aggregation, we deal with a fullerene molecule on (or within) a biological molecule. Yet another consequence of aggregation is the weakening of the photosensitizing ability of crystalline C_{60} (fullerite) compared to that of C_{60} in solution because the triplet state of fullerite undergoes rapid self-quenching.[198]

In some cases, the difference is more dramatic. For example, no ROS production from nano-C_{60} cluster prepared by prolonged sonication of a mixture of fullerene C_{60} with water was detected.[199] Therefore, it is obvious that the chemical nature of fullerene impacts its physical behaviour by bestowing unique optical and electronic properties, solubility, particle size and dispersion behaviour, which in turn dictate its interactions with biological entities.

Fullerenes in biological systems. There are several possible ways to introduce fullerenes into biological systems. One can use fullerite suspensions or aqueous colloidal dispersions (nano-C_{60}).[200, 201]

In the fullerite and nano-C_{60} particles the active entity is always the same, namely, pristine C_{60} as nanoparticles or some other forms. However, the sizes of these particles vary over a wide range, *e.g.*, from 200 to 1000 nm or more for suspensions[202] and from 50 to 600 nm for colloidal dispersions.[203] In the latter case, the particle size depends on the method of preparation.

The other way is to prepare water-soluble compositions, *viz.*, covalent derivatives containing polar groups or supramolecular complexes with polymers.

Polyhydroxylated fullerenes, or fullerenols, are very often used. The formula $C_{60}(OH)_n$ corresponds to the structure averaged over a mixture of fullerenols bearing different number of hydroxyl groups, each with its own stereoisomers. The solubility of fullerenols depends on the number of hydroxyl groups. Water-soluble fullerenols contain 20 or more OH groups. However, fullerenols have a significant disadvantage: in one of the first studies the authors pointed out that samples prepared in the same way nevertheless show a variability of both water solubility and biological effects, presumably reflecting uncontrolled differences in the number and location of oxygen-containing addends in the fullerene core.[204] The structures of some other fullerene derivatives (*e.g.*, some amino acid derivatives[205]) are also not always determined accurately. Nevertheless, for some compounds, the structures were defined accurately.[206]

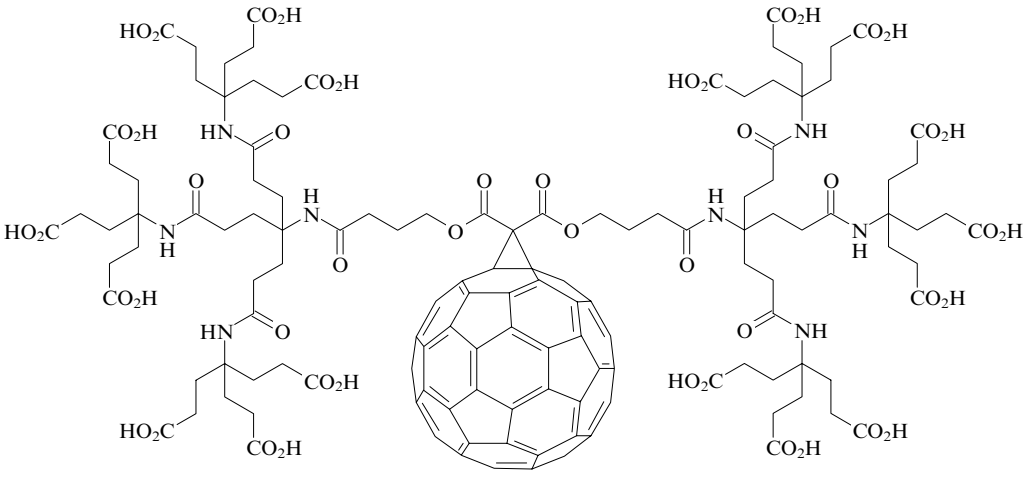
As mentioned above, there is a problem of aggregation originating from the hydrophobic nature of the fullerene core. The fullerene core strive to aggregation is so strong that often the attachment of only one substituent to the core is not enough to prevent it. Fullerene derivatives can form morphologically different nanoscale structures (spheres, nanorods and nanotubules) in water depending on the nature of the side chain attached to the fullerene core.[207, 208]

Therefore, fullerene molecules in biological systems simultaneously behave as molecules and nanoparticles. For example, they form aggregates in a solution but decompose into individual molecules and small aggregates (dimers, trimers) inside the membrane.[209] Even for nano-C_{60}, the cluster size depends on the method of preparation.[210]

Aggregation also leads to differences in the interaction with biological molecules. In particular, nano-C_{60} clusters with a particle size of more than 50 nm cannot enter into cell membranes whose thickness is merely 5 – 7 nm. Differences in the interaction of fullerene molecules and nanoparticles with proteins were discussed above.[195, 197, 211]

The same thing happens to fullerenes interacting with nucleic acids. In particular, only aminofullerenes can bind nucleic acids (these ionic complexes are used for gene delivery, see below).[212 – 214] However, fullerene aggregates (nano-C_{60}) can adsorb onto the surface of single-stranded DNA (ssDNA). Although the nano-C_{60} particles are negatively charged, ssDNA binds them due to strong $\pi - \pi$ stacking interactions between DNA bases and nano-C_{60}.[215]

A detailed analysis of the impact of the number and type of substituents on the solubility of fullerene derivatives in water and on their ability to aggregate shows that at least three ionic groups attached to the fullerene core are required to obtain a water-soluble form.[206] However, a drawback of multiple *exo*-functionalization is stronger disruption of the fullerene π-system with increasing number of addends. As a direct consequence,



I

Figure 11. Dendritic water-soluble fullerene mono-adduct of fullerene C_{60} **I**.[217]

the antioxidant or neuroprotective activities should decrease due to a lower electron or radical affinity.[216] Therefore, one of the most convenient ways is to synthesize dendrimer-type adducts since in this case it is possible to attach several polar groups and each addend does not strongly shield the fullerene core. For instance, the solubility of monoadduct **I** (second-generation dendrofullerene, Fig. 11) in water is 1.2×10^{-2} mol litre^{-1}, which is one of the highest values for fullerene derivatives.[218]

This substitution pattern also leads to another result, namely, due to the very effective shielding of the fullerene surface by the bulky dendritic branches, this compound is dispersed in monomeric form at a neutral pH.[219] Nevertheless, replacement of only one dendritic ligand by lipophilic octadecyl moiety results in a highly amphiphilic compound which aggregates into large clusters. The positively charged monoadduct **II** (Fig. 12)‡ with three ethylene glycol chains is water soluble at concentrations around 10^{-5} mol litre^{-1}, but the addend does not shield the fullerene core, and therefore **II** shows a pronounced tendency to form aggregates.[219]

However, the result is not good if both polymeric addends contain no charged groups. The nonionic but polar analogue of **I** (see Fig. 11) with two PEG chains is almost insoluble in water.

Nevertheless, obtaining a water-soluble fullerene derivative without charged ionic groups is possible. A derivative of 1,9-dihydro-1a-aza-1(2)a-homo(I_h-C_{60})[5,6]-fullerene **III** ('sugar ball', see Fig. 12) containing six α-D-mannose units is a good example. This compound is water soluble and forms only small micelles.[220]

Thus, using various polymers and fullerene derivatives, complexes with different solubility and aggregation ability can be obtained. In almost all cases, the most suitable compound for a given biological target can be synthesized.

‡ See P Rajagopalan, F Wudl, R F Schinazi, F D Boudinot *Antimicrob. Agents Chemother*. **40** 2262 (1996).

One more widely used approach is the preparation of water-soluble compositions by forming supramolecular complexes with hydrophilic polymers. These can be noncovalent water-soluble inclusion complexes with various biocompatible polymers, *viz*., PVP (C_{60}/PVP complex),[221] poly(2-ethyl-2-oxazoline) homopolymer (C_{60}R/PEtOx complex)[222] and a water-soluble diblock copolymer, poly(*N*-isopropylacrylamide)-*b*-poly(*N*-vinyl-2-pyrroridone).[223] Fullerenes can be included in liposomes,[224, 225] encapsulated in Triton X-100 micelles,[226] dissolved in PEG[227, 228] and solubilized through complexation with disaccharides.[229] To form supramolecular complexes with cyclodextrin-like structures and liposomal forms, surfactants can be used.

Fullerene C_{60} can also form water soluble supramolecular complexes with substituted cyclotriveratrylene.[230] All these forms differ in the fullerene concentration and in the degree of fullerene aggregation (*e.g*., the degree of aggregation in the C_{60}/PVP complex depends on the molecular mass of PVP and fullerene concentration[231]).

In some cases, such as compositions for topical cutaneous application, solutions of fullerene C_{60} in squalane and squalene can be used.[232, 233] A solution in a lipophilic solvent (olive oil) can also be used for oral administration of fullerene C_{60}.[2] It should be noted that aggregation of fullerene molecules in an inclusion complex of fullerene with γ-cyclodextrin C_{60}/2γ-CD is impossible.[234, 235]

Fullerenes in membranes. To predict or at least understand the biological properties of fullerenes and their behaviour in the body, one should know how they interact with lipid membranes. At low concentrations, fullerenes are present in the phospholipid membrane as single molecules. Their preferred location in the membrane is only slightly influenced by the derivatization because of the key role played by dispersion interactions between the highly polarizable fullerene cage and the tight hydrocarbon chains.[236]

Particular attention should be paid to two fullerene derivatives, *viz*., trisadducts *e*,*e*,*e*-$C_{63}(COOH)_6$ (C_3) and *trans-3*,*trans-3*,*trans-3*-$C_{63}(COOH)_6$ (D_3). They can be

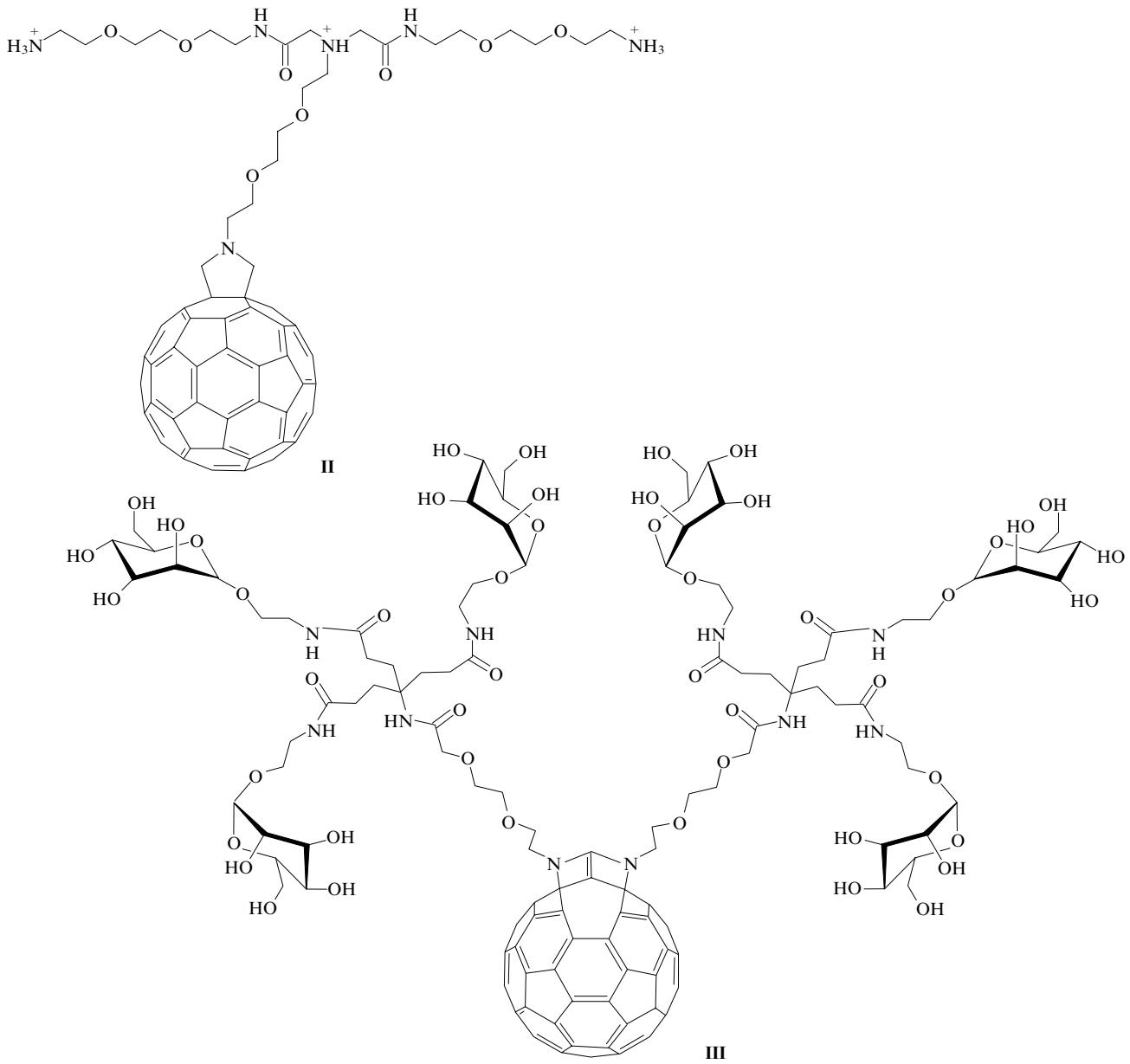


Figure 12. Fullerene C_{60} derivatives: mono-adduct with three positive charges **II** and 'sugar ball' **III**.[220]

synthesized with ease by the Bingel reaction and are well soluble even in neutral water. That is probably why they are the most frequently studied fullerene derivatives with respect to the antioxidant and neuroprotective activity *in vitro* and *in vivo*.[206]

It is these carboxyfullerens that provide one of the most striking examples of the contribution of membranotropic properties to the biological activity. Both compounds are powerful scavengers of hydroxyl radicals and superoxide radical anions.[204] However, they differ markedly in neuroprotective action and in effects on tissue cultures. According to EPR data, this is due to the difference in the interaction with membranes.[204]

The influence of membranotropic properties of these compounds is clearly seen when comparing their antiviral action. Namely, carboxyfullerene C_3 (10 μmol litre^{-1}) inactivated the Dengue-2 virus under illumination (*i.e.*, by the photochemical mechanism involving production of singlet oxygen or other ROS). This compound also could inactivate the Dengue-2 virus without light when its concentration was increased to 40 μmol litre^{-1}.[237] A study of the effect of C_3 on the Japanese encephalitis virus (JEV) and two nonenveloped viruses [*viz.*, Enterovirus 71 (EV71) and Coxsackie virus B3] revealed that this fullerene derivative selectively inactivated enveloped viruses (Dengue-2 virus and JEV), but was inactive against nonenveloped types,[237] which indicates possible involvement of a light-independent mechanism in the blockade of viral replication in the attachment and penetration stages.[237] Antimicrobial and bactericidal properties of fullerene derivatives are also associated with their membranotropic properties.[200, 238]

Antiviral effect of fullerene C_{60} in a complex with PVP is based on the interaction with membranes. This complex inhibits reproduction of influenza virus and can inhibit reproduction of DNA-containing viruses, in particular, herpes simplex virus.[239] An electron microscopy study of the intact influenza type A virions and the virions treated with the C_{60}/PVP complex showed a change in their morphology, namely, there were many defect virions and virions with damaged 'brush' and disturbances of lipid envelopes.[240]

The envelopes of viruses and bacteria are composed of not only lipids, but also proteins. Consequently, the aforementioned 'dark' antiviral effect of C_3 and virucidal action of C_{60} are most likely based on membrane destruction due to the interaction of fullerene molecules with proteins.

All the above data clearly demonstrate that the properties of the fullerene core (*e.g.*, lipophilicity) can play a crucial role in the interaction of fullerene and fullerene derivatives with biological objects *in vitro* and *in vivo*. However, it should be emphasized that fullerene molecules exhibit their membranotropic properties at low degree of aggregation only.

Fullerenes in photodynamic therapy. One of the fields where fullerenes may have a medical application is the light-based therapy called photodynamic therapy (PDT), which is a nonsurgical, minimally invasive approach that has been used in the treatment of solid tumours and many nonmalignant diseases.[241] Both pristine fullerenes C_{60} and C_{70}, as well as their derivatives, increase the intracellular ROS level, and so in biological systems, they are oxidants[242] and induce apoptosis.[243] They can therefore be lead compounds for antiviral and anticancer drug design.[244–246] Some relevant examples were given above (see also Refs 159 – 162).

The advantages of fullerenes over the traditional photosensitizers used for PDT are as follows:

— fullerenes are more photostable and undergo less photobleaching than many other photosensitizers;

— fullerenes show both kinds of photochemistry comprising type I (free radicals) and type II (singlet oxygen);

— fullerenes can be chemically modified for tuning their structures for the given activity in the given system;

— a light-harvesting antenna can be attached to the fullerene core in order to enhance the overall quantum yield and the ROS production and to extend the absorption spectrum of the photosensitizer in the long-wavelength region; and

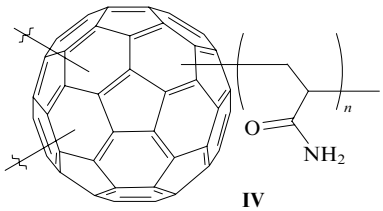
— molecular self-assembly of fullerenes into vesicles allows improved drug delivery and can produce self-assembled nanoparticles with tropism to different tissues.[184, 247]

The first demonstration of the photodynamic action of fullerene was the inactivation of enveloped viruses by fullerite suspensions.[248] Incorporation of fullerenes into polymeric environment usually does not deprive their photosensitizing properties, *viz.*, pristine C_{60} exhibits pronounced cytotoxicity under illumination with visible light in lipid membranes with a cationic surface[249] and in PEG-based block copolymer micelles.[250] Fullerene C_{60} in a complex with PEG demonstrates anticancer activity against fibrosarcoma cells, the effect being dependent on the concentration of the PEG – fullerene C_{60} complex and irradiation doses.[227, 228]

The photodynamic properties of fullerene C_{70} have also been widely studied. A comparison of the photodynamic activity of fullerenes C_{60} and C_{70} encapsulated in dimyristoylphosphatidylcholine liposomes against HeLa cells showed that C_{70} was five times more active than C_{60}. The difference has been attributed to an improved absorption spectrum of fullerene C_{70}.[251] The photodynamic activity of C_{70} and $C_{84}O_2$ fullerene derivatives functionalized with decacationic ethyleneamine chain was also described.[252]

It is known that aggregation weakens the photosensitizing properties. However, only aggregation leading to strong shielding of the fullerene core is undesirable. Aggregation of the entire polymer subunit may not influence the photosensitizing ability of a given compound provided that there is an oxygen generator near the fullerene core and the core is accessible to illumination.

For example, a fullerene-acrylamide copolymer **IV** can form particles with an average diameter of about 46 nm. The formation of 'nanoballs' does not affect the photodynamic activity of fullerene, thus indicating that aggregation does not lead to shielding of the fullerene core and is associated with the polymer system (Fig. 13).[253]



IV

Figure 13. Fullerene-acrylamide copolymer **IV**.

Yet another advantage of the use of polymers in the design of systems for photodynamic therapy is that the conjugate of fullerene C_{60} with PEG is accumulated predominantly in tumour tissue and can therefore be used for selective photodynamic action on the tumour.[254]

Modification of fullerene C_{60} with polysaccharide pullulan results leads to an effective photodynamic antitumour agent.[255, 256]

Mono- and polycationic fulleropyrrolidines can also be used as photosensitizers.[257, 258] These functionalized C_{60} fullerene derivatives are efficient broad-spectrum antimicrobial photosensitizers.[259, 260] Structure – activity studiess[258] showed that the most efficient antimicrobial photosensitizers are the quaternary C_{60} fullerene derivatives. It was assumed that they may be useful for the treatment of superficial infections, where light penetration into tissue is not problematic, *e.g.*, in wounds and burns.

A major challenge in PDT is the limited tissue penetration due to light absorption and scattering by biological tissues. Photosensitizing molecules which can only be excited by short-wavelength light (UV and blue light) are usually unfavorable in cancer therapy, espe-

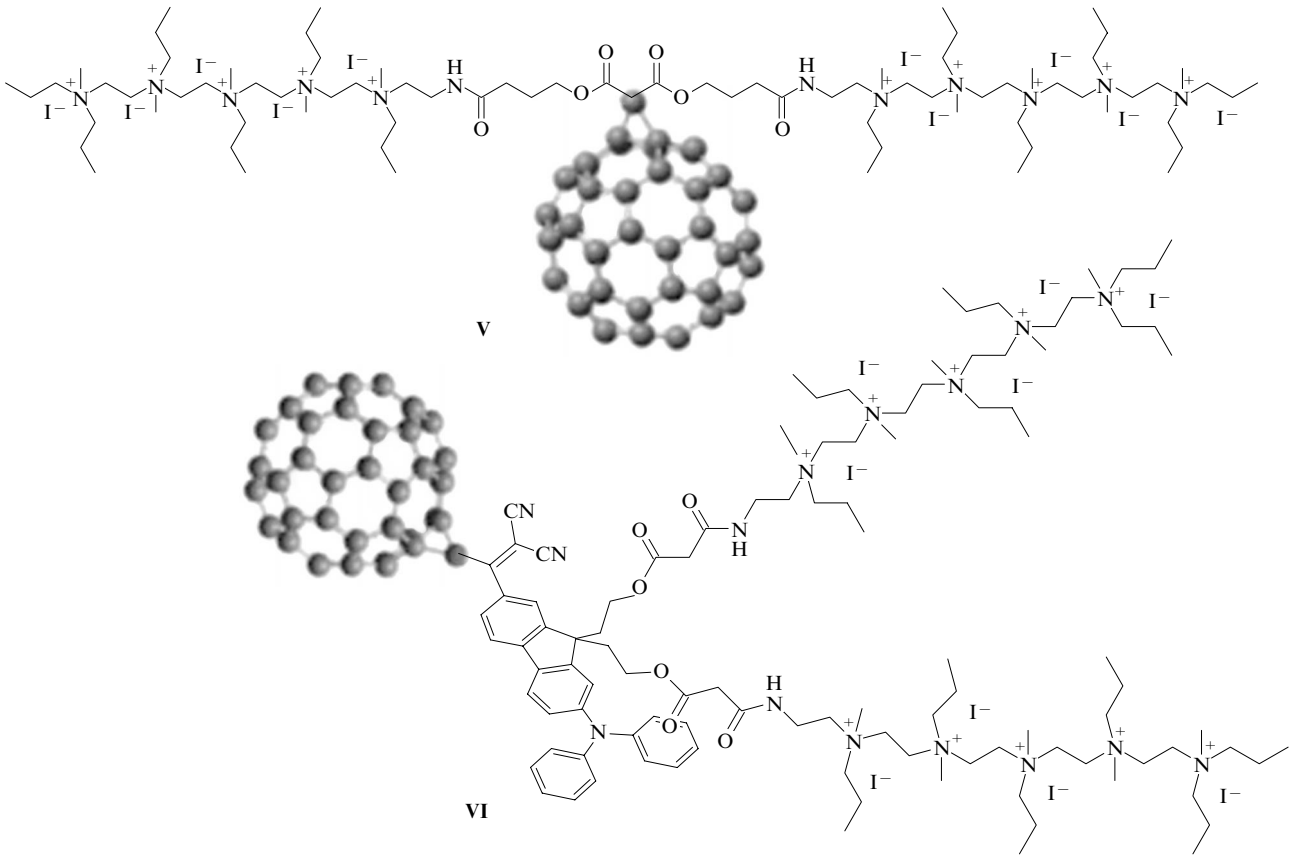


Figure 14. Decacationic fullerene C_{60} monoadducts **V** and **VI**.[261]

cially for solid tumour treatment, due to their extremely small tissue penetration depth.

The challenge can be overcome by inducing a red shift in the absorption spectrum through attachment of an electron-donating antenna to the fullerene core.

To this end, two compounds, namely, decacationic C_{60} fullerene derivative **V** and a conjugated monoadduct **VI** with a red light-harvesting antenna (Fig. 14) were synthesized. A study[261] on the possibility of using these compounds for cancer treatment on a HeLa cell model showed that attachment of the antenna **VI** enhances the photodynamic activity upon excitation by longer-wavelength light.

It is not necessary for a light-harvesting antenna moiety to be a fullerene addend. The antenna molecule can be included into lipid membrane bilayers together with fullerene C_{60} molecules.[262] For additional information on the light-harvesting antenna systems, see Ref. 47.

Polymers can 'help' fullerenes in the manifestation of biological activity, and fullerenes can enhance the biological effects of some oligomers. For example, squalene, (6*E*,10*E*,14*E*,18*E*)-2,6,10,15,19,23-hexamethyltetracosa-2,6,10,14,18,22-hexaene, an isoprenoid compound structurally similar to beta-carotene, can be used as an anticancer substance, antioxidant, drug carrier, detoxifier, skin hydrator and emollient both *in vivo* and *in vitro*.[263]

At the same time, a solution of fullerene C_{60} in squalene (C_{60}/Sqe) inhibited lipid peroxidation more markedly (1.2-fold) than squalene alone.[233] An assay showed that combining C_{60}/Sqe treatment and X-ray irradiation caused the lipid peroxidation level as malonic dialdehyde equivalent to increase in a manner dependent on X-ray dose.[233]

Fullerenes and biological polymers. Studies on the interactions of fullerenes and their derivatives with proteins and nucleic acids to form hybrid functional assemblies is a relatively new and promising research area.

Friedman and coworkers[182, 264] were the first who proposed the interaction of fullerenes with proteins. They assumed that the action of fullerene as HIV protease inhibitor is related to its ability to embed into the cylindrical cavity of the enzyme as a result of strong hydrophobic interaction between the C_{60} fullerene core and amino acid residues in the cavity region.[265]

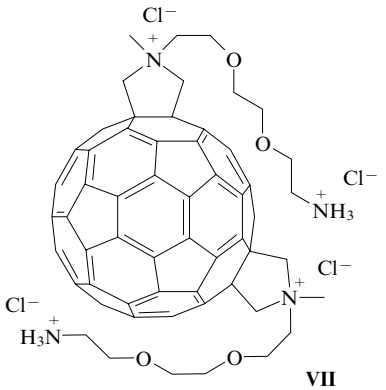
The available data on the interaction of fullerenes with biopolymers (proteins and nucleic acids) can be divided into two groups. One group includes the results which imply noncovalent or covalent interaction of fullerenes and their derivatives with polymers (indirect data based on biological response). The other group includes the results containing direct evidence of the formation of covalent or supramolecular fullerene–polymer complexes.

Studies which imply but do not directly show the interaction of fullerene or its derivatives with proteins first of all include the publications containing data on the effect of fullerenes as agonists or antagonists of receptors or enzymes, *e.g.*, the inhibitory effect of fullerene derivatives on glutathione reductase[266] and inac-

tivation of neuronal nitric oxide synthase by compounds $C_{60}C(COOR)_2$ [R = $(CH_2)_3OH$ or $(CH_2)_3NH_3^+$] (Ref. 267) or trismalonates $C_{60}[C(COOH)_2]_3$.[268]

Fullerenols $C_{60}(OH)_n$ (n = 18 – 20) were found to be glutamate receptor antagonists that inhibit the glutamate binding in dose-dependent manner.[269] Cationic bis-*N*,*N*-dimethylfulleropyrrolidinium salts are noncompetitive inhibitors of acetylcholinesterase.[270] More such examples can be found.

Fullerene derivatives can not only inhibit the action of enzymes, but also increase their expression, as is the case with the adenosine A_1 and A_{2A} receptors in SK-N-MC cells after treatment with the tetracationic fullerene derivative **VII** (Fig. 15).[191, 271]



VII

Figure 15. Tetracationic fullerene C_{60} derivative **VII**.[271]

One of the most striking proofs of the ability of fullerenes to interact with proteins is the formation of fullerene-specific antibodies obtained for the water-soluble C_{60} and C_{70} fullerene derivatives.[272] An X-ray study of a Fab fragment of an antibody showed that the fullerene-binding site contains amino acids of both chains. The site is formed by a cluster of hydrophobic amino acids; some of them are involved in π – π-stacking interactions with the fullerene core. The authors believe that the interaction proceeds by the induced fit mechanism.[273] The anti-fullerene C_{60} antibodies can also be produced using fullerenecarboxylic acids, thyroglobulin, BSA, *etc*.[274]

The formation of antibodies to fullerenes has a high theoretical significance because it demonstrates almost unlimited potential of the immune system, which can recognize even such an unusual structure as the fullerene molecule. There is also a practical value. Indeed, the application of fullerenes requires the development of relevant methods for the determination of these compounds in biological tissues and fluids and the immunoassay belongs to the most sensitive and relatively simple techniques. In particular, it is immunoassay that was used to determine the distribution of carboxyfullerene $C_{61}(COOH)_2$ within the cells.[275]

π – π-Stacking interactions can occur between the π-system of the fullerene core and aromatic amino acid residues.[276] An example of the direct interaction is provided by the synthesis of a 'peptide receptor', *i.e.*, a nonapeptide made up of six α-aminoisobutyric acid residues, a Gly spacer and two L-Tyr residues in positions 2 and 8 (here, hydroxyl groups were replaced by the ferrocenoyl moieties).[277] It was shown that the ability of this peptide to host fullerene C_{60} is due to the presence of electron-rich hydrophobic cavity formed by the ferrocenoyl residues.

Various complexes of fullerene C_{60} and its derivatives with natural proteins are available (Table 1). They were obtained by mixing aqueous solutions of fullerene C_{60} and lysozyme[278] as well as aqueous solutions of the trismalonate C_3 and proteins.[279, 280] Exchange reaction between supramolecular complexes of fullerene C_{60} with γ-cyclodextrin or PVP with proteins in solutions were used.[176, 281]

Table 1. Fullerene complexes with proteins.

Fullerene derivative	Protein	Ref.
C_{60}	Lysozyme	278
C_{60}	BSA	281
C_{60}	BSA, transthyretin	176
C_3	HSA	281
C_3	β-Lactoglobulin, HSA	282
C_{60}, C_3	BSA, HSA, HIV protease, fullerene-specific antibody	283
C_3	Apomyoglobin	280

The ability of fullerenes to form complexes with blood transport proteins (BSA and HSA) can be treated as a model for the interaction between carbonaceous nanomaterials and biomacromolecules and transport in biological systems. The exchange reaction between the C_{60}/lactoglobulin complex and HSA can be regarded as a model for carbonaceous nanomaterial delivery through epithelial barriers to the blood transport proteins.[282]

Experimental data and results of molecular docking calculations suggested that an amphiphilic, negatively charged ligand is bound to the HSA subdomain IIA (binding site is formed by hydrophobic side chains, with the entrance to the pocket being surrounded by positively charged amino acid residues). The binding constant of the C_3 isomer of trismalonic acid was found to be comparable with the published values for other organic molecules that strongly bind to the same HAS site, namely, bilirubin, iodipamide and some others.[284]

Fullerene C_{60} docking sites were studied[210] for more than 1200 proteins using the available experimental data on protein – C_{60} interaction.

Fullerenol $C_{60}(OH)_{20}$ can also interact with proteins, in particular, microtubules to give inclusion complexes.[285] Microtubules are the main component of the cytoskeleton and fullerenol inhibits their polymerization by the formation of a complex with tubulin in a molar ratio of 9 : 1.

Fullerenes can also influence the secondary structure of proteins. For instance, a water-soluble organophosphorus derivative of fullerene, $C_{60}O_m(OH)_n[C(PO_3Et_2)_2]_p$ ($m \approx 8$, $n \approx 12$, $p \approx 1$), forms a complex with HSA and disturbs the protein structure, *viz*., the number of α-helices and β-sheets increases while that of β-turns decreases. As a result, the protein becomes more compact upon association.[286]

Specific interaction between fullerene and proteins at the molecular level was mentioned above (see, *e.g.*, Ref. 278). However, it can also occur at the nanoparticle level. For example, nano-C_{60} can interact with and modulate the function of Ca^{2+}/calmodulin-dependent protein kinase II (CaMKII), a multimeric intracellular serine/threonine-specific kinase central to Ca^{2+} signal transduction, by a mechanism that competes with the well-documented interaction between the NMDA receptor subunit NR2B and CaMKII.[287] The example of specific interaction between nanoparticles and cellular signalling proteins may have significant implications for the potential therapeutic applications of fullerene C_{60}.

Amyloid deposits are implicated in the pathogenesis of many neurodegenerative diseases, *e.g.*, Alzheimer's disease. A fullerene C_{60} derivative, 1,2-(dimethoxylmethano)fullerene, inhibits the early stages of aggregation of β-amyloid peptides, the interaction being complementary. It was assumed that this compound can specifically bind to the central hydrophobic motif KLVFF, thus suppressing Aβ-fibrillation.[288]

The ability of fullerene C_{60} derivatives to inhibit the aggregation of amyloid peptides has repeatedly been shown[289 – 292] (see also a review[293]). It was assumed that C_{60} preferentially binds to the core part of the fibril and destabilizes the fibril structure.[294] A significant role in the inhibition of the Aβ(16 – 22) fragment is also ascribed to the fullerene six-membered rings.[295] Recent developments in the hybridization of carbon nanomaterials and amyloid fibrils, as well as the state of the art in the application of carbon nanomaterial – amyloid fibrils hybrids in bionanotechnology have been documented.[296, 297]

Inhibition of β-sheet formation has been considered as the primary therapeutic strategy for Alzheimer's disease. Therefore, the results obtained *in vitro* and *in vivo* provide hope that further work will give some possibilities for preventing the development of amyloidosis.

The use of fullerenes for gene transfer will be described later. Now we will dwell on publications concerning the interaction between fullerenes and nucleic acids which was studied using molecular dynamics simulations. It was shown that the nanoparticle binds to the minor grooves of double-stranded DNA (dsDNA) and triggers unwinding and disrupting of the DNA helix, which indicates that C_{60} can potentially inhibit the DNA replication and induce potential side effects.

The interaction of fullerene C_{60} with RNA occurs in different fashion. Namely, C_{60} only binds to the major grooves of the RNA helix, which stabilizes the RNA structure or transforms the RNA configuration from stretch to curl.[298] Also, atomistic molecular dynamics simulations showed that fullerenes strongly bind to nucleotides despite the hydrophobic nature of C_{60}. Binding of C_{60} to ssDNA causes significant deformation of nucleotides.[299]

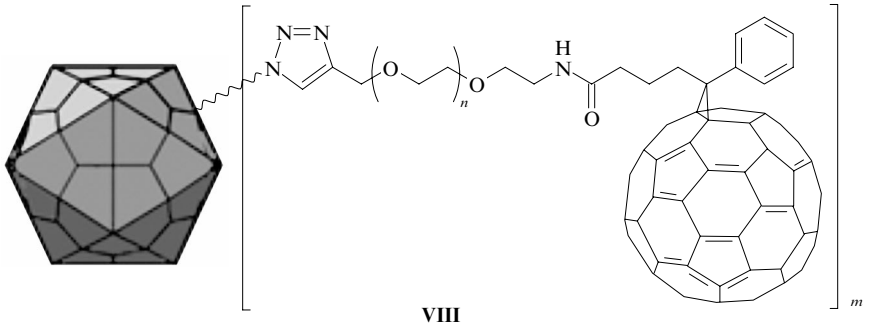
In an attempt[300] to understand the nature of the interaction between C_{60} and the Watson – Crick base pairs it was found that C_{60} forms stacking complexes with nucleobases and base pairs. The strength of the interaction of nucleobases with C_{60} is as follows: G > C > A > T > U, while the complex of fullerene C_{60} with the GC base pair is stronger than with the AT base pair.[300] However, practical value of these data remains unclear since lipophilic fullerene C_{60} can hardly be delivered to DNA or RNA through all membranes and cytosol in the living organism.

In 2009, the first complex of fullerenol $C_{60}(OH)_{24}$ with DNA was synthesized and its fluorescence enhancement was reported.[301] Fullerenol binds strongly to the phosphate backbone of native dsDNA and to base pairs within the major groove of sodium salt of dsDNA. Water-soluble fullerenols could bind to lambda DNA and remarkably improve the DNA stability against thermal degradation in a dose-dependent manner.[302]

And finally, why waste time on trifles, taking the molecules of proteins and nucleic acids separately, when we can take them all together in the form of a viral particle?

A fullerene derivative was covalently attached to Cowpea mosaic virus and bacteriophage Qβ virus-like particles, which are examples of naturally occurring viral nanoparticles (VNP). Two different water-soluble conjugates, VNP-C_{60} and VNP-PEG-C_{60}, were prepared and it was shown that the attached fullerene moiety did not inhibit the cellular uptake of dye-labelled VNP-PEG-C_{60} complexes **VIII** (Fig. 16) in a human cancer cell line.[303] This offers new prospects for the design of novel therapeutic strategies based on various delivery systems.

Fullerenes as vehicles in drug delivery systems. High lipophilicity of fullerene molecules make them useful and sometimes irreplaceable, as vehicles in drug delivery



VIII

Figure 16. Viral nanoparticle conjugated to fullerene derivative PEG-C_{60} (**VIII**).[303]

systems and as gene transfection agents. Initially, it was a system for targeted delivery of photosensitizers to DNA. An acridine residue attached to the nitrogen atom of aziridinofullerene was used as a vector. Acridine can intercalate between the pairs of nitrogen bases in a DNA molecule, thus immobilizing the fullerene core (ROS generator) near the target.[304] A conjugate of fullerene C_{60} with a 14-mer oligonucleotide capable of binding to a ssDNA and fixing the fullerene core about DNA was also synthesized.[305] To increase the specificity of binding, fullerene derivatives containing a moiety capable of binding to the minor groove of DNA were synthesized.[306]

A fullerene-containing polyacid prepared from 6-aminohexanoic acid and fullerene C_{60} in basic conditions can form ion pairs with hexamethonium. As a result, the highly polar molecule of peripheral acetylcholine receptor can penetrate into central nervous system (CNS), which is evident from the ability of the complex to block the central effects. Thus, fullerene C_{60} derivatives can be used as vehicles in systems for polar drug delivery to CNS.[307]

The ability of fullerene moiety to act as a vehicle increases significantly upon modification of the fullerene core with polymeric addends. In this connection, mention should be made of a dendrimer derivative of C_{60}, AF-1, where the fullerene core is modified with a Newkome-like dendrimer unit containing 18 carboxyl groups and five dodecyl malonate residues which are positioned octahedrally to the dendrimer.[308] This compound can self-assemble to form spherical nanostructures referred to as 'buckysomes'§ of size 100 – 200 nm in water.[309]

Empty buckysomes are not cytotoxic. The cellular internalization of buckysomes was confirmed using a hydrophobic fluorescent dye, which allowed one to use these systems as nanocarriers for anticancer drug paclitaxel. The suppression of MCF-7 breast cancer cell growth by the paclitaxel-embedded buckysomes demonstrates the possibility of using AF-1 as a vehicle for drug delivery systems.

Yet another dendrimer-like fullerene-based vehicle C_{60} – PEI – FAc (FAc is folic acid) was obtained *via* cationic polymerization of aziridine on the surface of C_{60}-NH_2 and subsequent encapsulation of C_{60} – PEI with FAc through an amide linker. The resulting dendrimer had the outer layer of FAc molecules which provided targeting. The drug delivery system was prepared by conjugating docetaxel (DTX) to C_{60} – PEI – FAc.

Compared to free DTX, the tumour-targeting drug delivery system could efficiently cross cell membranes, lead to more apoptosis and afford higher antitumour efficacy in cultured PC3 cells *in vitro*. Furthermore, in an *in vivo* murine tumour model, C_{60} – PEI – FA/DTX afforded higher antitumour efficacy than free DTX without obvious toxic effects to normal tissue.[310]

An example of a targeted drug delivery system based on polynucleotides is provided by a conjugate of trimalonic acid-modified fullerene C_{70} (TF70) with an aptamer named R13. It significantly enhances the PDT efficiency of TF70 against A549 lung cancer cells. The TF70-R13 conjugate is preferably localized in lysosomes and can produce intracellular ROS that efficiently kill cells under illumination.[311]

One more approach to designing delivery systems is based on the concept of a modular carrier system. The system employs diverse units or modules: a therapeutic unit, an addressing unit (*e.g.*, an antibody) which serves to direct the drug to its target, and a multiplying unit which increases the number of biologically active moieties the system can carry. The role of the fullerene-based multiplying unit can be played by, *e.g.*, a [5 : 1]-fullerene hexa-adduct.[312] It has five malonate spacers capable of binding two therapeutic units (photosensitizer pyropheophorbide-*a*; a total of ten units) each, and a longer malonate spacer conjugated to the addressing unit (monoclonal antibody rituximab). It was shown that such a modular delivery system is useful for PDT and can potentially be used in any therapy in which a high selectivity and affinity for the target is required.[312]

The lipophilicity of fullerene core can be used to design compositions capable of penetrating lipophilic barriers. Indeed, amphiphilic lipophilic derivatives $C_{60}C(COOH)_2$ {(3′*H*-cyclopropa[1,9](I_h-C_{60})[5,6]fullerene-3′,3′-dicarboxylic acid} and $C_{60}C[COO(CH_2)_4SO_2Na]$ {sodium salt of di(4-sulfoxybutyl)-3′*H*-cyclopropa[1,9](I_h-C_{60})[5,6]fullerene-3′,3′-dicarboxylate} were used to transfer arginine-rich cell-penetrating peptides like oligoarginines across bilayer membranes.[313, 314]

Not only drug delivery systems, but also gene transfection agents can be designed on the basis of fullerenes. The 'two-handed' fullerene derivative **IX** was the first representative of a new class of artificial vectors for gene transfection.

This compound binds duplex DNA and transfers it into cells, causing the cells to acquire the ability to express novel genes. Upon complexation with the fullerene, the plasmid containing a green fluorescent protein (GFP) reporter gene is taken up by the cultured cells through phagocytosis and then the gene is expressed in these cells.[212, 315, 316]

Efficient *in vitro* transfection was achieved using two positively charged derivatives of fullerene C_{60}, namely, an octa-amino derivative **Xa** and a dodeca-amino derivative **Xb** (Fig. 17).[317] It was found that a higher positive charge of the fullerene derivatives was a dominant physical attribute necessary for optimal ratio of C_{60}/DNA structural features leading to increased transfection efficiency and that aggregation is the major factor that negatively affected the cytotoxicity profiles of the C_{60}-vector/DNA complexes. This means that the compound forms supramolecular complexes with DNA-type ion pairs, which are transported into the cell more efficiently than the gene itself.

Theranostics and theranostic agents. Design of theranostic agents is yet another field of application of fullerene derivatives that is closely related to the development of delivery systems. It is nanomedicine that combines two active principles, therapeutic and diagnostic, in a single particle. Theranostic tools are often developed using polymer platforms.[318] And, of course, efforts to integrate polymers and carbon nanostructures for the design of theranostic agents are underway.[319, 320]

§ From '**bucky**ball' and 'lipo**somes**'.

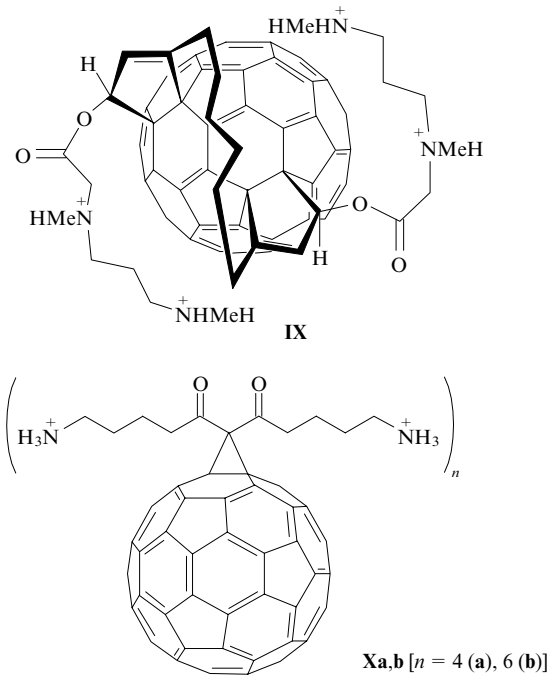


Figure 17. 'Two-handed' fullerene derivative **IX** and amino derivatives of C_{60} **Xa,b**.

Fullerenes can be treated as nanoparticles that provide a lot of possibilities for combining the two principles mentioned above in the same molecule. They are very suitable as basis or auxiliary units in the design of theranostic tools. The most remarkable is the fact that fullerene-based theranostic agents can be single molecules rather than nanoparticles [*e.g.*, a methano-C_{60} derivative with hydrophilic spacers covalently tethered to two doxorubicin (DOX) units, conjugate **XI**] (Fig. 18).[321]

Since highly effective anticancer drug DOX possesses strong absorption and fluorescence in the visible region, incorporation of two DOX units into the fullerene core enables the tracking of DOX-containing conjugates by optical techniques. It was found that conjugate **XI** was distributed mostly in the cytoplasm, which is significantly different from free DOX molecules predominantly accumulated in the cell nucleus.[322]

One more theranostic nanoparticle was designed on the basis of fullerenol $C_{60}(OH)_{24}$. Tumours injected with fullerenols were imaged using photoacoustic tomography and photothermally treated with a near-IR laser. As a result, the tumour size decreased by 72% within two hours of treatment and only a blister was visible after 20 h.[323, 324]

Theranostic tools on the basis of EMFs can be developed with relative ease. For example, a conjugate of a derivative of the EMF $Gd@C_{82}$, namely, $Gd@C_{82}O_6(OH)_{16}(NHCH_2CH_2COOH)_8$, with the antibody of GFP (anti-GFP) presents a model for tumour-targeted imaging contrast agent based on EMFs.[325]

A macromolecular MRI contrast agent Gd-DTPA-HSA (DTPA is diethylenetriamine pentaacetate) can be modified by trimalonate $C_{60}[C(COOH)_2]_3$. The Gd-DTPA-HSA-C_{60} conjugate exhibits a maximum relaxivity reported so far, which is comparable with the theoretical maximum.[326] Being included in the same molecule, HSA and carboxylfullerene exhibit a synergistic effect. Since two modalities, therapeutic (fullerene core as photosensitizer) and diagnostic (gadolinium as MRI contrast agent), are present in the same composition, it can be considered as a theranostic system.

Theranostic agents containing radioactive atoms can also be designed on the basis of corresponding EMFs. An example is provided by a conjugate ^{177}Lu-DOTA-f-$Gd_3N@C_{80}$ with a TNT-EMF (as MRI contrast agent) and a ^{177}Lu complex with DOTA (as therapeutic agent). For the imaging capabilities of this theranostic agent, see Ref. 327. Regarding therapeutic efficacy *in vivo*, see Ref. 328.

New theranostic molecules can also be prepared on the basis of a nanoplatform from 3-aminophenylboronic acid functionalized with up-conversion nanoparticles (APBA – UCNPs) and hyaluronated fullerene (HA – C_{60}) *via* a specific diol-borate condensation. In

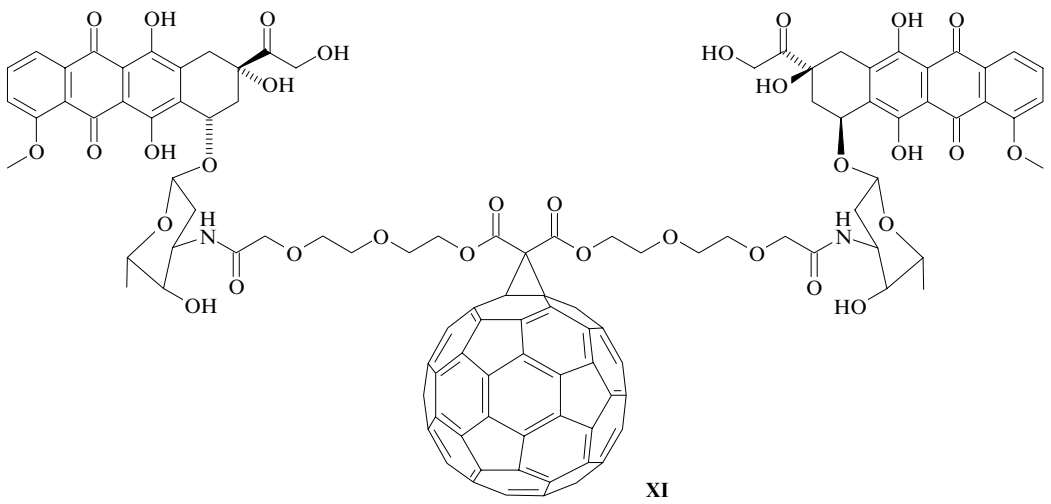


Figure 18. Fullerene C_{60} derivative tethered to two doxorubicin units (**XI**).[321]

this conjugate, the two specific ligands provide synergistic targeting effects, high targetability, and hence a dramatically increased uptake of the nanoplatform by cancer cells. High yield of $^1O_2$ due resonance energy transfer between APBA-UCNPs (donor) and HA – C_{60} (acceptor) also favours effective therapy. The nanoplatform shows a great potential for highly selective tumour-targeted imaging-guided PDT.[329]

'Wrapping' in PEG of iron oxide nanoparticles (IONP) and fullerene C_{60} enhances the photodynamic effect of fullerenes. Hematoporphyrin monomethyl ether (HMME), a new photodynamic anticancer drug, conjugated to C_{60} – IONP – PEG forms a C_{60} – IONP – PEG/HMME drug delivery system, which demonstrated an excellent magnetic targeting ability in cancer therapy. Since C_{60} – IONP – PEG can be further used as a T_2-contrast agent for *in vivo* MRI, it was concluded that the C_{60} – IONP – PEG/HMME system has a great potential for cancer theranostic applications.[330]

It is the impression that EMFs were designed by nature as a basis for contrast agents. In these molecules, the carbon cage protects a metal atom (or a group of atoms) from the external environment. Therefore, the encapsulated metal atoms do not interact with the biological environment, do not take part in any biochemical reactions in the body and are thus nontoxic.[331] The state-of-the-art in the application of EMFs in biology and medicine has been considered in a comprehensive review.[332] Two more reviews are also available.[320, 333]

Endometallofullerenes exhibit unique properties that differ distinctly from those of empty fullerenes because of the presence of metal atoms and hybridization effects as a result of electron transfer. In some details, they are similar, however. For example, the reactivity of carbon atoms of the EMF core is quite sufficient to obtain water-soluble derivatives, and the set of possible EMF derivatives coincides with that of the 'empty' fullerene derivatives. For instance, the application of $[Gd@C_{82}(OH)_{22}]_n$ can repair the functions of injured liver as well as kidney tissue,[334] *i.e.*, there is a very good correlation of the effect of $[Gd@C_{82}(OH)_{22}]_n$ with that of fullerenol $C_{60}(OH)_{24}$ *in vivo*.[335]

Magnetic resonance imaging is one of the most common techniques for diagnostic examination using a magnetic field and pulses of radiofrequency energy to visualize organs and structures inside the body. The visibility of the internal body structures in MRI can be drastically improved using contrast agents, which can change the proton relaxation times in tissues and body fluids.

To this end, organic chelates of rare-earth metals with paramagnetic properties (in particular, gadolinium chelates) are used in clinics.[336] Unfortunately, inside the body, these chelates partially release highly toxic Gd^{3+} ions. In this case, the cage protection of the toxic metal ions in EMFs is several times more effective.

Thus, metal ions (*e.g.*, gadolinium ions) can be shielded from the chemical activity within the body and the unwanted release of metals can be minimized or even avoided. The large surface area of the fullerene core also enables multiple hydrophilic functionalizations and the attachment of some tissue-targeting ligands. All these features provide opportunities for the application of endometallofullerenes $Gd@C_n$ in MRI.[333]

To date, various water-soluble derivatives of $Gd@C_n$ systems have been synthesized and investigated for their imaging properties. The archetypes of these species are hydroxylated EMFs $Gd@C_{82}(OH)_x$ (Ref. 337) and $Gd@C_{60}(OH)_x$.[338] It was mentioned that all the reported systems including $Gd@C_{60}[C(COOH_yNa_{1-y})_2]$,[339] $Gd@C_{82}(OH)_6(NHC_2H_4SO_3H)$,[332] and $Gd@C_{82}O_6(OH)_{16}(NHC_2H_4CO_2H)_8$ (AAD – $Gd@C_{82}$, Ref. 340) generally show much higher relaxivities than Gd – DTPA.

Due to the high stability, high relative yield, and encapsulation of three Gd^{3+} ions per molecule, TNT-EMFs have certain advantages, *e.g.*, high contrast. Among related EMFs, a high ^1H NMR relaxivity was shown for hydroxylated $Gd_3N@C_{84}(OH)_x$.[341] Mixed-metal metallofullerenes simultaneously containing gadolinium and lutetium or holmium and lutetium and having the composition $Lu_{3-x}A_xN@C_{80}$ (A = Gd, Ho; $x = 0-2$) were proposed for X-ray tomography and MRI multifunctional diagnostic products.[342]

Not the last role in the design of biologically acceptable compositions with EMF belongs to polymers. For example, the system $Gd_3N@C_{80}[DiPEG(OH)_x]$ with two PEG units at the exohedral carbon atom shows the highest relaxivity among the EMF derivatives used as MRI contrast agents.[343] Endometallofullerenes are suitable for the design of not only contrast agents for MRI, but also other methods of investigation. For example, an atherosclerotic-targeting contrast agent can be prepared on the basis of $Gd_3N@C_{80}$.[344]

Radiopharmaceuticals based on EMFs. Endohedral metallofullerenes with encapsulated radioactive metal atoms (^{166}Ho, ^{177}Lu) are expected to act as radiotracers or as delivery systems for brachytherapy. A biodistribution study of $^{166}Ho_x@C_{82}(OH)_y$ demonstrated the feasibility of using this compound as a radiotracer.[345] A significant advantage of such a strategy is elimination of the undesired toxicity of radionuclides that might be leaked from their conventional complexes.

Recently, radioactive EMFs for radioimmunotherapy of cancer have been developed.[346] It was also shown that a conjugate of radiolabelled cluster $^{177}Lu_xLu_{(3-x)}N@C_{80}$ with the 1L-13 peptide and a fluorescent tag (tetramethyl-6-carboxyrhodamine, TAMRA) can be used for radiotherapeutic and radiodiagnostic applications.[327]

Endometallofullerenes and chemotherapeutic pharmaceuticals. Anticancer drugs can also be designed on the basis of EMFs containing no radioactive atoms. In particular, polyhydroxylated EMF $Gd@C_{82}(OH)_{22}$ exhibits high antineoplastic activity in mice in a dose of 10^{-7} mol kg^{-1}.[347] This high antitumour activity belongs to the $[Gd@C_{82}(OH)_{22}]_n$ particles about 22 nm in diameter in saline. Being practically nontoxic, as confirmed by *in vitro* and *in vivo* tests, these particles inhibit tumour growth by interfering in the processes of tumour invasion in normal muscle tissue.

In other words, the $Gd@C_{82}(OH)_{22}$ nanoparticles do not kill the tumour cells directly, which is in sharp contrast to conventional antineoplastic chemicals. The mechanism of antitumour effect has not yet been fully clarified. According to more recent studies, the actual functions of the $Gd@C_{82}(OH)_{22}$ nanoparticles might involve improving immunity (for details, see Ref. 348).

Some other interesting properties of $Gd@C_{82}(OH)_{22}$ nanoparticles have been documented.[349] It was also assumed that, having fullerene derivatives with appropriately modified surface, the dream of the oncologist to design a highly potent but low toxic anticancer drug can be realized.[347]

Fullerene distribution and metabolism. Two essential parameters of all pharmaceuticals are their pharmacokinetic and metabolic properties. The dynamic distribution of fullerenes in the body is influenced by several factors including the particle size, the type and degree of functionalization and the administration pathways. Orally administered ^{14}C-labelled fullerene C_{60} is excreted primarily in feces. Unlike this, C_{60} injected intravenously is cleared from the blood circulation rapidly, accumulates mainly within the liver, remains there for a long time, and then is removed slowly from the liver (nearly completely 13 days after injection). All these results suggest that the liver is a potential target for fullerene accumulation.[202, 350, 351]

Certainly, much more is known about the distribution of EMFs in the body, since their monitoring is easier. Therefore, there is more data available on their fate in the body compared with nonradioactive fullerenes. After administration of $^{140}La@C_{82}$ to rats no more than 20% of the total radioactivity was eliminated in 24 h, and the remaining 80% was accumulated in the liver, blood, and brain.[352] A more detailed study of the $^{166}Ho_x@C_{82}(OH)_y$ distribution in rats showed that the agent was distributed throughout the entire body, except for tissues with limited blood flow, as early as 1 h after the tail vein injection.[345]

The concentration of ^{166}Ho increased only in the liver and bone from 1 to 4 h, especially in bone, which subsequently displayed a slight increase in the concentration over a period of 48 h. These results were consistent with those of a biodistribution study of $[Gd@C_{82}(OH)_{22}]_n$ particles, which were delivered to almost all observed tissues but accumulated mostly in bone. This suggested that the fullerene cage was not destroyed in organisms and that the encapsulated Gd^{3+} was well protected in the cage.

The concentration of gadolinium in the brain was close to the baseline, thus suggesting that the $[Gd@C_{82}(OH)_{22}]_n$ nanoparticles could not pass through the blood – brain barrier.[334] Similar results obtained in the biodistribution studies of $C_{60}(OH)_x$ and $C_{82}(OH)_y$ showed that the biological properties would not be expected to change upon encapsulation of metal atom in the fullerene cage.[320]

Toxicity. No one has observed any manifestations of the acute toxicity of fullerenes.[2, 202, 353 – 355] The widely advertised data in Ref. 356 is negligible (see Refs 357 and 358). Only some derivatives are toxic.[359, 360] At the same time, fullerenol $C_{60}(OH)_{24}$ showed no cytotoxicity up to its limit of solubility.[320]

Chronic toxicity, especially in connection with the established accumulation of fullerenes in the liver,[361] has not been studied well enough. It was demonstrated that fullerene C_{60} can react *in vivo* inside liver cells with vitamin A, thereby undergoing *in vivo* a Diels – Alder-like reaction.[362] There is still no definitive answer to the question of whether fullerene metabolizes, and how. All these uncertainties cause some circumspection in the use of fullerenes in drug design.

III.4. Sensors and actuators

Unique features of fullerene derivatives have been used in the development of new sensors for biological and medical applications.[363 – 365]

Two types of polymer films, *viz.*, a polythiophene film and a didodecyldimethylammonium bromide (DDAB) one, were studied by electrochemical techniques.[363] Both films were modified with the EMF $Dy@C_{82}$. Preliminary results on the redox properties and sensor applications of the modified films were described. It was found that $Dy@C_{82}$ in the DDAB membrane promotes the encapsulation of hemoglobin through the attractive interaction, and hemoglobin can catalyze the reduction of $Dy@C_{82}$.

Sharma *et al.*[364] presented the conception of molecularly imprinted polymer (MIP) film for adenosine-5′ triphosphate (ATP) using reductive electropolymerization and fullerene derivatives. ATP plays a key role in the energy turnover in a living cell. It transports metabolic energy and, therefore, can be considered a biological 'energy unit'. The use of fullerenes with attached recognizing groups may be useful in the sensing field because the presence of these groups in the fullerene – MIP film improves electrochemical characteristics of the film by decreasing its resistivity.

Three types of fullerene derivatives were employed as functional monomers, namely, *N*-phenyl-4-(fullero-*N*-methylpyrrolidin-2-yl)benzamide, 4-(fullero-*N*-methylpyrrolidin-2-yl)benzoic acid and 4-(fullero-*N*-methylpyrrolidin-2-yl)uracil. Amide groups were used for complexation with the phosphate moieties of ATP. The presence of the ribose vicinal diol in the ATP molecule allowed one to use a carboxy monomer of C_{60} as one more functional monomer for imprinting. The uracil-containing functional monomer can form hydrogen bonding due to complementary base pairing of adenine, adenosine and ATP. The hydrogen bond involved in this pairing is a directional secondary valence force compared to other noncovalent bonds, such as electrostatic, van der Waals, and hydrophobic interactions. This feature was used in the last step of the MIP – ATP film preparation. The complex of ATP with the fullerene derivatives is schematically shown in Fig. 19.

The ATP template was present in the MIP – ATP film due to electropolymerization.[364] The subsequent absence of this template after extraction proved the formation of the pre-polymerization complex in solution, and then deposition of the polymerized molecular imprint. This fullerene based MIP – ATP film was integrated with two different transducers, an Au-film electrode of a quartz crystal resonator and the Pt electrode, for fabrication of piezoelectric microgravimetry and the capacitive impedimetric chemosensor, respectively.

A nanocomplex of glucose oxidase (GOD) with hydroxylated fullerene immobilized on a glassy carbon electrode and protected with a chitosan membrane (Fig. 20) was studied.[365] The possible secondary structure and the catalytic properties of GOD were characterized by different experimental methods including UV/Vis absorption spectrometry, TEM and circular dichroism.

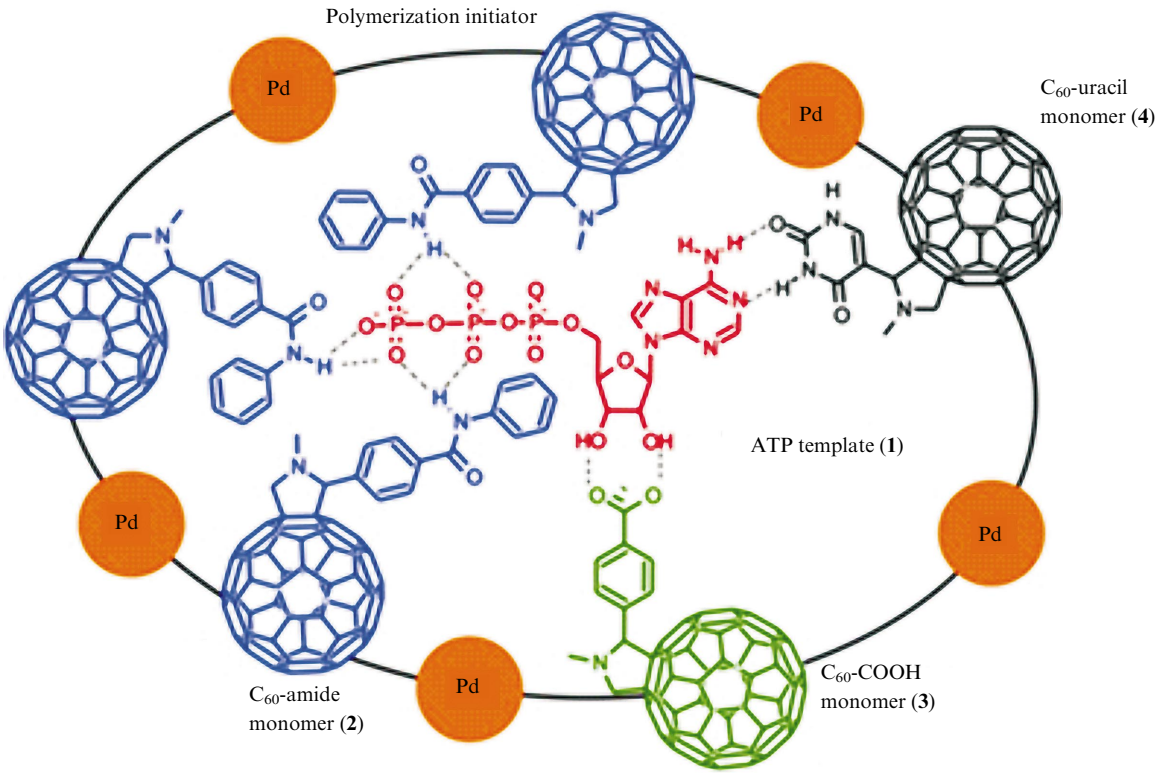


Figure 19. Simplified possible structure of the pre-polymerization complex of ATP (**1**) with functional monomers: *N*-phenyl-4-(fullero-*N*-methylpyrrolidin-2-yl)benzamide (**2**), 4-(fullero-*N*-methylpyrrolidin-2-yl)benzoic acid (**3**), 4-(fullero-*N*-methylpyrrolidin-2-yl)uracil (**4**) and $Pd(OAc)_2$ cross-linker.[364]

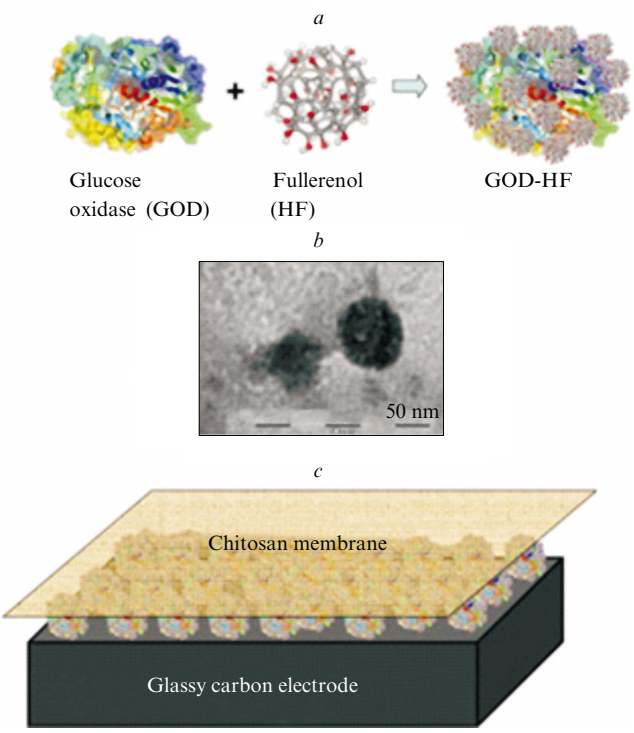


Figure 20. Possible structure of glucose oxidase complexes with hydroxylated fullerenes (*a*), a TEM image of a chitosan membrane with nanoparticles of these complexes (*b*) and a schematic structure of a glassy carbon electrode modified with nanoparticles of the complexes and coated with chitosan membrane (*c*).[365]

A possible application of the modified electrode is a third-generation glucose biosensor with high sensitivity and selectivity. An additional benefit of these methods is the fact that conformation of GOD is maintained. Consequently, the catalytic properties of the modified GOD are similar to those of the native GOD.

Practical application of this method is complicated by the fact that real samples (*e.g.*, blood) may contain high concentrations of other components (carbon dioxide, bicarbonate, hemoglobin, plasma proteins, phosphate). Some of them can cover the electrode surface or block channels in the chitosan membrane and thus seriously affect the detection results. However, the authors believed [365] that the undesired effects may be eliminated or strongly reduced by diluting the blood samples to be analyzed.

A topical application field of polymers is to use them in the design of actuators. Stimuli-responsive polymer actuators are smart materials capable of responding to external stimuli and performing large-deformation mechanical work. This is especially important when creating artificial muscle. A distinctive feature of actuator materials is the possibility to change their mechanical properties under the action of an external field (typically, electric field). In practice, an actuator should be able to provide a large actuation under low voltage. Due to its electrical properties, fullerenol allows improving the mechanical properties of polymer actuators. Also, an important feature of the use of fullerenol in main actuator systems is the water solubility of this fullerene derivative. A number of studies on the appli-

cation of fullerenol-modified polymers in the design of actuators are available.

Kyokane and co-workers[366–368] studied actuators based on fullerenol-doped PUE.

Monomorph actuators were fabricated[367] from a PUE film and two kinds of metal electrodes of different thickness. The working voltage of the PUE actuator (film 200 μm thick) was more than 1 kV, which was high for the commercial device used. The monomorph actuators were doped with fullerenol (0.1% and 0.25%) in order to provide large bends at low voltage. To understand the results obtained, a fullerene-modified PUE was studied. The bend of the PUE actuator doped with fullerenol was independent of the thickness of the metallic electrode and of the electrode material. Since the PUE films contain many polar groups in the soft segment, it was assumed that the bend of the actuator occurred when the molecular chain was stretched due to orientation of the polar groups in electric field. Also, the bend of the fullerenol-doped PUE actuators increased with increasing fullerenol concentration and reached a maximum value at 0.25%. At 300 V and 0.25% of fullerenol, the fullerenol-doped actuator was found to bend about three times larger than undoped films. The bend of the C_{60}-modified PUE actuator was smaller that that of the pure PUE actuator. Thus, the best results were obtained for the fullerenol-doped actuator. The large bend of this actuator was due to the crosslinking density that increased in the PUE films due to combination of hydroxyl groups of the star-shaped fullerenol which were incorporated into hard segments. That is, the apparent number of polar groups in the soft segment increased with increasing the crosslinking density of the PUE films. Other improved properties include an increased dielectric constant and induced e.m.f. of the fullerenol-doped films compared to other PUE films.

In a continuation of research on actuators based on fullerenol-doped PUE films Kyokane and co-workers.[368] showed that the bend, the forced actuation, and the induced voltage increased with the increase in the number of hydroxyl groups in fullerenol. Also, a piezoelectric effect was found in the fullerenol-doped PUE films in contrast to the undoped films.

New nanofibrous actuators based on electrospun cellulose acetate with fullerenol additives (0.1% or 0.5%) were developed.[369] The morphology of nanofibrous membranes resembled the porous structure of extracellular matrix of natural muscles. A chemical interaction between the hydroxyl groups of fullerenols and carboxylate groups was revealed by FT-IR spectroscopy. Using X-ray diffraction and differential scanning calorimetry, it was shown that the degree of crystallinity and labile bonding of polymer chains to the fullerenol surface increased and led to the formation of novel crystalline structures. Actuation tests showed more than a threefold increase in the tip displacement even at minute concentrations of fullerenol. This improvement of actuation performance was caused by superposition of three effects, namely, higher degree of crystallinity, piezoelectric behaviour of cellulose acetate, and electrostrictive effect of fullerenol. The results obtained demonstrate that minute concentrations of fullerenol significantly influence the structural and electroactive properties of biocompatible nanoporous actuators based on cellulose acetate. Changes in mechanical properties of the modified membranes were also observed. Adding 0.5 mass % of fullerenol to cellulose acetate fibres increased the tensile strength from 1.6 MPa to 2.75 MPa, *i.e.*, by more than 75%. Undoubtedly, this effect is a result of interactions between the cellulose acetate moieties and fullerenol molecules. Fullerenol is a zero-dimensional nanosized filler; its particles are smaller than the length scale of the cellulose acetate polymer chain. Therefore, some fullerenol molecules may be physically entrapped in the free volume, which leads to labile bonding of cellulose acetate chains with the fullerenol surface, resulting in a substantial increase in the tensile strength. The increase in tensile strength was also accompanied by a drastic decrease of nearly 100% in elongation at break, indicating that the addition of fullerenol increases the stiffness of the membranes.

Electroactive artificial muscles based on fullerenol and sulfonated polyetherimide (SPEI) were studied.[370] Being an electroactive polymer, SPEI is a good candidate material for electromechanical actuators because of its high mechanical strength, thermal stability, cost efficiency, stable film-forming properties, reasonably high water uptake and ion-exchange capacity.

It was established that incorporation of fullerene (0.5 mass %) into the polymer led to fundamental changes in proton conductivity and water uptake. These properties are vital parameters for high-performance actuators. The fullerenol–SPEI actuators showed larger bending deformation under the action of harmonic and step inputs as compared to the pristine SPEI actuator. Moreover, the straightening-back phenomenon, a critical drawback of ionic polymer actuators, was not observed for the fullerenol–SPEI actuators. The movement of hydrated fullerenol molecules in the nanoscale ionic channels of the fullerenol–SPEI membranes results in much larger bending deformation under the action of electric field. Also, it is important that fullerenes and SPEI are biocompatible and eco-friendly, so these fullerenol–SPEI actuators may appear to be promising candidates for the use in biomedical devices, artificial muscles and biomimetic robots.

Panwar *et al.*[371] fabricated and studied composite membranes for ionic polymer metal composite (IPMC) actuators. The membrane material contained fullerenol (0.1 mass %, 0.3 mass % and 0.5 mass %), polyvinylidene fluoride, PVP and polystyrene sulfonic acid. It was established that incorporation of fullerenol into the membrane significantly and rapidly improved the function of the IPMC actuator at d.c. and a.c. voltages of 0.5–1.5 V. For comparison, experiments with cellulose acetate–fullerenol[369] and SPEI–fullerenol membranes[370] required a voltage of 3 and 5 V, respectively. The largest normalized tip displacement was obtained at d.c. voltages of 0.5–1.5 V for the IPMC actuator containing 0.3 mass % of fullerenol and characterized by highest capacitance and electric current. The water uptake, proton conductivity, and tensile strain of the fullerenol-doped membranes were higher than those the untreated membranes and led to an increase in the electric current, capacitance and tensile strain of the

IPMC samples. Improved hydrophilic behaviour and proton conduction in the fullerenol-containing composite membrane were confirmed by X-ray photoelectron spectroscopy and impedance spectroscopy. Therefore, the fullerenol-doped IPMC actuators provide fast and large actuation at d.c. and a.c. voltages of 0.5 – 1.5 V.

It was assumed [371] that the enhanced and fast actuation performance of these IPMC actuators can be very useful for utilizing them in active guide wires and swimming micro-robots applications.

III.5. Optoelectronics and optical-limiting materials

The main idea of using fullerene derivatives in optoelectronics is the mixing of fullerene derivatives and conjugated polymers to obtain organic semiconductor materials that can be used for new optoelectronic devices. A typical structure of an optoelectronic device comprises a conjugated polymer acting as an electron donor and a fullerene-containing material acting as an electron acceptor. Absorption of light leads to generation of excitons that encounter the donor/acceptor interface and dissociate. Exciton dissociation is followed by electron transfer from the polymer to the fullerene cage and generation of photocurrent.

One of the famous methanofullerenes used for this purpose is PCBM. Itskos *et al.*[372] systematically studied the optical properties of pristine samples as well as binary and ternary blends of a conjugated polymer (P3HT), fullerene derivative (PCBM) and colloidal nanocrystals (oleic acid capped PbS quantum dots) using a combination of steady-state and time-resolved optical methods. Steady-state absorption measurements revealed a modest increase in the red and near-IR light harvesting efficiency upon addition of the quantum dots. Photoluminescence experiments performed in the emission regions of P3HT and quantum dots showed partial quenching of the photoluminescence of the blends compared to the emission of the pristine films. Emission quenching in the polymer region was attributed to re-absorption by the quantum dots and to electron transfer mostly to PCBM and, to a lesser degree, to the nanocrystals. On the other hand, emission of the quantum dots was predominantly quenched due to electron transfer to PCBM and/or to hole transfer to P3HT. Ultrafast transient absorption measurements revealed a variety of relaxation pathways of the photogenerated P3HT species in the blends. At shorter times, relaxation in all samples was dominated by linear hot exciton relaxation effects. At longer times, long-lived components associated with charge-transfer excitons were observed. The formation of such species occurred efficiently in the samples containing a significant amount of P3HT and PCBM, but the process was quenched in the P3HT sample doped with quantum dots and in the pristine P3HT film. At short probe wavelengths corresponding to the ground state of the P3HT singlet exciton, a long-lived photobleaching of the state was observed in the blends containing quantum dots. Overall, both steady-state photoluminescence experiments and transient absorption measurements showed that interfacial charge transfer processes occurred more efficiently at the fullerene/polymer and fullerene/nanocrystal interfaces compared to the polymer/nanocrystal interfaces. Thus, doping with fullerene seems to facilitate exciton dissociation in the ternary blends studied.

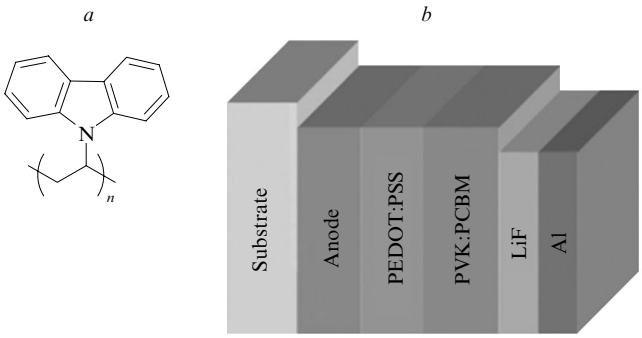


Figure 21. The chemical structure of poly(*N*-vinylcarbazole) (*a*) and the organic light-emitting diode architecture (*b*).[373]
PEDOT is poly(3,4-ethylenedioxythiophene) and PSS is poly(styrene sulfonate).[373]

The possibility to use poly(*N*-vinylcarbazole) (PVK) doped with PCBM to detect UV light was demonstrated [373] in relation to a well understood device structure for organic light-emitting diodes and organic photovoltaics with a high work function anode and a low work function cathode. The chemical structure of PVK as well as the device architecture are shown in Fig. 21. It was established that PVK:PCBM devices generate a substantial open-circuit voltage upon illumination with UV light. The UV sensing potential of this system was confirmed by UV/Vis spectroscopy in addition to the importance of the substrate and anode material. Different substrate materials (quartz or normal glass) in the devices led to different results under illumination. In the case of quartz glass, devices performed better. The limiting factors for the performance of the devices include the anode material (indium-tin-oxide) and possible shunts in the active layer.

Practical application of polymer – fullerene derivative films in electronic devices and solar cells requires that the heat resistance problem be solved. Heating can lead to the formation of large clusters of fullerene materials in the films, which can cause poor phase separation in the donor/acceptor mixed films, thus influencing the performance of the devices. To improve the thermal stability of the polymer – fullerene derivative materials, it was proposed [374] to use a fullerene derivative containing an adamantane group instead of traditional fullerene materials like PCBM. Incorporation of the adamantane unit into polymers significantly improved their stability including enhancement of heat resistance and glass transition temperature.

Liao *et al.*[374] systematically studied [6,6]-phenyl-C_{61}-butyric acid 1-adamantylmethyl ester ($PC_{60}BAd$) in P3HT:$PC_{60}BAd$ films as well as its optoelectronic properties and thermal stability. In an organic field-effect transistor device, the electron mobility of $PC_{60}BAd$ was found to be as high as 0.01 $cm^2\ V^{-1}\ s$ with a high on-off (I_{on}/I_{off}) ratio of 4.9×10^6, which is useful for logic device applications. The PCE of the optimized P3HT:$PC_{60}BAd$ organic photovoltaic devices was found to reach a value of 3.31%. The active layer of P3HT:$PC_{60}BAd$ was found to exhibit superior thermal stability over that of P3HT:PCBM. After heating at

150 °C for 20 h, the P3HT:PC_{60}BAd device still showed a PCE of 2.44%, thus demonstrating the applicability of PC_{60}BAd.

Yet another interesting direction of methanofullerene applications is the surface modification of semiconductor nanocrystals. Inorganic colloidal nanocrystals possess necessary properties for being used in optoelectronics as active elements of light-emitting diodes and photovoltaic devices. These applications require that the surface of the nanocrystals be thoroughly controlled because the ligand shell is important to prevent aggregation. Many crucial features of the nanocrystals, such as solubility, reactivity, processability and, most importantly, electronic properties with direct effects on conduction and optical activity can be controlled by tuning the surface design.

Binding yet another fullerene derivative, 3,4-dihexyloxyphenyl-C_{61}-butyric acid (dPCBA), to PbS and CdSe nanocrystals[375] is a new method of nanocrystal surface modification using electroactive fullerene derivatives. The occurrence of a ligand exchange reaction was confirmed by UV/Vis spectroscopy, photoluminescence and time-resolved photoluminescence measurements indicating photoinduced charge transfer from the nanocrystals to dPCBA molecules. The current–voltage characteristics of the complexes of dPCBA with nanocrystals showed enhanced photocurrents due to charge carrier transfer and a decrease in the potential barrier between nanocrystals. This also indicated that the complexes under study can be promising building blocks for photovoltaic devices.

The self-assembly strategy was utilized[376] to form monolayer structures. This approach increases the potential of fabrication of electronic devices with improved interfacial contact, and, therefore, it should lead to enhanced electron transfer between the acceptor and donor materials. Four water-soluble fullerene derivatives, namely, methanofullerenes with phosphonate groups attached to the C_{60} core were studied. Different electrode substrates (indium-tin-oxide, Au and Si) with specific anchoring groups (zirconium, cysteamine and amino-silane) were used to form self-assembled monolayers. The conclusion about the formation of surfaces was based on the results obtained by different experimental methods including AFM, IR spectroscopy, contact angle measurements and cyclic voltammetry (CV). It was established by CV that the reduction potentials of substituted methanofullerenes, both in solution and in monolayer, were slightly higher than the formal potentials of the redox reactions of fullerene C_{60}. The AFM results showed that the fullerene molecules produce surface features with an apparent height of about 2 nm.

The application of methanofullerenes in ultrafast spectroscopic holography was proposed[377] taking cholestanoxy methanofullerenes in luminescent polymers from the polyphenylenevinylene family as examples. These materials were studied in detail using tunable non-degenerate four-wave mixing. The role of the methanofullerenes was to enhance charge transfer in the polymer systems, which is important for the holography processes. The results of experiments demonstrated that the potential holographic information processing density of these objects is up to 12 orders of magnitude higher compared to other holographic nonlinear optical materials. Using transient absorption spectroscopy, the complex photoinduced index of refraction was determined in the photon energy range of 1–2.5 eV. Having performed the Kramers–Kronig transformation of the broadband photoinduced absorption spectrum, a reliable diffraction efficiency spectrum was obtained.

The possibility of fabricating new optical devices based on poly(propylene carbonate) containing fullerenol $C_{60}(OH)_n$ as terminal unit was demonstrated.[378] The material was obtained by copolymerization of propylene oxide and CO_2 using the $Et_2Zn-C_{60}(OH)_n$ catalytic system. The emission spectrum of the material exhibits an emission band with a few peaks in the UV region, which are absent in the spectra of individual $C_{60}(OH)_n$ and polymer. Thus, $C_{60}(OH)_n$ derivatives can be used as new kinds of chemical sensors or other optical devices due to the change in emission wavelength of the $C_{60}(OH)_n$ fragment in polymers.

The main goal of optical limiters is eye and sensor protection from high-intensity laser pulses. It is known that fullerenes possess excellent nonlinear optical-limiting properties. However, the poor solubility of fullerenes and poor adhesion between fullerenes and polymers usually hinders their utilization in such devices. These difficulties can be avoided by functionalization of fullerenes to give fullerenols or methanofullerenes. In this direction, complexes of fullerene derivatives with polymers were studied both in solution (see, for example, Refs 379 and 380) and in blends.[381–384] We will focus on fullerene derivative–polymer blends because the use of solid devices is largely preferred for technical purposes due to greater ease of handling compared to liquid solutions.

Multifunctional fullerenols were utilized in fullerenol–polymer composites,[381,382] with poly(styrene-*co*-4-vinylpyridine) (PSVPy) and poly(styrene-*co*-butadiene) being the polymer matrices. The optical-limiting properties of fullerenol were studied at 532 nm with nanosecond laser pulses. Compared to fullerene C_{60}, fullerenol showed a weaker nonlinear optical response, which may be ascribed to the disturbance of the π-electron system of the parent C_{60} molecule due to multifunctionalization. Polystyrene does not significantly change the optical-limiting performance of the fullerenol solution, while PSVPy containing 32 mol.% of vinylpyridine slightly improves the optical-limiting performance of the concentrated fullerenol solution.

Nonlinear optical (NLO) absorption of a blend of poly(3-octylthiophene) (P3OT) and a methanofullerene was studied[383] using nanosecond laser pulses at wavelengths from 620 to 960 nm (1.3–2.0 eV) with [6,6]-phenyl-C_{61}-butyric acid cholesteryl ester ([6,6]-PCBCR) as the methanofullerene. Solid films containing [6,6]-PCBCR (1 : 1 by mass, approximately one acceptor for every five repeating units of P3OT) were synthesized. For comparison, pure methanofullerene films and pure P3OT films were measured by the same technique as the blend. Thick films (20–30 μm) for nonlinear optical absorption experiments at off-resonant wavelengths were cast from filtered solution onto fused silica substrates. Thin films (0.1–0.2 μm) for measurements near resonance and for the third harmonic generation experiments were prepared by spin coating.

Enhanced NLO optical absorption of the polymer – methanofullerene blend was observed. Individual components of the material did not demonstrate such an effect. For instance, the NLO absorption of the blend film at 760 nm enhanced by more than two orders of magnitude compared to the films prepared from the pure components. The high nonlinearity results from efficient photoinduced intermolecular charge transfer from the polymer to methanofullerene followed by absorption in the charge separated excited state. It was established that when pumped at 760 nm, the transmitted energy saturates at an average fluence of approximately 0.1 J cm^{-2}. The damage threshold was 15 mJ $pulse^{-1}$ ($\sim$1 J cm^{-2} in average fluence), above which there was a permanent change in the linear transmission. It was assumed [383] that NLO absorption of P3OT – methanofullerene blends is high enough that the photoinduced charge transfer films be promising as optical limiters.

Nonlinear absorption and the optical-limiting properties of a ternary blend including a conjugated polymer (electron donor), a fullerene (electron acceptor) and a plasticizer were studied.[384] The blends of MEH-PPV and PCBM are well known to show efficient one-photon induced charge carrier generation and have been studied extensively as solar cell materials. However, these blends have a poor optical quality, which restricts their utility in optical-limiting devices. To solve this problem, a plasticizer (dioctyl phthalate, DOP) was added to the MEH-PPV – PCBM system. This made it possible to obtain thick films (25 μm) of high optical quality. For comparison, nonlinear absorption of the blend containing no methanofullerene (MEH-PPV – DOP) was measured. In the femtosecond regime, two-photon absorption induced excited-state absorption of MEH-PPV dominated the suppression, and a $\sim$10 dB of suppression was observed for both samples with and without PCBM. In the nanosecond regime, the suppression was enhanced by the accumulation of absorbing charge carriers over the long pulse duration and a contribution of one-photon absorption to the carrier generation due to a ground-state charge-transfer complex of MEH-PPV and PCBM, especially at the shorter wavelengths studied. The blend with the methanofullerene showed a significantly reduced turn-on threshold and increased suppression of 15 dB relative to the sample containing no PCBM. Thus, the MEH-PPV – PCBM – DOP blend showed stronger suppression than what had been reported to date for organic optical-limiting materials containing methanofullerenes in the 750 – 900 nm range.

IV. Conclusion

The applications of fullerenes and their complexes with conjugated polymers as well as supramolecular complexes of fullerenes are now extensive and diverse, and fullerene-containing polymer compositions are important tools for various fields. The medicinal chemistry of fullerenes allows one to select the derivatives for the desired biological effects and to perform fine tuning of the structure, thus showing that fullerene derivatives have already found their place in this area, similarly to all other classes of organic compounds.

Recently, fullerene derivatives have been playing a crucial role in the rapidly emerging field of organic photovoltaics, stimulating research interest in understanding the physical processes that would help to increase the performance of organic solar cells. It is hard not to be captivated by the recent progress in photovoltaic devices, with the improvements in the efficiency when new functionalized fullerenes are used. The PCE limit of 10% has now been surpassed,[385] and there are no doubts that this value is still far away from the possible physical limit of organic solar cell performance.[386]

Intensive research is ongoing in both fundamental and applied directions. First, it is important to get clear understanding of physics of interfacial molecular processes involving donor and acceptor materials — exciton dissociation, charge separation, and recombination. Second, progress in organic solar cell performance is fuelled by the creation of new fullerene acceptors with more interesting properties and by the design and development of new types of highly efficient devices.

The possibility of performing fullerene sensitization of well-known oxide photocatalysts through a charge transfer mechanism has met with a generous response from researchers and led to great potential for many photocatalytic applications. Fullerene derivatives including particularly attractive biocompatible water-soluble fullerenols allowed researchers to extend the range of irradiation wavelengths corresponding to active photocatalytic processes to the visible region.

This led to emergence of new application areas of fullerenes, such as oxidative degradation of pollutants (*e.g.*, dyes) and biological objects (*e.g.*, microbes, viruses and biological cells). The ability to be involved in photogeneration of active radicals (singlet oxygen and others) belongs to the family of unique properties of functionalized fullerenes, which ensures stable interest in these materials and novel fullerene-based applications.[387]

The use of metallofullerenes as catalysts helps to promote different organic reactions: cycloadditions, Bingel reactions, Prato reactions, and Diels – Alder type cycloadditions. The electronic properties of metallofullerenes can also be used to control the catalytic activity of proteins *in vivo*. Metallofullerenes have also been suggested as alternative catalysts with ultralow Pt loading for PEM fuel cells.

Fullerenol bearing OH groups is successfully used as a hydrogen-bond catalyst for different reactions (Henry reaction, aldol reaction, Michael addition reaction, Friedel – Crafts reaction, *etc.*) because the high electron affinity of the C_{60} cage makes the surface hydroxyl group a better hydrogen bond donor.

Sensors based on fullerene derivatives are a new field of application of these carbon materials. The main direction of the sensoric application is biomedicine. The possibilities to create hemosensors for identification or capture of biological objects using fullerene derivatives were demonstrated.

Stimuli-responsive polymer actuators provide large deformation under the action of an external field (typically, electric field). Fullerenols can be utilized as fillers of polymer matrices for actuators because (i) fullerene molecules allow one to improve the electrical properties

of the polymer matrix for large actuation under low voltage and (ii) the good solubility of fullerenol in water is necessary for actuator systems.

The main goal of using fullerene derivatives in optical limiters and optoelectronic devices is to improve the dispersion of fullerene in polymer matrices in order to obtain nonlinear optical-limiting and organic semiconductor materials. In this context, the most effective carbon filler is methanofullerene which is highly compatible with polymers; however, fullerenols can also be used. Fullerene derivatives facilitate the dispersion of fullerenes in polymer matrices. Moreover, the functional groups of fullerene derivatives can be used as modifiers or as cross-linking agents in polymer systems.

Modification of polymers with fullerene derivatives in membrane processes helps to prepare membrane materials with specified transport properties since targeted changes in the membrane morphology, polymer structure and free volume can be done with ease.

This work was supported by the Florida State University Research Foundation (USA), the Fellowship of the President of the Russian Federation (SP-1153.2015.1), the Russian Foundation for Basic Research (Project No. 15-58-04034), the FP7 European Union's Research and Innovation Funding Programme (FP7 – IRSES Grant No. 269138) and the Government of the Russian Federation (Grant No. 074-U01).

Figure 2 is Copyright 2012 V.Milic Torres, V.Dragojevic Simic. Published in Ref. 17 under CC BY 3.0 license. Available from: http://dx.doi.org/10.5772/34692

Figures 3, 4, 6, 7, 9 and 11 are given with permission from The Royal Society of Chemistry.

Figure 8 is Copyright John Wiley and Sons.

Figures 10 and 14 are Copyright Elsevier.

Figures 15, 16, 18, 19, 20 and 21 are Copyright American Chemical Society.

References

1. Z Zhang, L Wei, X Qin, Y Li *Nano Energy* **15** 490 (2015)
2. T Baati, F Bourasset, N Gharbi, L Njim, M Abderrabba, A Kerkeni, H Szwarc, F Moussa *Biomaterials* **33** 4936 (2012)
3. S Saga, H Matsumoto, K Saito, M Minagawa, A Tanioka *J. Power Sources* **176** 16 (2008)
4. G A Polotskaya, A V Penkova, A M Toikka, Z Pientka, L Brozova, M Bleha *Sep. Sci. Technol.* **42** 333 (2007)
5. A V Penkova, G A Polotskaya, A M Toikka, M Trchova, M Šlouf, M Urbanová, J Brus, L Brožová, Z Pientka *Macromol. Mater. Eng.* **294** 432 (2009)
6. G Polotskaya, Y Biryulin, V Rozanov *Fullerenes Nanotubes Carbon Nanostruct.* **12** 371 (2004)
7. X Jin, J Y Hu, M L Tint, S L Ong, Y Biryulin, G Polotskaya *Desalination* **214** 83 (2007)
8. S L Ong, J Y Hu, Yu F Biryulin, G A Polotskaya *Fullerenes Nanotubes Carbon Nanostruct.* **14** 463 (2006)
9. A Penkova, A Toikka, T Kostereva, N Sudareva, G Polotskaya *Fullerenes Nanotubes Carbon Nanostruct.* **16** 666 (2008)
10. G A Polotskaya, A V Pen'kova, N N Sudareva, A E Polotskii, A M Toikka *Russ. J. Appl. Chem.* **81** 236 (2008)
11. N N Sudareva, A V Penkova, T A Kostereva, A E Polotskii, G A Polotskaya *Express Polym. Lett.* **6** 178 (2012)
12. E Badamshina, M Gafurova *J. Mater. Chem.* **22** 9427 (2012)
13. A V Penkova, S F A Acquah, M E Dmitrenko, M P Sokolova, M T Mikhailova, E S Polyakov, S S Ermakov, D A Markelov, D Roizard *Mater. Des.* **96** 416 (2016)
14. K N Semenov, N A Charykov, V N Postnov, V V Sharoyko, I V Vorotyntsev, M M Galagudza, I V Murin *Prog. Solid State Chem.* **44** 59 (2016)
15. N Wang, L Sun, X Zhang, X Bao, W Zheng, R Yang *RSC Adv.* **4** 25886 (2014)
16. Z Wang, S Wang, Z Lu, X Gao *J. Cluster Sci.* **26** 375 (2015)
17. V Milic Torres, V Dragojevic Simic, in *Cardiotoxicity of Oncologic Treatments* (Ed. M Fiuza) (Rijeka: InTech, 2012) p. 89
18. J Zhao, X Huang, P Jin, Z Chen *Coord. Chem. Rev.* **289 – 290** 315 (2015)
19. A Rodríguez-Fortea, A L Balch, J M Poblet *Chem. Soc. Rev.* **40** 3551 (2011)
20. B C Thompson, J M Frechet *Angew. Chem., Int. Ed.* **47** 58 (2008)
21. Y He, Y Li *Phys. Chem. Chem. Phys.* **13** 1970 (2011)
22. D Jariwala, V K Sangwan, L J Lauhon, T J Marks, M C Hersam *Chem. Soc. Rev.* **42** 2824 (2013)
23. Z Yang, J Ren, Z Zhang, X Chen, G Guan, L Qiu, Y Zhang, H Peng *Chem. Rev.* **115** 5159 (2015)
24. Y N Biglova, D K Susarova, A F Akbulatov, A V Mumyatov, P A Troshin *Mendeleev Commun.* **25** 473 (2015)
25. Y N Biglova, D K Susarova, A F Akbulatov, A G Mustafin, P A Troshin, M S Miftakhov *Mendeleev Commun.* **25** 348 (2015)
26. A R Tuktarov, A A Khuzin, A R Akhmetov, L M Khalilov, A R Tulyabaev, V A Barachevskii, O V Venediktova, U M Dzhemilev *Mendeleev Commun.* **26** 143 (2016)
27. J Yan, B R Saunders *RSC Adv.* **4** 43286 (2014)
28. J L Delgado, P A Bouit, S Filippone, M Ángeles Herranz, N Mártin *Chem. Commun.* **46** 4853 (2010)
29. D Arvizu, P Balaya, L Cabeza, T Hollands, A Jíger-Waldau, M Kondo, C Konseibo, V Meleshko, W Stein, Y Tamaura, H Xu, R Zilles, in *IPCC Special Report on Renewable Energy Sources and Climate Change Mitigation* (Eds O Edenhofer, R Pichs-Madruga, Y Sokona, K Seyboth, P Matschoss, S Kadner, T Zwickel, P Eickemeier, G Hansen, S Schlömer, C von Stechow) (Cambridge, New York: Cambridge University Press, 2011) p. 333
30. *World Energy Outlook 2010* (Paris: International Energy Agency, 2010)
31. *Renewable Energy Technologies. Solar Energy Perspectives* (Paris: International Energy Agency, 2011)
32. S B Darling, F You *RSC Adv.* **3** 17633 (2013)
33. M C Scharber, N S Sariciftci *Prog. Polym. Sci.* **38** 1929 (2013)
34. K A Mazzio, C K Luscombe *Chem. Soc. Rev.* **44** 78 (2015)
35. N S Sariciftci, L Smilowitz, A J Heeger, F Wudl *Science* **258** 1474 (1992)
36. N S Sariciftci, D Braun, C Zhang, V I Srdanov, A J Heeger, G Stucky, F Wudl *Appl. Phys. Lett.* **62** 585 (1993)
37. J C Bernède *J. Chil. Chem. Soc.* **53** 1549 (2008)
38. J C Hummelen, B W Knight, F LePeq, F Wudl, J Yao, C L Wilkins *J. Org. Chem.* **60** 532 (1995)

39. V D Mihailetchi, H Xie, B de Boer, L J A Koster, P W M Blom *Adv. Funct. Mater.* **16** 699 (2006)
40. A V Akkuratov, P A Troshin *Polym. Sci., Ser. B* **56** 414 (2014)
41. T Xu, L Yu *Mater. Today* **17** 11 (2014)
42. G Yu, J Gao, J C Hummelen, F Wudl, A J Heeger *Science* **270** 1789 (1995)
43. W Ma, C Yang, X Gong, K Lee, A J Heeger *Adv. Funct. Mater.* **15** 1617 (2005)
44. G Li, V Shrotriya, J Huang, Y Yao, T Moriarty, K Emery, Y Yang *Nat. Mater.* **4** 864 (2005)
45. Y Liang, D Feng, Y Wu, S-T Tsai, G Li, C Ray, L Yu *J. Am. Chem. Soc.* **131** 7792 (2009)
46. V D Mihailetchi, J K J van Duren, P W M Blom, J C Hummelen, R A J Janssen, J M Kroon, M T Rispens, W J H Verhees, M M Wienk *Adv. Funct. Mater.* **13** 43 (2003)
47. S M Tuladhar, D Poplavskyy, S A Choulis, J R Durrant, D D C Bradley, J Nelson *Adv. Funct. Mater.* **15** 1171 (2005)
48. B Ebenhoch, S A J Thomson, K Genevičius, G Juška, I D W Samuel *Org. Electron.* **22** 62 (2015)
49. P Hunhomme *EPJ Photovoltaics* **4** 40401 (2013)
50. S Foster, F Deledalle, A Mitani, T Kimura, K-B Kim, T Okachi, T Kirchartz, J Oguma, K Miyake, J R Durrant, S Doi, J Nelson *Adv. Energy Mater.* **4** 1400311 (2014)
51. M M Wienk, J M Kroon, W J Verhees, J Knol, J C Hummelen, P A van Hal, R A Janssen *Angew. Chem., Int. Ed.* **42** 3371 (2003)
52. Y Liang, Y Wu, D Feng, S-T Tsai, H-J Son, G Li, L Yu *J. Am. Chem. Soc.* **131** 56 (2009)
53. S H Park, A Roy, S Beaupré, S Cho, N Coates, J S Moon, D Moses, M Leclerc, K Lee, A J Heeger *Nat. Photonics* **3** 297 (2009)
54. M Williams, N R Tummala, S G Aziz, C Risko, J L Brédas *J. Phys. Chem. Lett.* **5** 3427 (2014)
55. P Romero-Gomez, R Betancur, A Martinez-Otero, X Elias, M Mariano, B Romero, B Arredondo, R Vergaz, J Martorell *Sol. Energy Mater. Sol. Cells* **137** 44 (2015)
56. J A Bartelt, J D Douglas, W R Mateker, A E Labban, C J Tassone, M F Toney, J M J Fréchet, P M Beaujuge, M D McGehee *Adv. Energy Mater.* **4** Art. No. 1301733 (2014)
57. W Li, W S Roelofs, M M Wienk, R A Janssen *J. Am. Chem. Soc.* **134** 13787 (2012)
58. K H Hendriks, G H Heintges, V S Gevaerts, M M Wienk, R A Janssen *Angew. Chem., Int. Ed.* **52** 8341 (2013)
59. J K Lee, W L Ma, C J Brabec, J Yuen, J S Moon, J Y Kim, K Lee, G C Bazan, A J Heeger *J. Am. Chem. Soc.* **130** 3619 (2008)
60. M-S Su, C-Y Kuo, M-C Yuan, U-S Jeng, C-J Su, K-H Wei *Adv. Mater.* **23** 3315 (2011)
61. D Huang, Y Li, Z Xu, S Zhao, L Zhao, J Zhao *Phys. Chem. Chem. Phys.* **17** 8053 (2015)
62. L Lu, T Xu, W Chen, J M Lee, Z Luo, I H Jung, H I Park, S O Kim, L Yu *Nano Lett.* **13** 2365 (2013)
63. Y Li, Z Xu, S Zhao, D Huang, L Zhao, C Zhang, J Zhao, P Wang, Y Zhu *Org. Electron.* **28** 275 (2016)
64. K Sun, Z Xiao, S Lu, W Zajaczkowski, W Pisula, E Hanssen, J M White, R M Williamson, J Subbiah, J Ouyang, A B Holmes, W W Wong, D J Jones *Nat. Commun.* **6** 6013 (2015)
65. Z He, B Xiao, F Liu, H Wu, Y Yang, S Xiao, C Wang, T P Russell, Y Cao *Nat. Photonics* **9** 174 (2015)
66. Z He, C Zhong, S Su, M Xu, H Wu, Y Cao *Nat. Photonics* **6** 593 (2012)
67. B J Tremolet de Villers, K A O'Hara, D P Ostrowski, P H Biddle, S E Shaheen, M L Chabinyc, D C Olson, N Kopidakis *Chem. Mater.* **28** 876 (2016)
68. G Susanna, L Salamandra, C Ciceroni, F Mura, T M Brown, A Reale, M Rossi, A Di Carlo, F Brunetti *Sol. Energy Mater. Sol. Cells* **134** 194 (2015)
69. D J Burke, D J Lipomi *Energy Environ. Sci.* **6** 2053 (2013)
70. S H Liao, H-J Jhuo, Y-S Cheng, S-A Chen *Adv. Mater.* **25** 4766 (2013)
71. F B Kooistra, V D Mihailetchi, L M Popescu, D Kronholm, P W M Blom, J C Hummelen *Chem. Mater.* **18** 3068 (2006)
72. K Shibata, Y Kubozono, T Kanbara, T Hosokawa, A Fujiwara, Y Ito, H Shinohara *Appl. Phys. Lett.* **84** 2572 (2004)
73. S R Cowan, W L Leong, N Banerji, G Dennler, A J Heeger *Adv. Funct. Mater.* **21** 3083 (2011)
74. W L Leong, S R Cowan, A J Heeger *Adv. Energy Mater.* **1** 517 (2011)
75. L Kaake, X-D Dang, W L Leong, Y Zhang, A Heeger, T-Q Nguyen *Adv. Mater.* **25** 1706 (2013)
76. L M Popescu, P van't Hof, A B Sieval, H T Jonkman, J C Hummelen *Appl. Phys. Lett.* **89** 213507 (2006)
77. J Jo, S-S Kim, S-I Na, B-K Yu, D-Y Kim *Adv. Funct. Mater.* **19** 866 (2009)
78. J Peet, J Y Kim, N E Coates, W L Ma, D Moses, A J Heeger, G C Bazan *Nat. Mater.* **6** 497 (2007)
79. Y He, G Zhao, B Peng, Y Li *Adv. Funct. Mater.* **20** 3383 (2010)
80. C J Brabec, A Cravino, D Meissner, N S Sariciftci, T Fromherz, M T Rispens, L Sanchez, J C Hummelen *Adv. Funct. Mater.* **11** 374 (2001)
81. L J A Koster, V D Mihailetchi, R Ramaker, P W M Blom *Appl. Phys. Lett.* **86** 123509 (2005)
82. M C Scharber, D Mühlbacher, M Koppe, P Denk, C Waldauf, A J Heeger, C J Brabec *Adv. Mater.* **18** 789 (2006)
83. J J M Halls, J Cornil, D A dos Santos, R Silbey, D-H Hwang, A B Holmes, J L Brédas, R H Friend *Phys. Rev. B* **60** 5721 (1999)
84. C J Brabec, C Winder, N S Sariciftci, J C Hummelen, A Dhanabalan, P A van Hal, R A Janssen *Adv. Funct. Mater.* **12** 709 (2002)
85. F Zhang, J Bijleveld, E Perzon, K Tvingstedt, S Barrau, O Inganäs, M R Andersson *J. Mater. Chem.* **18** 5468 (2008)
86. R B Ross, C M Cardona, D M Guldi, S G Sankaranarayanan, M O Reese, N Kopidakis, J Peet, B Walker, G C Bazan, E Van Keuren, B C Holloway, M Drees *Nat. Mater.* **8** 208 (2009)
87. L J A Koster, V D Mihailetchi, P W M Blom *Appl. Phys. Lett.* **88** 093511 (2006)
88. D Mmhlbacher, M Scharber, M Morana, Z Zhu, D Waller, R Gaudiana, C Brabec *Adv. Mater.* **18** 2884 (2006)
89. M Lenes, G-J A H Wetzelaer, F B Kooistra, S C Veenstra, J C Hummelen, P W M Blom *Adv. Mater.* **20** 2116 (2008)
90. M Lenes, S W Shelton, A B Sieval, D F Kronholm, J C (Kees) Hummelen, P W M Blom *Adv. Funct. Mater.* **19** 3002 (2009)
91. M H Yun, G-H Kim, C Yang, J Y Kim *J. Mater. Chem.* **20** 7710 (2010)
92. B Kim, H R Yeom, W-Y Choi, J Y Kim, C Yang *Tetrahedron* **68** 6696 (2012)
93. H Kang, C-H Cho, H-H Cho, T E Kang, H J Kim, K-H Kim, S C Yoon, B J Kim *ACS Appl. Mater. Interfaces* **4** 110 (2012)

94. D Di Nuzzo, G-J A H Wetzelaer, R K M Bouwer, V S Gevaerts, S C J Meskers, J C Hummelen, P W M Blom, R A J Janssen *Adv. Energy Mater.* **3** 85 (2013)
95. H-W Liu, D-Y Chang, W-Y Chiu, S-P Rwei, L Wang *J. Mater. Chem.* **22** 15586 (2012)
96. L Ye, S Zhang, D Qian, Q Wang, J Hou *J. Phys. Chem. C* **117** 25360 (2013)
97. H Chen, J Peet, Y-C Hsiao, B Hu, M Dadmun *Chem. Mater.* **26** 3993 (2014)
98. N C Cates, R Gysel, Z Beiley, C E Miller, M F Toney, M Heeney, I McCulloch, M D McGehee *Nano Lett.* **9** 4153 (2009)
99. J H Choi, K-I Son, T Kim, K Kim, K Ohkubo, S Fukuzumi *J. Mater. Chem.* **20** 475 (2010)
100. Y Li *Chem. – Asian J.* **8** 2316 (2013)
101. K Vandewal, K Tvingstedt, A Gadisa, O Inganäs, J V Manca *Nat. Mater.* **8** 904 (2009)
102. K Vandewal, A Gadisa, W D Oosterbaan, S Bertho, F Banishoeib, I Van Severen, L Lutsen, T J Cleij, D Vanderzande, J V Manca *Adv. Funct. Mater.* **18** 2064 (2008)
103. M D Perez, C Borek, S R Forrest, M E Thompson *J. Am. Chem. Soc.* **131** 9281 (2009)
104. X Guo, N Zhou, S J Lou, J Smith, D B Tice, J W Hennek, R P Ortiz, J T L Navarrete, S Li, J Strzalka, L X Chen, R P H Chang, A Facchetti, T J Marks *Nat. Photonics* **7** 825 (2013)
105. Y-S Kim, B-K Yu, J W Kim, Y-H Suh, D-Y Kim, W B Kim *J. Mater. Chem. A* **1** 5015 (2013)
106. N Ćelić, E Pavlica, M Borovšak, J Strle, J Buh, J Zavašnik, G Bratina, P Denk, M Scharber, N S Sariciftci, D Mihailovic *Synth. Met.* **212** 105 (2016)
107. T Salim, H-W Lee, L H Wong, J H Oh, Z Bao, Y M Lam *Adv. Funct. Mater.* **26** 51 (2016)
108. Y Zhang, T P Basel, B R Gautam, X Yang, D J Mascaro, F Liu, Z V Vardeny *Nat. Commun.* **3** 1043 (2012)
109. A Rao, P C Chow, S Géinas, C W Schlenker, C-Z Li, H L Yip, A K-Y Jen, D S Ginger, R H Friend *Nature (London)* **500** 435 (2013)
110. A E Jailaubekov, A P Willard, J R Tritsch, W-L Chan, N Sai, R Gearba, L G Kaake, K J Williams, K Leung, P J Rossky, X Y Zhu *Nat. Mater.* **12** 66 (2013)
111. J R Ochsmann, D Chandran, D W Gehrig, H Anwar, P K Madathil, K S Lee, F Laquai *Macromol. Rapid Commun.* **36** 1122 (2015)
112. B Bernardo, D Cheyns, B Verreet, R D Schaller, B P Rand, N C Giebink *Nat. Commun.* **5** 3245 (2014)
113. J Niklas, K L Mardis, B P Banks, G M Grooms, A Sperlich, V Dyakonov, S Beaupré, M Leclerc, T Xu, L Yu, O G Poluektov *Phys. Chem. Chem. Phys.* **15** 9562 (2013)
114. J Niklas, S Beaupré, M Leclerc, T Xu, L Yu, A Sperlich, V Dyakonov, O G Poluektov *J. Phys. Chem. B* **119** 7407 (2015)
115. J L Brédas, J E Norton, J Cornil, V Coropceanu *Acc. Chem. Res.* **42** 1691 (2009)
116. L Sanchez, M Ángeles Herranz, N Martín *J. Mater. Chem.* **15** 1409 (2005)
117. J Ge, J Liu, X Guo, Y Qin, H Luo, Z-X Guo, Y Li *Chem. Phys. Lett.* **535** 100 (2012)
118. J L Delgado, E Espíldora, M Liedtke, A Sperlich, D Rauh, A Baumann, C Deibel, V Dyakonov, N Martín *Chem-Eur. J.* **15** 13474 (2009)
119. J Liu, X Guo, Y Qin, S Liang, Z-X Guo, Y Li *J. Mater. Chem.* **22** 1758 (2012)
120. J L Segura, N Martín *Chem. Soc. Rev.* **29** 13 (2000)
121. Y Morinaka, M Nobori, M Murata, A Wakamiya, T Sagawa, S Yoshikawa, Y Murata *Chem. Commun.* **49** 3670 (2013)
122. Y Liu, C-C Chen, Z Hong, J Gao, Y (M) Yang, H Zhou, L Dou, G Li, Y Yang *Sci. Rep.* **3** 3356 (2013)
123. Q Zhang, B Kan, F Liu, G Long, X Wan, X Chen, Y Zuo, W Ni, H Zhang, M Li, Z Hu, F Huang, Y Cao, Z Liang, M Zhang, T P Russell, Y Chen *Nat. Photonics* **9** 35 (2014)
124. J Y Kim, K Lee, N E Coates, D Moses, T-Q Nguyen, M Dante, A J Heeger *Science* **317** 222 (2007)
125. J You, L Dou, K Yoshimura, T Kato, K Ohya, T Moriarty, K Emery, C-C Chen, J Gao, G Li, Y Yang *Nat. Commun.* **4** 1446 (2013)
126. D Sukeguchi, S P Singh, M R Reddy, H Yoshiyama, R A Afre, Y Hayashi, H Inukai, T Soga, S Nakamura, N Shibata, T Toru *Beilstein J. Org. Chem.* **5** 7 (2009)
127. D Baran, S Erten-Ela, A Kratzer, T Ameri, C J Brabec, A Hirsch *RSC Adv.* **5** 64724 (2015)
128. W Cambarau, U F Fritze, A Viterisi, E Palomares, M von Delius *Chem. Commun.* **51** 1128 (2015)
129. D Mi, J-H Kim, H U Kim, F Xu, D-H Hwang *J. Nanosci. Nanotechnol.* **14** 1064 (2014)
130. A A Popov, S Yang, L Dunsch *Chem. Rev.* **113** 5989 (2013)
131. H Cong, B Yu, T Akasaka, X Lu *Coord. Chem. Rev.* **257** 2880 (2013)
132. M Rudolf, S Wolfrum, D M Guldi, L Feng, T Tsuchiya, T Akasaka, L Echegoyen *Chem. – Eur. J.* **18** 5136 (2012)
133. S Stevenson, G Rice, T Glass, K Harich, F Cromer, M R Jordan, J Craft, E Hadju, R Bible, M M Olmstead, K Maitra, A J Fisher, A L Balch, H C Dorn *Nature (London)* **401** 55 (1999)
134. J Zhang, S Stevenson, H C Dorn *Acc. Chem. Res.* **46** 1548 (2013)
135. J R Pinzón, D C Gasca, S G Sankaranarayanan, G Bottari, T Torres, D M Guldi, L Echegoyen *J. Am. Chem. Soc.* **131** 7727 (2009)
136. J R Pinzón, C M Cardona, M Ángeles Herranz, M E Plonska-Brzezinska, A Palkar, A J Athans, N Martín, A Rodríguez-Fortea, J M Poblet, G Bottari, T Torres, S S Gayathri, D M Guldi, L Echegoyen *Chem. – Eur. J.* **15** 864 (2009)
137. J R Pinzón, M E Plonska-Brzezinska, C M Cardona, A J Athans, S S Gayathri, D M Guldi, M Ángeles Herranz, N Martín, T Torres, L Echegoyen *Angew. Chem., Int. Ed.* **47** 4173 (2008)
138. C M Cardona, A Kitaygorodskiy, A Ortiz, M Ángeles Herranz, L Echegoyen *J. Org. Chem.* **70** 5092 (2005)
139. C Shu, W Xu, C Slebodnick, H Champion, W Fu, J E Reid, H Azurmendi, C Wang, K Harich, H C Dorn, H W Gibson *Org. Lett.* **11** 1753 (2009)
140. M N Chaur, A J Athans, L Echegoyen *Tetrahedron* **64** 11387 (2008)
141. M Liedtke, A Sperlich, H Kraus, A Baumann, C Deibel, M J Wirix, J Loos, C M Cardona, V Dyakonov *J. Am. Chem. Soc.* **133** 9088 (2011)
142. L Feng, M Rudolf, S Wolfrum, A Troeger, Z Slanina, T Akasaka, S Nagase, N Martín, T Ameri, C J Brabec, D M Guldi *J. Am. Chem. Soc.* **134** 12190 (2012)
143. A Fujii, T Umeda, T Shirakawa, T Akasaka, K Yoshino *Jpn. J. Appl. Phys. Part 1* **41** 2254 (2002)
144. Shang Yang, L Fan, Shihe Yang *Chem. Phys. Lett.* **388** 253 (2004)

145. Shang Yang, L Fan, Shihe Yang *J. Phys. Chem. B* **108** 4394 (2004)
146. L Fan, Shang Yang, Shihe Yang *Thin Solid Films* **483** 95 (2005)
147. Y Takano, M Ángeles Herranz, N Martín, S G Radhakrishnan, D M Guldi, T Tsuchiya, S Nagase, T Akasaka *J. Am. Chem. Soc.* **132** 8048 (2010)
148. D M Guldi, L Feng, S G Radhakrishnan, H Nikawa, M Yamada, N Mizorogi, T Tsuchiya, T Akasaka, S Nagase, M Ángeles Herranz, N Mártin *J. Am. Chem. Soc.* **132** 9078 (2010)
149. P W Dunk, M Mulet-Gas, Y Nakanishi, N K Kaiser, A Rodríguez-Fortea, H Shinohara, J M Poblet, A G Marshall, H W Kroto *Nat. Commun.* **5** 5844 (2014)
150. G Zhang, G Kim, W Choi *Energy Environ. Sci.* **7** 954 (2014)
151. Y Park, N J Singh, K S Kim, T Tachikawa, T Majima, W Choi *Chem. – Eur. J.* **15** 10843 (2009)
152. B Chai, T Peng, X Zhang, J Mao, K Li, X Zhang *Dalton Trans.* **42** 3402 (2013)
153. S Wang, C Liu, K Dai, P Cai, H Chen, C Yang, Q Huang *J. Mater. Chem. A* **3** 21090 (2015)
154. C-B Liu, Y Cong, H-Y Sun, G-B Che, J-S Zhang *CrystEngComm* **16** 5275 (2014)
155. W-C Oh, F-J Zhang, M-L Chen *J. Ind. Eng. Chem.* **16** 299 (2010)
156. L Zhang, Y Wang, T Xu, S Zhu, Y Zhu *J. Mol. Catal. A: Chem.* **331** 7 (2010)
157. J Lim, D Monllor-Satoca, J S Jang, S Lee, W Choi *Appl. Catal. B: Environ.* **152 – 153** 233 (2014)
158. M Yang, H Jha, N Liu, P Schmuki *J. Mater. Chem.* **21** 15205 (2011)
159. J Lee, S Mahendra, P J J Alvarez *ACS Nano* **4** 3580 (2010)
160. Y Li, J Niu, E Shang, J C Crittenden *Environ. Sci. Technol.* **49** 965 (2015)
161. J P Kamat, T P A Devasagayam, K I Priyadarsini, H Mohan *Toxicology* **155** 55 (2000)
162. W Bai, V Krishna, J Wang, B Moudgil, B Koopman *Appl. Catal., B: Environ.* **125** 128 (2012)
163. V Krishna, N Noguchi, B Koopman, B Moudgil *J. Colloid Interface Sci.* **304** 166 (2006)
164. V Krishna, D Yanes, W Imaram, A Angerhofer, B Koopman, B Moudgil *Appl. Catal., B: Environ.* **79** 376 (2008)
165. A R Badireddy, E M Hotze, S Chellam, P Alvarez, M R Wiesner *Environ. Sci. Technol.* **41** 6627 (2007)
166. L Brunet, D Y Lyon, E M Hotze, P J J Alvarez, M R Wiesner *Environ. Sci. Technol.* **43** 4355 (2009)
167. J Lee, Y Mackeyev, M Cho, D Li, J-H Kim, L J Wilson, P J J Alvarez *Environ. Sci. Technol.* **43** 6604 (2009)
168. G Liu, C Chen, H Ji, W Ma, J Zhao *Sci. China Chem.* **55** 1953 (2011)
169. L Bazinet, A Doyen *Crit. Rev. Food Sci. Nutr.* **57** 677 (2017)
170. M Aslam, A Charfi, G Lesage, M Heran, J Kim *Chem. Eng. J.* **307** 897 (2017)
171. B Swain *Sep. Purif. Technol.* **172** 388 (2017)
172. Y K Ong, G M Shi, N L Le, Y P Tang, J Zuo, S P Nunes, T-S Chung *Prog. Polym. Sci.* **57** 1 (2016)
173. M Shestakova, M Sillanpii *Chemosphere* **93** 1258 (2013)
174. A V Penkova, Z Pientka, G A Polotskaya *Fullerenes Nanotubes Carbon Nanostruct.* **19** 137 (2011)
175. A Friedl *FEMS Microbiol. Lett.* **363** Art. No. fnw073 (2016)
176. A V Penkova, S F A Acquah, M E Dmitrenko, B Chen, K N Semenov, H W Kroto *Carbon* **76** 446 (2014)
177. A V Penkova, S F A Acquah, M P Sokolova, M E Dmitrenko, A M Toikka *J. Membr. Sci.* **491** 22 (2015)
178. R Dobashi, K Matsunaga, M Tajima *J. Appl. Polym. Sci.* **131** Art. No. 39986 (2014)
179. F C Chen, Z Gao, R O Loutfy, M Hecht *Fuel Cells* **3** 181 (2004)
180. K Tasaki, R DeSousa, H Wang, J Gasa, A Venkatesan, P Pugazhendhi, R O Loutfy *J. Membr. Sci.* **281** 570 (2006)
181. D V Postnov, N A Melnikova, V N Postnov, K N Semenov, I V Murin *Rev. Adv. Mater. Sci.* **39** 20 (2014)
182. S H Friedman, D L DeCamp, R P Sijbesma, G Srdanov, F Wudl, G L Kenyon *J. Am. Chem. Soc.* **115** 6506 (1993)
183. R Sijbesma, G Srdanov, F Wudl, J A Castoro, C Wilkins, S H Friedman, D L DeCamp, G L Kenyon *J. Am. Chem. Soc.* **115** 6510 (1993)
184. S K Sharma, L Y Chiang, M R Hamblin *Nanomedicine* **6** 1813 (2011)
185. A Montellano, T Da Ros, A Bianco, M Prato *Nanoscale* **3** 4035 (2011)
186. A Dellinger, Z Zhou, J Connor, A B Madhankumar, S Pamujula, C M Sayes, C L Kepley *Nanomedicine* **8** 1191 (2013)
187. X Yang, A Ebrahimi, J Li, Q Cui *Int. J. Nanomed.* **9** 77 (2014)
188. S V Kurmaz, N A Obraztsova *Mendeleev Commun.* **25** 350 (2015)
189. O L Kobzar, V V Trush, V Y Tanchuk, I I Voronov, A S Peregudov, P A Troshin, A I Vovk *Mendeleev Commun.* **25** 199 (2015)
190. I A Avilova, A V Chernyak, A V Zhilenkov, P A Troshin, V I Volkov *Mendeleev Commun.* **26** 146 (2016)
191. K B Hartman, L J Wilson, M G Rosenblum *Mol. Diagn. Ther.* **12** 1 (2008)
192. M L Matson, L J Wilson *Future Med. Chem.* **2** 491 (2010)
193. E Nakamura, H Isobe *Acc. Chem. Res.* **36** 807 (2003)
194. R Martin, H-L Wang, J Gao, S Iyer, G A MontaKho, J Martinez, A P Shreve, Y Bao, C-C Wang, Z Chang, Y Gao, R Iyer *Toxicol. Appl. Pharmacol.* **234** 58 (2009)
195. B Belgorodsky, L Fadeev, J Kolsenik, M Gozin *ChemBioChem* **7** 1783 (2006)
196. S Li, X Zhao, Y Mo, P T Cummings, W T Heller *J. Nanopart. Res.* **15** Art. No. 1769 (2013)
197. S Deguchi, T Yamazaki, S Mukai, R Usami, K Horikoshi *Chem. Res. Toxicol.* **20** 854 (2007)
198. L Kong, R G Zepp *Environ. Toxicol. Chem.* **31** 136 (2012)
199. J Lee, Y Yamakoshi, J B Hughes, J-H Kim *Environ. Sci. Technol.* **42** 3459 (2008)
200. S Bosi, T Da Ros, G Spalluto, M Prato *Eur. J. Med. Chem.* **38** 913 (2003)
201. R Bakry, R M Vallant, M Najam-ul-Haq, M Rainer, Z Szabo, C W Huck, G K Bonn *Int. J. Nanomed.* **2** 639 (2007)
202. N Gharbi, M Pressac, M Hadchouel, H Szwarc, S R Wilson, F Moussa *Nano Lett.* **5** 2578 (2005)
203. J A Brant, J Labille, J Y Bottero, M R Wiesner *Langmuir* **22** 3878 (2006)
204. L L Dugan, D M Turetsky, C Du, D Lobner, M Wheeler, C R Almli, C K-F Shen, T-Y Luh, D W Choi, T-S Lin *Proc. Natl. Acad. Sci. USA* **94** 9434 (1997)
205. Z Hu, W Guan, W Wang, L Huang, X Tang, H Xu, Z Zhu, X Xie, H Xing *Carbon* **46** 99 (2008)
206. F Beuerle, R Lebovitz, A Hirsch, in *Medicinal Chemistry and Pharmacological Potential of Fullerenes and Carbon Nanotubes (Carbon Materials: Chemistry and Physics)* Vol. 1 (Eds F Cataldo, T Da Ros) (Springer, 2008) p. 51

207. D M Guldi, M Prato *Acc. Chem. Res.* **33** 695 (2000)
208. V Georgakilas, F Pellarini, M Prato, D M Guldi, M Melle-Franco, F Zerbetto *Proc. Natl. Acad. Sci. USA* **99** 5075 (2002)
209. J Wong-Ekkabut, S Baoukina, W Triampo, I-M Tang, D P Tieleman, L Monticelli *Nat. Nanotechnol.* **3** 363 (2008)
210. J Brant, H Lecoanet, M R Wiesner *J. Nanopart. Res.* **7** 545 (2005)
211. M Calvaresi, F Zerbetto *ACS Nano* **4** 2283 (2010)
212. H Isobe, W Nakanishi, N Tomita, S Jinno, H Okayama, E Nakamura *Chem. – Asian J.* **1** 167 (2006)
213. H Isobe, W Nakanishi, N Tomita, S Jinno, H Okayama, E Nakamura *Mol. Pharm.* **3** 124 (2006)
214. R Maeda-Mamiya, E Noiri, H Isobe, W Nakanishi, K Okamoto, K Doi, T Sugaya, T Izumi, T Homma, E Nakamura *Proc. Natl. Acad. Sci. USA* **107** 5339 (2010)
215. H Li, Y Zhang, Y Luo, X Sun *Small* **7** 1562 (2011)
216. B de La Vaissière, J P B Sandall, P W Fowler, P de Oliveira, R V Bensasson *J. Chem. Soc., Perkin Trans. 2* 821 (2001)
217. P Witte, F Beuerle, U Hartnagel, R Lebovitz, A Savouchkina, S Sali, D Guldi, N Chronakis, A Hirsch *Org. Biomol. Chem.* **5** 3599 (2007)
218. M Brettreich, A Hirsch *Tetrahedron Lett.* **39** 2731 (1998)
219. F Beuerle, P Witte, U Hartnagel, R Lebovitz, C Parng, A Hirsch *J. Exp. Nanosci.* **2** 147 (2007)
220. H Kato, C Böttcher, A Hirsch *Eur. J. Org. Chem.* 2659 (2007)
221. Y N Yamakoshi, T Yagami, K Fukuhara, S Sueyoshi, N Miyata *J. Chem. Soc., Chem. Commun.* 517 (1994)
222. J Tong, M C Zimmerman, S Li, X Yi, R Luxenhofer, R Jordan, A V Kabanov *Biomaterials* **32** 3654 (2011)
223. S-I Yusa, S Awa, M Ito, T Kawase, T Takada, K Nakashima, D Liu, S Yamago, Y Morishima *J. Polym. Sci., Part A: Polym. Chem.* **49** 2761 (2011)
224. Z Zhou, R P Lenk, A Dellinger, S R Wilson, R Sadler, C L Kepley *Bioconjug. Chem.* **21** 1656 (2010)
225. Z Zhou *Pharmaceutics* **5** 525 (2013)
226. I Ramakanth, A Patnaik *Carbon* **46** 692 (2008)
227. F Liao, Y Saitoh, N Miwa *Oncol. Res.* **19** 203 (2011)
228. R Asada, F Liao, Y Saitoh, N Miwa *Mol. Cell. Biochem.* **390** 175 (2014)
229. V I Bhoi, S Kumar, C N Murthy *Carbohydr. Res.* **359** 120 (2012)
230. Y Rio, J F Nierengarten *Tetrahedron Lett.* **43** 4321 (2002)
231. L B Piotrovsky, M Y Eropkin, E M Eropkina, M A Dumpis, O I Kiselev, in *Medicinal Chemistry and Pharmacological Potential of Fullerenes and Carbon Nanotubes (Carbon Materials: Chemistry and Physics)* Vol. 1 (Eds F Cataldo, T Da Ros) (Springer, 2008) p. 139
232. L Xiao, H Aoshima, Y Saitoh, N Miwa *Biomaterials* **31** 5976 (2010)
233. S Kato, M Kimura, N Miwa *Radiat. Phys. Chem.* **97** 134 (2014)
234. A Ikeda, T Sato, K Kitamura, K Nishiguchi, Y Sasaki, J Kikuchi, T Ogawa, K Yogo, T Takeya *Org. Biomol. Chem.* **3** 2907 (2005)
235. A Ikeda, T Genmoto, N Maekubo, J Kikuchi, M Akiyama, T Mochizuki, S Kotani, T Konishi *Chem. Lett.* **39** 1256 (2010)
236. M Bortolus, G Parisio, A L Maniero, A Ferrarini *Langmuir* **27** 12560 (2011)
237. Y-L Lin, H-Y Lei, Y-Y Wen, T-Y Luh, C-K Chou, H-S Liu *Virology* **275** 258 (2000)
238. N Tsao, T-Y Luh, C-K Chou, T-Y Chang, J-J Wu, C-C Liu, H-Y Lei *J. Antimicrob. Chemother.* **49** 641 (2002)
239. L B Piotrovsky, O I Kiselev *Fullerenes Nanotubes Carbon Nanostruct.* **12** 397 (2004)
240. L B Piotrovsky, in *Carbon Nanotechnology: Recent Developments in Chemistry, Physics, Materials Science and Device Applications* (Ed. L Dai) (Amsterdam: Elsevier, 2006) p. 235
241. P Mroz, G P Tegos, H Gali, T Wharton, T Sarna, M R Hamblin *Photochem. Photobiol. Sci.* **6** 1139 (2007)
242. M Horie, K Nishio, H Kato, N Shinohara, A Nakamura, K Fujita, S Kinugasa, S Endoh, Y Yoshida, Y Hagihara, H Iwahashi *Chemosphere* **93** 1182 (2013)
243. C Nishizawa, N Hashimoto, S Yokoo, M Funakoshi-Tago, T Kasahara, K Takahashi, S Nakamura, T Mashino *Free Radical Res.* **43** 1240 (2009)
244. Z Chen, R Mao, Y Liu *Curr. Drug Metab.* **13** 1035 (2012)
245. Z Dou, Y Xu, H Sun, Y Liu *Nanoscale* **4** 4624 (2012)
246. L Cheng, C Wang, L Feng, K Yang, Z Liu *Chem. Rev.* **114** 10869 (2014)
247. Y-Y Huang, S K Sharma, R Yin, T Agrawal, L Y Chiang, M R Hamblin *J. Biomed. Nanotechnol.* **10** 1918 (2014)
248. F Käsermann, C Kempf *Rev. Med. Virology* **8** 143 (1998)
249. A Ikeda, Y Doi, K Nishiguchi, K Kitamura, M Hashizume, J-i Kikuchi, K Yogo, T Ogawa, T Takeya *Org. Biomol. Chem.* **5** 1158 (2007)
250. M Akiyama, A Ikeda, T Shintani, Y Doi, J-i Kikuchi, T Ogawa, K Yogo, T Takeya, N Yamamoto *Org. Biomol. Chem.* **6** 1015 (2008)
251. Y Doi, A Ikeda, M Akiyama, M Nagano, T Shigematsu, T Ogawa, T Takeya, T Nagasaki *Chem. – Eur. J.* **14** 8892 (2008)
252. F F Sperandio, S K Sharma, M Wang, S Jeon, Y-Y Huang, T Dai, S Nayka, S C O M de Sousa, L Y Chiang, M R Hamblin *Nanomed. Nanotechnol. Biol. Med.* **9** 570 (2013)
253. G C Jiang, Q X Zheng, D Z Yang *J. Appl. Polym. Sci.* **99** 2874 (2006)
254. Y Tabata, Y Ikada *Pure Appl. Chem.* **71** 2047 (1999)
255. J Liu, Y Tabata *J. Drug Target.* **18** 602 (2010)
256. J Liu, Y Tabata *J. Biomater. Sci., Polym. Ed.* **22** 297 (2011)
257. Z Lu, T Dai, L Huang, D B Kurup, G P Tegos, A Jahnke, T Wharton, M R Hamblin *Nanomedicine* **5** 1525 (2010)
258. K Mizuno, T Zhiyentayev, L Huang, S Khalil, F Nasim, G P Tegos, H Gali, A Jahnke, T Wharton, M R Hamblin *J. Nanomed. Nanotechnol.* **2** Art. No. 109 (2011)
259. M B Spesia, A E Milanesio, E N Durantini *Eur. J. Med. Chem.* **43** 853 (2008)
260. L Huang, M Terakawa, T Zhiyentayev, Y-Y Huang, Y Sawayama, A Jahnke, G P Tegos, T Wharton, M R Hamblin *Nanomed. Nanotechnol. Biol. Med.* **6** 442 (2010)
261. R Yin, M Wang, Y-Y Huang, H-C Huang, P Avci, L Y Chiang, M R Hamblin *Nanomed. Nanotechnol. Biol. Med.* **10** 795 (2014)
262. A Ikeda, M Akiyama, T Ogawa, T Takeya *ACS Med. Chem. Lett.* **1** 115 (2010)
263. S-K Kim, F Karadeniz, in *Marine Medicinal Foods: Implications and Applications — Animals and Microbes (Advances in Food and Nutrition Research)* Vol. 65 (1st Edn) (Ed. S-K Kim) (Amsterdam: Academic Press, 2012) p. 223
264. S H Friedman, P S Ganapathi, Y Rubin, G L Kenyon *J. Med. Chem.* **41** 2424 (1998)
265. Z W Zhu, D I Schuster, M E Tuckerman *Biochemistry* **42** 1326 (2003)
266. T Mashino, K Okuda, T Hirota, M Hirobe, T Nagano, M Mochizuki *Fullerene Sci. Technol.* **9** 191 (2001)

267. D J Wolff, K Mialkowski, C F Richardson, S R Wilson *Biochemistry* **40** 37 (2001)
268. D J Wolff, A D P Papoiu, K Mialkowski, C F Richardson, D I Schuster, S R Wilson *Arch. Biochem. Biophys.* **378** 216 (2000)
269. H Jin, W Q Chen, X W Tang, L Y Chiang, C Y Yang, J V Schloss, J Y Wu *J. Neurosci. Res.* **62** 600 (2000)
270. G Pastorin, S Marchesan, J Hoebeke, T Da Ros, L Ehret-Sabatier, J-P Briand, M Prato, A Bianco *Org. Biomol. Chem.* **4** 2556 (2006)
271. D Giust, D León, I Ballesteros-Yañez, T Da Ros, J L Albasanz, M Martín *ACS Chem. Neurosci.* **2** 363 (2011)
272. B-X Chen, S R Wilson, M Das, D J Coughlin, B F Erlanger *Proc. Natl. Acad. Sci. USA* **95** 10809 (1998)
273. B C Braden, F A Goldbaum, B-X Chen, A N Kirschner, S R Wilson, B F Erlanger *Proc. Natl. Acad. Sci. USA* **97** 12193 (2000)
274. O D Hendrickson, N S Fedyunina, A A Martianov, A V Zherdev, B B Dzantiev *J. Nanopart. Res.* **13** 3713 (2011)
275. S Foley, C Crowley, M Smaihi, C Bonfils, B F Erlanger, P Seta, C Larroque *Biochem. Biophys. Res. Commun.* **294** 116 (2002)
276. W H Noon, Y F Kong, J P Ma *Proc. Natl. Acad. Sci. USA* **99** 6466 (2002)
277. A Bianco, C Corvaja, M Crisma, D M Guldi, M Maggini, E Sartori, C Toniolo *Chem. – Eur. J.* **8** 1544 (2002)
278. C Ratna Prabha, R Patel, C N Murthy *Fullerenes Nanotubes Carbon Nanostruct.* **12** 405 (2005)
279. B Belgorodsky, L Fadeev, V Ittah, H Benyamini, S Zelner, D Huppert, A B Kotlyar, M Gozin *Bioconjug. Chem.* **16** 1058 (2005)
280. J Kolsenik, B Belgorodsky, L Fadeev, M Gozin *J. Nanosci. Nanotechnol.* **7** 1389 (2007)
281. M Calvaresi, F Zerbetto *Nanoscale* **3** 2873 (2011)
282. B Belgorodsky, L Fadeev, J Kolsenik, M Gozin *Bioconjug. Chem.* **18** 1095 (2007)
283. H Benyamini, A Shulman-Peleg, H J Wolfson, B Belgorodsky, L Fadeev, M Gozin *Bioconjug. Chem.* **17** 378 (2006)
284. U Kragh-Hansen, V T G Chuang, M Otagiri *Biol. Pharm. Bull.* **25** 695 (2002)
285. T A Ratnikova, P N Govindan, E Salonen, P C Ke *ACS Nano* **5** 6306 (2011)
286. X-f Zhang, C-y Shu, L Xie, C-r Wang, Y-z Zhang, J-f Xiang, L Li, Y-l Tang *J. Phys. Chem. C* **111** 14327 (2007)
287. Y Miao, J Xu, Y Shen, L Chen, Y Bian, Y Hu, W Zhou, F Zheng, N Man, Y Shen, Y Zhang, M Wang, L Wen *ACS Nano* **8** 6131 (2014)
288. J E Kim, M Lee *Biochem. Biophys. Res. Commun.* **303** 576 (2003)
289. I Ya Podolski, Z A Podlubnaya, E A Kosenko, E A Mugantseva, E G Makarova, L G Marsagishvili, M D Shpagina, Y G Kaminsky, G V Andrievsky, V K Klochkov *J. Nanosci. Nanotechnol.* **7** 1479 (2007)
290. A G Bobylev, A B Kornev, L G Bobyleva, M D Shpagina, I S Fadeeva, R S Fadeev, D G Deryabin, J Balzarini, P A Troshin, Z A Podlubnaya *Org. Biomol. Chem.* **9** 5714 (2011)
291. A G Bobylev, M D Shpagina, L G Bobyleva, A D Okuneva, L B Piotrovsky, Z A Podlubnaya *Biophysics* **57** 300 (2012)
292. E G Makarova, R Ya Gordon, I Ya Podolski *J. Nanosci. Nanotechnol.* **12** 119 (2012)
293. I Ya Podolski, Z A Podlubnaya, O V Godukhin *Biophysics* **55** 71 (2010)
294. S A Andujar, F Lugli, S Höfinger, R D Enriz, F Zerbetto *Phys. Chem. Chem. Phys.* **14** 8599 (2012)
295. L Xie, Y Luo, D Lin, W Xi, X Yang, G Wei *Nanoscale* **6** 9752 (2014)
296. M Mahmoudi, H R Kalhor, S Laurent, I Lynch *Nanoscale* **5** 2570 (2013)
297. C Li, R Mezzenga *Nanoscale* **5** 6207 (2013)
298. X Xu, X Wang, Y Li, Y Wang, L Yang *Nucleic Acids Res.* **40** 7622 (2012)
299. X Zhao, A Striolo, P T Cummings *Biophys. J.* **89** 3856 (2005)
300. M K Shukla, M Dubey, E Zakar, R Namburu, J Leszczynski *Chem. Phys. Lett.* **493** 130 (2010)
301. M Pinteala, A Dascalu, C Ungurenasu *Int. J. Nanomed.* **4** 193 (2009)
302. H An, B Jin *Environ. Sci. Technol.* **45** 6608 (2011)
303. N F Steinmetz, V Hong, E D Spoerke, P Lu, K Breitenkamp, M G Finn, M Manchester *J. Am. Chem. Soc.* **131** 17093 (2009)
304. Y N Yamakoshi, T Yagami, S Sueyoshi, N Miyata *J. Org. Chem.* **61** 7236 (1996)
305. A S Boutorine, H Tokuyama, M Takasugi, H Isobe, E Nakamura, C Hélène *Angew. Chem., Int. Ed. Engl.* **33** 2462 (1994)
306. T Da Ros, E Vázquez, G Spalluto, S Moro, A Boutorine, M Prato *J. Supramol. Chem.* **2** 327 (2002)
307. L B Piotrovskiy, E V Litasova, M A Dumpis, D N Nikolaev, E E Yakovleva, O A Dravolina, A Y Bespalov *Dokl. Biochem. Biophys.* **468** 173 (2016)
308. R Partha, M Lackey, A Hirsch, S Ward Casscells, J L Conyers *J. Nanobiotechnol.* **5** Art. No. 6 (2007)
309. R Partha, L R Mitchell, J L Lyon, P P Joshi, J L Conyers *ACS Nano* **2** 1950 (2008)
310. J Shi, H Zhang, L Wang, L Li, H Wang, Z Wang, Z Li, C Chen, L Hou, C Zhang, Z Zhang *Biomaterials* **34** 251 (2013)
311. Q Liu, L Xu, X Zhang, N Li, J Zheng, M Guan, X Fang, C Wang, C Shu *Chem. – Asian J.* **8** 2370 (2013)
312. F Rancan, M Helmreich, A Mölich, E A Ermilov, N Jux, B Röder, A Hirsch, F Böhm *Bioconjug. Chem.* **18** 1078 (2007)
313. F Perret, M Nishihara, T Takeuchi, S Futaki, A N Lazar, A W Coleman, N Sakai, S Matile *J. Am. Chem. Soc.* **127** 1114 (2005)
314. M Nishihara, F Perret, T Takeuchi, S Futaki, A N Lazar, A W Coleman, N Sakai, S Matile *Org. Biomol. Chem.* **3** 1659 (2005)
315. E Nakamura, H Isobe, N Tomita, M Sawamura, S Jinno, H Okayama *Angew. Chem., Int. Ed.* **39** 4254 (2000)
316. E Nakamura, H Isobe *Chem. Rec.* **10** 260 (2010)
317. B Sitharaman, T Y Zakharian, A Saraf, P Misra, J Ashcroft, S Pan, Q P Pham, A G Mikos, L J Wilson, D A Engler *Mol. Pharm.* **5** 567 (2008)
318. A Puri, R Blumenthal *Acc. Chem. Res.* **44** 1071 (2011)
319. Z Liu, X-J Liang *Theranostics* **2** 235 (2012)
320. Z Chen, L Ma, Y Liu, C Chen *Theranostics* **2** 238 (2012)
321. F Lu, Sk A Haque, S-T Yang, P G Luo, L Gu, A Kitaygorodskiy, H Li, S Lacher, Y-P Sun *J. Phys. Chem. C* **113** 17768 (2009)
322. J-H Liu, L Cao, P G Luo, S-T Yang, F Lu, H Wang, M J Meziani, Sk A Haque, Y Liu, S Lacher, Y-P Sun *ACS Appl. Mater. Interfaces* **2** 1384 (2010)

323. V Krishna, A Singh, P Sharma, N Iwakuma, Q Wang, Q Zhang, J Knapik, H Jiang, S R Grobmyer, B Koopman, B Moudgil *Small* **6** 2236 (2010)
324. V Krishna, N Stevens, B Koopman, B Moudgil *Nat. Nanotechnol.* **5** 330 (2010)
325. C-Y Shu, X-Y Ma, J-F Zhang, F D Corwin, J H Sim, E-Y Zhang, H C Dorn, H W Gibson, P P Fatouros, C-R Wang, X-H Fang *Bioconjug. Chem.* **19** 651 (2008)
326. M Zhen, J Zheng, L Ye, S Li, C Jin, K Li, D Qiu, H Han, C Shu, Y Yang, C Wang *ACS Appl. Mater. Interfaces* **4** 3724 (2012)
327. M D Shultz, J C Duchamp, J D Wilson, C-Y Shu, J Ge, J Zhang, H W Gibson, H L Fillmore, J I Hirsch, H C Dorn, P P Fatouros *J. Am. Chem. Soc.* **132** 4980 (2010)
328. J D Wilson, W C Broaddus, H C Dorn, P P Fatouros, C E Chalfant, M D Shultz *Bioconjug. Chem.* **23** 1873 (2012)
329. X Wang, C-X Yang, J-T Chen, X-P Yan *Anal. Chem.* **86** 3263 (2014)
330. J Shi, X Yu, L Wang, Y Liu, J Gao, J Zhang, R Ma, R Liu, Z Zhang *Biomaterials* **34** 9666 (2013)
331. R Injac, M Prijatelj, B Strukelj, in *Oxidative Stress and Nanotechnology: Methods and Protocols (Methods in Molecular Biology)* Vol. 1028 (Eds D Armstrong, D J Bharali) (New York, Heidelberg: Springer, 2013) p. 75
332. X Lu, L Feng, T Akasaka, S Nagase *Chem. Soc. Rev.* **41** 7723 (2012)
333. R D Bolskar *Nanomedicine* **3** 201 (2008)
334. J Wang, C Chen, B Li, H Yu, Y Zhao, J Sun, Y Li, G Xing, H Yuan, J Tang, Z Chen, H Meng, Y Gao, C Ye, Z Chai, C Zhu, B Ma, X Fang, L Wan *Biochem. Pharmacol.* **71** 872 (2006)
335. R Injac, M Perse, M Cerne, N Potocnik, N Radic, B Govedarica, A Djordjevic, A Cerar, B Strukelj *Biomaterials* **30** 1184 (2009)
336. I Rašović *Mater. Sci. Technol.* **33** 777 (2017)
337. M Mikawa, H Kato, M Okumura, M Narazaki, Y Kanazawa, N Miwa, H Shinohara *Bioconjug. Chem.* **12** 510 (2001)
338. É Tóth, R D Bolskar, A Borel, G González, L Helm, A E Merbach, B Sitharaman, L J Wilson *J. Am. Chem. Soc.* **127** 799 (2005)
339. R D Bolskar, A F Benedetto, L O Husebo, R E Price, E F Jackson, S Wallace, L J Wilson, J M Alford *J. Am. Chem. Soc.* **125** 5471 (2003)
340. C-Y Shu, L-H Gan, C-R Wang, X-l Pei, H-b Han *Carbon* **44** 496 (2006)
341. J Zhang, Y Ye, Y Chen, C Pregot, T Li, S Balasubramaniam, D B Hobart, Y Zhang, S Wi, R M Davis, L A Madsen, J R Morris, S M LaConte, G T Yee, H C Dorn *J. Am. Chem. Soc.* **136** 2630 (2014)
342. E B Iezzi, J C Duchamp, K R Fletcher, T E Glass, H C Dorn *Nano Lett.* **2** 1187 (2002)
343. J Zhang, P P Fatouros, C Shu, J Reid, L S Owens, T Cai, H W Gibson, G L Long, F D Corwin, Z-J Chen, H C Dorn *Bioconjug. Chem.* **21** 610 (2010)
344. A Dellinger, J Olson, K Link, S Vance, M G Sandros, J Yang, Z Zhou, C L Kepley *J. Cardiovasc. Magn. Reson.* **15** Art. No. 7 (2013)
345. D W Cagle, S J Kennel, S Mirzadeh, J M Alford, L J Wilson *Proc. Natl. Acad. Sci. USA* **96** 5182 (1999)
346. M D Diener, J M Alford, S J Kennel, S Mirzadeh *J. Am. Chem. Soc.* **129** 5131 (2007)
347. C Chen, G Xing, J Wang, Y Zhao, B Li, J Tang, G Jia, T Wang, J Sun, L Xing, H Yuan, Y Gao, H Meng, Z Chen, F Zhao, Z Chai, X Fang *Nano Lett.* **5** 2050 (2005)
348. J Meng, X Liang, X Chen, Y Zhao *Integr. Biol.* **5** 43 (2013)
349. Y Liu, F Jiao, Y Qiu, W Li, F Lao, G Zhou, B Sun, G Xing, J Dong, Y Zhao, Z Chai, C Chen *Biomaterials* **30** 3934 (2009)
350. S Yamago, H Tokuyama, E Nakamura, K Kikuchi, S Kananishi, K Sueki, H Nakahara, S Enomoto, F Ambe *Chem. Biol.* **2** 385 (1995)
351. R Bullard-Dillard, K E Creek, W A Scrivens, J M Tour *Bioorg. Chem.* **24** 376 (1996)
352. K Kobayashi, M Kuwano, K Sueki, K Kikuchi, Y Achiba, H Nakahara, N Kananishi, M Watanabe, K Tomura *J. Radioanal. Nucl. Chem.* **192** 81 (1995)
353. G L Baker, A Gupta, M L Clark, B R Valenzuela, L M Staska, S J Harbo, J T Pierce, J A Dill *Toxicol. Sci.* **101** 122 (2008)
354. T Mori, H Takada, S Ito, K Matsubayashi, N Miwa, T Sawaguchi *Toxicology* **225** 48 (2006)
355. V A Popov, M A Tyunin, O B Zaitseva, R H Karaev, N V Sirotinkin, M A Dumpis, L B Piotrovsky *Fullerenes Nanotubes Carbon Nanostruct.* **16** 693 (2008)
356. E Oberdörster *Environ. Health Perspect.* **112** 1058 (2004)
357. E Oberdörster, S Q Zhu, T M Blickley, P McClellan-Green, M L Haasch *Carbon* **44** 1112 (2006)
358. T B Henry, F-M Menn, J T Fleming, J Wilgus, R N Compton, G S Sayler *Environ. Health Perspect.* **115** 1059 (2007)
359. P Rajagopalan, F Wudl, R F Schinazi, F D Boudinot *Antimicrob. Agents Chemother.* **40** 2262 (1996)
360. C Cusan, T Da Ros, G Spalluto, S Foley, J-M Janot, P Seta, C Larroque, M C Tomasini, T Antonelli, L Ferraro, M Prato *Eur. J. Org. Chem.* 2928 (2002)
361. F Moussa, F Trivin, R Céolin, M Hadchouel, P-Y Sizaret, V Greugny, C Fabre, A Rassat, H Szwarc *Fullerene Sci. Technol.* **4** 21 (1996)
362. F Moussa, S Roux, M Pressac, E Génin, M Hadchouel, F Trivin, A Rassat, R Céolin, H Szwarc *New J. Chem.* **22** 989 (1998)
363. L Fan, Shang Yang, Shihe Yang *Fullerenes Nanotubes Carbon Nanostruct.* **13** (Suppl. 1) 155 (2005)
364. P S Sharma, M Dabrowski, K Noworyta, T-P Huynh, C B Kc, J W Sobczak, P Pieta, F D'Souza, W Kutner *Anal. Chim. Acta* **844** 61 (2014)
365. Y-F Gao, T Yang, X-L Yang, Y-S Zhang, B-L Xiao, J Hong, N Sheibani, H Ghourchian, T Hong, A A Moosavi-Movahedi *Biosens. Bioelectron.* **60** 30 (2014)
366. J Kyokane, H Ishimoto, H Yugen, T Hirai, T Ueda, K Yoshino *Synth. Met.* **103** 2366 (1999)
367. J Kyokane, K Tokugi, D Uranishi, M Miyata, T Ueda, K Yoshino *Synth. Met.* **121** 1129 (2001)
368. Y Nakama, J Kyokane, K Tokugi, T Ueda, K Yoshino *Synth. Met.* **135 – 136** 749 (2003)
369. J Li, S Vadahanambi, C-D Kee, I-K Oh *Biomacromolecules* **12** 2048 (2011)
370. M Rajagopalan, I-K Oh *ACS Nano* **5** 2248 (2011)
371. V Panwar, S Y Ko, J-O Park, S Park *Sens. Actuators, B* **183** 504 (2013)
372. G Itskos, A Othonos, T Rauch, S F Tedde, O Hayden, M V Kovalenko, W Heiss, S A Choulis *Adv. Energy Mater.* **1** 802 (2011)
373. A Lange, H Flügge, B Fischer, H Schmidt, C Boeffel, M Wegener, T Riedl, W Kowalsky *Synth. Met.* **162** 522 (2012)

374. X-X Liao, T Wang, J Wang, J-C Zheng, C Wang, V W-W Yam *ACS Appl. Mater. Interfaces* **5** 9579 (2013)
375. K Szendrei, D Jarzab, M Yarema, M Sytnyk, S Pichler, J C Hummelen, W Heiss, M A Loi *J. Mater. Chem.* **20** 8470 (2010)
376. P Damlin, M Hätönen, S E Domínguez, T Ääritalo, H Kivelä, C Kvarnström *RSC Adv.* **4** 8391 (2014)
377. B Kraabel, D McBranch, B Hsieh, F Wudl *Synth. Met.* **101** 281 (1999)
378. S Aikawa, Y Yoshida, S Nishiyama, H Noguchi, A Shoji *Mol. Cryst. Liq. Cryst.* **445** 315 (2006)
379. Y-P Sun, J E Riggs *Int. Rev. Phys. Chem.* **18** 43 (1999)
380. H I Elim, J Ouyang, S H Goh, W Ji *Thin Solid Films* **477** 63 (2005)
381. J Ouyang, S H Goh, H I Elim, G C Meng, W Ji *Chem. Phys. Lett.* **366** 224 (2002)
382. H I Elim, W Ji, G C Meng, J Ouyang, S H Goh *J. Nonlinear Opt. Phys. Mater.* **12** 175 (2003)
383. M Cha, N S Sariciftci, A J Heeger, J C Hummelen, F Wudl *Appl. Phys. Lett.* **67** 3850 (1995)
384. S H Chi, J M Hales, M Cozzuol, C Ochoa, M Fitzpatrick, J W Perry *Opt. Express* **17** 22062 (2009)
385. I Etxebarria, J Ajuria, R Pacios *Org. Electron.* **19** 34 (2015)
386. N Li, D Baran, G D Spyropoulos, H Zhang, S Berny, M Turbiez, T Ameri, F C Krebs, C J Brabec *Adv. Energy Mater.* **4** 1400084 (2014)
387. S F A Acquah, A V Penkova, D A Markelov, A S Semisalova, B E Leonhardt, J M Magi, *ECS J. Solid State Sci. Technol.* **6** M3155 (2017)